

hep-th/0412290

AEI-2004-124

Hamburger Beiträge zur Mathematik Nr. 209

December 2004

TFT CONSTRUCTION OF RCFT CORRELATORS
 IV : STRUCTURE CONSTANTS
 AND CORRELATION FUNCTIONS

Jurgen Fuchs¹ Ingo Runkel² Christoph Schweigert³

¹ Institutionen for fysik, Karlstads Universitet
 Universitetsgatan 5, S-651 88 Karlstad

² Max-Planck-Institut für Gravitationsphysik, Albert-Einstein-Institut
 Am Mühlenberg 1, D-14476 Golm

³ Fachbereich Mathematik, Universität Hamburg
 Schwerpunkt Algebra und Zahlentheorie
 Bundesstraße 55, D-20146 Hamburg

Abstract

We compute the fundamental correlation functions in two-dimensional rational conformal field theory, from which all other correlators can be obtained by sewing: the correlators of three bulk fields on the sphere, one bulk and one boundary field on the disk, three boundary fields on the disk, and one bulk field on the cross cap. We also consider conformal defects and calculate the correlators of three defect fields on the sphere and of one defect field on the cross cap.

Each of these correlators is presented as the product of a structure constant and the appropriate conformal two- or three-point block. The structure constants are expressed as invariants of ribbon graphs in three-manifolds.

Contents

1	Introduction and summary	3
1.1	Correlators from sewing of world sheets	3
1.2	Correlators from 3-d TFT and algebras in tensor categories	4
1.3	Plan of the paper	7
2	Fusing matrices for modules and bimodules	8
2.1	Fusing matrices for modules	8
2.2	Fusing matrices for bimodules	12
2.3	Expressions in a basis	18
2.4	Example: The Cardy case	20
3	Ribbon graph representation of field insertions	22
3.1	A note on conventions	23
3.2	Boundary fields	25
3.3	Bulk fields	31
3.4	Defect fields	35
4	Ribbon graphs for structure constants	42
4.1	Standard bases of conformal blocks on the sphere	43
4.2	Boundary three-point function on the disk	44
4.3	One bulk and one boundary field on the disk	46
4.4	Three bulk fields on the sphere	51
4.5	Three defect fields on the sphere	55
4.6	One bulk field on the cross cap	57
4.7	One defect field on the cross cap	60
4.8	Example: The Cardy case	64
5	Conformal blocks on the complex plane	68
5.1	Chiral vertex operators	69
5.2	Spaces of conformal blocks	72
5.3	Relation to TFT state spaces	75
5.4	The braid matrices	79
6	The fundamental correlation functions	83
6.1	Riemannian world sheets	83
6.2	Boundary three-point function on the upper half plane	87
6.3	One bulk and one boundary field on the upper half plane	89
6.4	Three bulk fields on the complex plane	90
6.5	Three defect fields on the complex plane	91
6.6	One bulk field on the cross cap	92
6.7	One defect field on the cross cap	93

1 Introduction and summary

This paper constitutes part IV of the series announced in [1], in which the relation [2,3,4] between rational two-dimensional conformal field theory (RCFT) and three-dimensional topological quantum field theory (TFT) is combined with non-commutative algebra in modular tensor categories to obtain a universal, model independent, construction of CFT correlation functions. In the previous parts of the series, we concentrated on the description of correlators without field insertions, i.e. partition functions [I], on the special features that arise when the world sheet is unoriented [II], and on the case that the CFT is obtained as a simple current construction [III]. In the present part we give the fundamental correlation functions of the CFT, i.e. a finite set of correlators from which all others can be obtained [5,6,7] via sewing and chiral Ward identities.

1.1 Correlators from sewing of world sheets

The correlators of a CFT should be single-valued functions of the world sheet moduli, like the positions of the field insertions or, more generally, the world sheet metric. Further, the correlators are subject to factorisation, or sewing, constraints. These constraints arise when a world sheet is cut along a circle or an interval and a sum over intermediate states is inserted on the cut boundaries. This procedure allows one to express a correlator on a complicated world sheet (e.g. of higher genus) in terms of simpler building blocks. The fundamental building blocks are [5,6,7] the correlators $h_{\dots i}$ for three bulk fields on the sphere, $h_{\dots i}$ for one bulk field and one boundary field on the disk, $h_{\dots i}$ for three boundary fields on the disk, and $h_{\dots i}$ for one bulk field on the cross cap. Actually, the requirement of covariance under global conformal transformations determines each of these correlators up to the choice of a non-zero vector in the relevant coupling space. The components of these vectors are called structure constants.

Depending on what class of surfaces one allows as world sheets for the CFT, different sets of these fundamental correlators (or, equivalently, structure constants) are required:

class of world sheets	fundamental correlators
(1) oriented, with empty boundary	$h_{\dots i}$
(2) unoriented, with empty boundary	$h_{\dots i}, h_{\dots i}$
(3) oriented, with empty or non-empty boundary	$h_{\dots i}, h_{\dots i}, h_{\dots i}$
(4) unoriented, with empty or non-empty boundary	$h_{\dots i}, h_{\dots i}, h_{\dots i}, h_{\dots i}$

The factorisation of a given correlator into the fundamental building blocks is not unique. Requiring that the different ways to express a correlator in terms of sums over intermediate states agree gives rise to an infinite system of constraints for the data $h_{\dots i}, h_{\dots i}, h_{\dots i}, h_{\dots i}$. One way to define a CFT is thus to provide a collection of candidates for the fundamental correlators that are required in (1) – (4) and show that they solve these factorisation constraints and lead to single-valued correlators.

Holomorphic bulk fields (like the component T of the stress tensor) lead to conserved charges and chiral Ward identities, which constrain the form of the correlation functions. Solutions to the chiral Ward identities are called conformal blocks. In rational CFT the space of conformal blocks for a given correlator is finite-dimensional. Another important consequence of rationality

is that the fundamental correlators have to be given only for a finite collection of fields; for all other fields they are then determined by the chiral Ward identities.

The conformal blocks that are relevant for the correlators on a given world sheet X are actually to be constructed on the double \hat{X} of X . The surface \hat{X} is obtained as the orientation bundle over X , divided by the equivalence relation that identifies the two possible orientations above points on the boundary of X :

$$\hat{X} = \text{Or}(X) = \text{with } (x; \text{or}) \quad (x; \text{or}) \text{ for } x \in \partial X : \quad (1.1)$$

For example, if X is orientable and has empty boundary, then \hat{X} just consists of two copies of X with opposite orientation. A correlator $C(X)$ on the world sheet X is an element in the space of conformal blocks on the double,

$$C(X) \in H(\hat{X}) : \quad (1.2)$$

This is known as the principle of holomorphic factorisation [8].

The conformal blocks on a surface are generically multivalued functions of the moduli of X . Upon choosing bases in the spaces $H(\cdot)$, the behaviour of the blocks under analytic continuation and factorisation can be expressed through braiding and fusing matrices B and F [9, 10, 11]. These matrices are in fact already determined by the four-point blocks on the Riemann sphere. One can then express the constraints on the fundamental correlators coming from factorisation and single-valuedness in terms of fusing and braiding matrices. It turns out that there is a finite set of equations which the structure constants must obey in order to yield a consistent CFT. These are the so-called sewing constraints [5, 6].

The first class of CFTs for which explicit solutions for the structure constants have been calculated are the A-series Virasoro minimal models. The constants for $h_{i,i}$, $h_{i,i}$, $h_{i,i}$ and $h_{i,i}$ are given in [12, 13, 14, 7], respectively. By now many more solutions are known; pertinent references will be given at the end of sections 4.2 { 4.6, in which the calculation of the individual structure constants in the TFT framework is carried out.

Remarkably, one can also obtain exact expressions for some of the fundamental correlation functions in a few examples of non-rational CFTs in which the chiral algebra V is too small to make all spaces of conformal blocks finite-dimensional. The most complete answers are known for Liouville theory, see e.g. [15, 16, 17] and references cited therein. The structure of the expressions found in this case is very similar to the Cardy case of a rational CFT. This similarity might serve as a guideline when trying to extend aspects of the TFT-based construction beyond the rational case.

1.2 Correlators from 3-d TFT and algebras in tensor categories

The sewing constraints form a highly overdetermined system of polynomial equations, which is difficult to solve directly. Instead, one can try to identify an underlying algebraic structure that encodes all information about a solution. In our TFT-based construction, this underlying structure is an algebra A in a certain tensor category. The associativity of this algebra is in fact a sewing constraint, applied to a disk with four insertions on the boundary. This turns out to be the only non-linear constraint to be solved in the TFT approach; all other relevant equations are linear.

We will consider CFTs that can be defined on world sheets of type (3) or type (4). Each of these two cases requires slightly different properties of the algebra A , but they can, and will, be treated largely in parallel.

Our construction of CFT correlators takes two pieces of data as an input:

(i) The chiral algebra V .

This fixes the minimal amount of symmetry present in the CFT to be constructed. More specifically, the holomorphic (and anti-holomorphic) bulk fields contain as a subset the fields in V , and all boundary conditions and defect lines preserve V (with trivial gluing automorphism).

We demand V to be a rational conformal vertex algebra and denote by $\text{Rep}(V)$ its representation category. The properties¹ of V then imply that $\text{Rep}(V)$ is a modular tensor category (see section I2.1 for definition, references and our notational conventions). To any modular tensor category C one can associate a three-dimensional topological field theory TFT (C), see e.g. [19,20] as well as section I2.4 and section 3.1 below. The TFT supplies two assignments. The first, $E \mapsto H(E)$ associates to an (extended) surface E the space $H(E)$ of states, a finite-dimensional vector space. The second assignment takes a cobordism $E^M \xrightarrow{!} E^0$, i.e. a three-manifold with ‘in-going’ boundary E^0 and ‘out-going’ boundary E^M together with an embedded ribbon graph, and assigns to it a linear map $Z(M) : H(E^0) \rightarrow H(E^M)$. In the case of Chern-Simons theory, the state spaces of the TFT can be identified with the spaces of conformal blocks of the corresponding WZW model [2]. In the case of three points on the sphere, for a general RCFT the identification of the state spaces of the TFT with spaces of conformal blocks is a consequence of the definition of the tensor product; for more general situations it follows by the hypothesis of factorisation.

According to the principle (1.2), in order to specify a CFT we must assign to every world sheet X a vector $C(X)$ in $H(\hat{X})$. This will be done with the help of TFT (C), by specifying for every X a cobordism $M \xrightarrow{!} \hat{X}$ and setting $C(X) = Z(M_X)$. Since $C = \text{Rep}(V)$ encodes all the monodromy properties of the conformal blocks, the question whether the collection $\{C(X)\}$ of candidate correlators satisfies the requirements of single-valuedness and factorisation can be addressed solely at the level of the category C . In particular, the analysis does not require the knowledge of the explicit form of V or of the conformal blocks. The first input in the TFT construction is thus

a modular tensor category C

which determines in particular also TFT (C).

For the construction of the vector $C(X) \in H(\hat{X})$ it is actually not necessary that C is the representation category of a vertex algebra; only the defining properties of a modular tensor categories are used. The vertex algebra and its conformal blocks are relevant only when one wishes to determine the correlators as actual functions. In particular, in those cases where non-isomorphic vertex algebras have equivalent representation categories (as it happens e.g. for WZW theories based on $so(2n+1)$ at level 1 with n taking different values congruent modulo 8), the TFT approach yields the same link invariants in the description of the correlators. It

¹ To be precise, V must obey certain conditions on its homogeneous subspaces, be self-dual, have a semi-simple representation category, and fulfill Zhu’s C_2 connectedness condition [18].

is only after substituting multivalued functions for the conformal blocks that two such models have different correlators as actual functions of moduli and insertion points.

(ii) An algebra A in C .

There are generically several distinct CFTs which share the same chiral algebra V , the best known example being the A-D-E classification of minimal models [21]. The additional datum we need to specify the CFT uniquely is an algebra A in the tensor category C .

More precisely, what is needed is

a symmetric special Frobenius algebra (see section I:3) for obtaining a CFT defined on world sheets of type (3);

a Jandl algebra, i.e. a symmetric special Frobenius algebra together with a reversion (see section II:2), for obtaining a CFT defined on world sheets of type (4).

At the level of the CFT, specifying a symmetric special Frobenius algebra corresponds to providing the structure constants for three boundary fields on the disk (denoted $h_{\bar{i}i}$ above) for a single boundary condition. To obtain a Jandl algebra, one must [II] in addition provide a reversion (a braided analogue of an involution) on the boundary fields that preserve the given boundary condition.

Suppose now we are given such a pair $(C; A)$ of data. The correlators C_A of the conformal field theory CFT (A) associated to this pair are obtained as follows. Given a world sheet X , one constructs a particular cobordism M_X , the connecting manifold [4] together with a ribbon graph R_X embedded in M_X . The different ingredients of X , like field insertions, boundary conditions and defect lines, are represented by specific parts of the ribbon graph R_X , and also the algebra A enters in the definition of R_X ; this will be described in detail in section 3. Next one uses TFT (C) to define the correlator of CFT (A) on X as $C_A(X) = Z(M_X)$.

One can prove [V] that the correlators supplied by the assignment $X \mapsto C_A(X)$ are single-valued and consistent with factorisation or, equivalently, with its inverse operation, sewing. This implies in particular that the fundamental correlators $h_{\bar{i}i}$, $h_{\bar{i}i}$, $h_{\bar{i}i}$ and $h_{\bar{i}i}$ obtained in this manner solve the sewing constraints.

We conjecture that, conversely, every CFT build from conformal blocks of the rational vertex algebra V defined on world sheets of types (3) and (4) can be obtained from a suitable pair $(C; A)$ with $C = \text{Rep}(V)$. This converse assignment is not unique: several different algebras lead to one and the same CFT. This corresponds to the freedom of choosing the particular boundary condition whose structure constants are used to define the algebra structure. All such different algebras are, however, Morita equivalent.

For theories defined on world sheets of type (3), it has been advocated in [22, 23, 24, 25] that aspects of the fundamental correlators are captured by the structure of a weak Hopf algebra, respectively an O -cyclic double triangle algebra. Indeed, a weak Hopf algebra furnishes (see [26], and e.g. [27] for a review) a non-canonical description of a module category over a tensor category, i.e. of the situation that in our TFT-based construction is described by the algebra A in the tensor category $\text{Rep}(V)$.

1.3 Plan of the paper

In section 2 we introduce the fusing matrices for the categories \mathcal{C}_A of A -modules and ${}_A\mathcal{C}_A$ of A -bimodules. These are useful for obtaining compact expressions for the structure constants. In section 3 the ribbon graph representation of eld insertions is described. We will consider three kinds of elds: boundary elds, bulk elds, and defect elds. By a boundary eld we mean either a eld that lives on a boundary with a given boundary condition or a eld that changes the boundary condition. Likewise, a defect eld can either live on a defect line of a given type, or change the defect type. A bulk eld can thus be regarded as a special type of defect eld, namely one that connects the invisible defect to the invisible defect.

In section 4 the ribbon invariants for the fundamental correlators $h_{i,i}h_{i,i}h_{i,i}$ and $h_{i,i}$ are computed, as well as the correlators $h_{i,i}$ of three defect elds on the sphere, and $h_{i,i}$ of one defect eld on the cross cap. Up to this point the discussion proceeds entirely at the level of the tensor category \mathcal{C} , ie. of the monodromy data of the conformal blocks.

We would also like to obtain the fundamental correlators as explicit functions of the eld insertion points. The necessary calculations, which are presented in section 6, require additional input beyond the level of \mathcal{C} , namely the vertex algebra V with representation category $\text{Rep}(V)$ and the notions of intertwiners between V -representations and of conformal blocks, as well as the isomorphism between the state spaces of the TFT and the spaces of conformal blocks. These additional ingredients are the subject of section 5. Unlike them atematical prerequisites employed in the earlier sections 2–4, some of this machinery is not yet fully developed in the literature. However, in section 6 we only need the two- and three-point conformal blocks, which are well understood.

The formulas which give our results for correlators of boundary elds, bulk elds and defect elds are listed in the following table.

Correlator	Ribbon invariant	Ribbon invariant in a basis	Ribbon invariant in Cardy case $A = 1$	Correlation function
$h_{i,i}$	eq. (4.5)	eq. (4.12)	eq. (4.67)	eq. (6.16)
$h_{i,i}$	eq. (4.16)	eq. (4.23)	eq. (4.72)	eq. (6.26)
$h_{i,i}$	eq. (4.28)	eq. (4.34)	eq. (4.69)	eq. (6.31)
$h_{i,i}$	eq. (4.38)	eq. (4.42)	eq. (4.68)	eq. (6.36)
$h_{i,i}$	eq. (4.48)	eq. (4.52)	eq. (4.76)	eq. (6.42)
$h_{i,i}$	eq. (4.54)	eq. (4.60)	eq. (4.75)	eq. (6.44)

Acknowledgements. We are indebted to N. Potyitsina-Kube for her skillful help with the numerous illustrations. J.F. is supported by VR under project no. 621{2003{2385, and C.S. is supported by the DFG project SCHW 1162/1-1.

2 Fusing matrices for modules and bimodules

To exhibit the mathematical structure encoded by the bulk and boundary structure constants, we make use of the concept of module [28, 29, 30, 26] and bimodule categories. As the main focus of this paper lies on the computation of correlators, we do not develop the mathematical formalism in all detail.

Given a tensor category C , a right module category over C comes by definition with a prescription for tensoring objects of M with objects of C from the right,

$$M : M \otimes C \rightarrow M : \quad (2.1)$$

The tensor product M must be compatible with the tensor product of C in the sense that there are associativity isomorphisms

$$(M \otimes_M U) \otimes_M V = M \otimes_M (U \otimes V) \quad (2.2)$$

for $U, V \in \text{Obj}(C)$ and $X \in \text{Obj}(M)$, such that the corresponding pentagon identity is satisfied, as well as unitality isomorphisms $M \otimes_M 1 = M$ obeying appropriate triangle identities.

A bimodule category B is a straightforward extension of this concept, allowing both for a left action of a tensor category C and a right action of a possibly different tensor category D ,

$$\begin{matrix} \mathbf{l}_B : C \otimes B \rightarrow B \\ \mathbf{r}_B : B \otimes D \rightarrow B \end{matrix} \quad \text{and} \quad (2.3)$$

The compatibility conditions of the different tensor products are given by associativity isomorphisms

$$\begin{aligned} U \mathbf{l}_B (V \mathbf{l}_B X) &= (U \otimes_C V) \mathbf{l}_B X && \text{(left action)}; \\ (X \mathbf{r}_B R) \mathbf{r}_B S &= X \mathbf{r}_B (R \otimes_D S) && \text{(right action)}; \\ U \mathbf{l}_B (X \mathbf{r}_B R) &= (U \otimes_B X) \mathbf{r}_B R && \text{(left and right action commute)} \end{aligned} \quad (2.4)$$

for $U, V \in \text{Obj}(C), R, S \in \text{Obj}(D)$ and $X \in \text{Obj}(B)$. Again the various associators must fulfill the corresponding pentagon identities, and again there are also unitality isomorphisms satisfying triangle identities. In our application it is natural to take the category B to be a tensor category as well; then there are also the corresponding additional associators and pentagon identities.

In section 4 we will see that the boundary structure constants encode the associator of a module category, while the structure constants of bulk and defect fields give the associator of a bimodule category. In the present section we define the expansion of these associators in a basis. This gives the fusing matrices for modules and bimodules.

2.1 Fusing matrices for modules

The right module category relevant for our purposes is the category \mathcal{G}_A of left A -modules, where A is an algebra in a tensor category C (see e.g. section I.4, or section 2.3 of [31]; we take C to be strict.) Given a left A -module $M = (M, \mathbf{l}_M)$, we can tensor with any object U of C from the right so as to obtain again a (generically different) left A -module $M \otimes U = (M \otimes U, \mathbf{l}_{M \otimes U})$ (with all tensor products taken in C). This defines a right action $\mathbf{r}_M : \mathcal{G}_A \otimes C \rightarrow \mathcal{G}_A$.

We take A to be a symmetric special Frobenius algebra and C to be a modular tensor category. Then also \mathcal{G}_A is semisimple and has a finite number of non-isomorphic simple objects

[32,33]. Let fU_i jg be a set of representatives of isomorphism classes of simple objects of C and fM_j $2Jg$ a set of representatives of isomorphism classes of simple left A -modules. Thus lower case roman letters i, j, k, \dots appear as labels for simple objects U_i, U_j, U_k, \dots of C , while lower case greek letters $\alpha, \beta, \gamma, \dots$ from the upper range of the alphabet appear as labels for simple A -modules $M_\alpha, M_\beta, M_\gamma, \dots$ (later on, we will use such greek letters also for simple bimodules).

As a first step towards defining the fusing matrices for C_A we choose bases in the spaces $\text{Hom}_A(M_j, U_i; M_\alpha)$,

$$\begin{array}{ccc}
 & M & \\
 & \downarrow & \\
 (i) & \cong & \text{Hom}_A(M_j, U_i; M_\alpha) : \\
 & \downarrow & \\
 & M & \\
 & \downarrow & \\
 & U_i &
 \end{array} \tag{2.5}$$

We do not restrict this choice of basis in any way, except for $i=0$, i.e. when $U_i=1$. In this case we demand the basis element to be $(0) = \text{id}_M$. Both the basis morphisms (2.5) and the basis morphisms $(ij)k$ $2\text{Hom}(U_i, U_j; U_k)$ that were chosen in (I2.29) will be labelled by lower case greek letters $\alpha, \beta, \gamma, \dots$, chosen from the beginning of the alphabet.

We also need bases in the spaces $\text{Hom}_A(M_j; M_\alpha, U_i)$, which we denote by $f^{(i)}g$. We choose these bases such that they are dual to the (i) in the sense that $(i) = \alpha, \text{id}_M$. Just as for the morphisms $(ij)k$ in (I2.31), owing to the semisimplicity of C_A the morphisms (i) obey the completeness relation

$$\begin{array}{ccc}
 & M & U_i \\
 & \downarrow & \downarrow \\
 X & \xrightarrow{\alpha} & M \\
 & \downarrow & \downarrow \\
 & M & U_i \\
 & \downarrow & \downarrow \\
 2J & = 1 & M \\
 & \downarrow & \downarrow \\
 & M & U_i \\
 & \downarrow & \downarrow \\
 & M & U_i
 \end{array} = \begin{array}{c} M \\ \downarrow \\ M \\ \downarrow \\ M \\ \downarrow \\ M \end{array} \tag{2.6}$$

Here we abbreviate the dimension of the morphism space $\text{Hom}_A(M_j, U_i; M_\alpha)$ by A_{ij} ; according to proposition I5.22, these non-negative integers give the annulus coefficients of the CFT.

The fusing matrices $G[A]$ relate two different bases of the space $\text{Hom}_A(M_j, U_i, U_j; M_\alpha)$. We denote these bases by $\text{fb}_k^{(1)}g$ and $\text{fb}_k^{(2)}g$, with the individual vectors given by

$$\begin{array}{ccc}
 & M & \\
 & \downarrow & \\
 b^{(1)} & \cong & M \\
 & \downarrow & \\
 & M & \\
 & \downarrow & \\
 & U_i & U_j \\
 & \downarrow & \downarrow \\
 & M & U_i & U_j
 \end{array} \text{ and } \begin{array}{ccc}
 & M & \\
 & \downarrow & \\
 b_k^{(2)} & \cong & M \\
 & \downarrow & \\
 & M & \\
 & \downarrow & \\
 & U_i & U_k \\
 & \downarrow & \downarrow \\
 & M & U_i & U_j
 \end{array} \tag{2.7}$$

Let us verify that these are indeed bases. Linear independence can be seen by composing with the corresponding dualbasis elements. Completeness of $fb_k^{(1)} g$ is seen by applying (2.6) twice. A similar reasoning establishes completeness of $fb_k^{(2)} g$. Also note that there are $A_i A_j$ basis elements of type $b^{(1)}$ and $\sum_k N_{ij}^k A_k$ basis elements of type $b^{(2)}$. That these two numbers are indeed equal has been established in theorem I.5.20(v). In CFT, equality of the two sums means that the annulus coefficients furnish a NIM rep of the fusion rules [34,22,35].

The fusing matrix of the module category \mathcal{C}_A describes a change of basis from $b^{(1)}$ to $b^{(2)}$. There exists a unique set of numbers $G[\mathbb{A}]^{(ij)}_{;k}$ such that

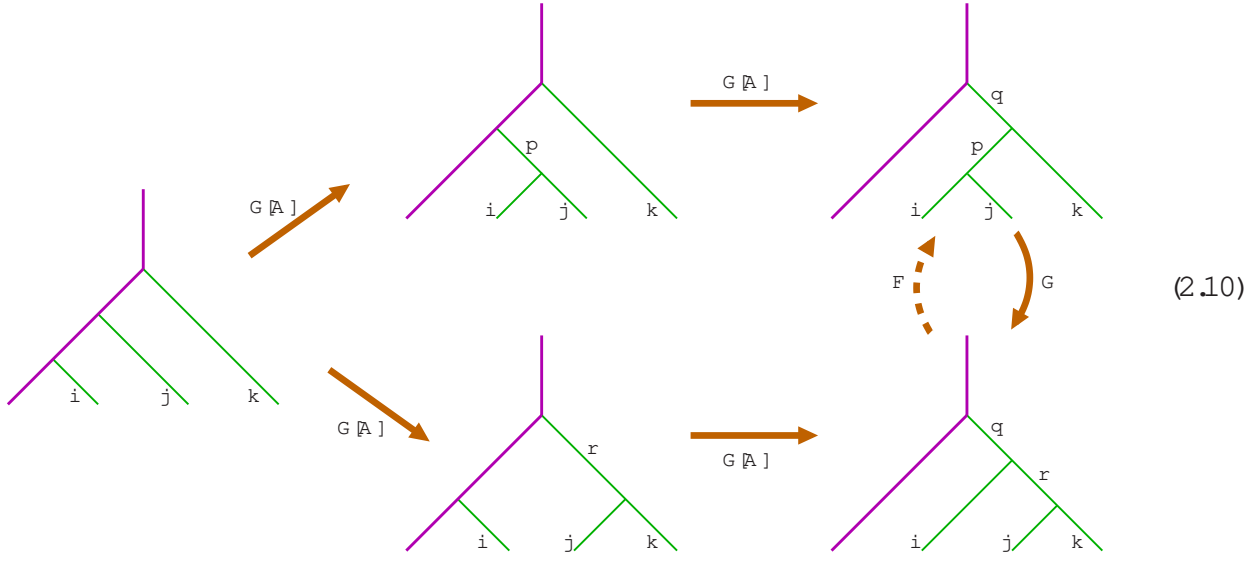
$$\begin{array}{ccc}
 \begin{array}{c} M \\ \text{---} \\ M \\ \text{---} \\ M \end{array} & = & \begin{array}{c} X \quad \sum_k \sum_{ij}^k \\ \text{---} \quad = 1 \quad = 1 \\ G[\mathbb{A}]^{(ij)}_{;k} \end{array} \\
 & & \begin{array}{c} M \\ \text{---} \\ M \\ \text{---} \\ M \end{array}
 \end{array}
 \quad (2.8)$$

We denote the fusing matrix arising here by $G[\mathbb{A}]$ rather than by $F[\mathbb{A}]$, because in the Cardy case $A = 1$ it reduces to the inverse fusing matrix G of \mathcal{C} , see (I.2.40). By composing (2.8) with the basis of $\text{Hom}_A(M \otimes M \otimes U_i \otimes U_j)$ dual to $fb_k^{(2)} g$, one arrives at the following ribbon invariant for $G[\mathbb{A}]$:

$$\begin{array}{ccc}
 \begin{array}{c} M \\ \text{---} \\ M \\ \text{---} \\ M \end{array} & = & \begin{array}{c} M \\ \text{---} \\ M \\ \text{---} \\ M \end{array}
 \end{array}
 \quad (2.9)$$

A possibility to compute these numbers is to first find all simple A -modules M by decomposing induced modules (see section I.4.3), which is a linear (and finite) problem. Next one needs to identify the spaces $\text{Hom}_A(M \otimes U_i; M)$ as subspaces of $\text{Hom}(M \otimes U_i; M)$. This can be done by finding the eigenspaces of the projector $f \otimes f$ that takes a morphism $f \in \text{Hom}(M \otimes U_i; M)$ to its A -averaged morphism \bar{f} , which is known to lie in the subspace $\text{Hom}_A(M \otimes U_i; M)$, see definition I.4.3 and lemma I.4.4. This is again a linear problem. These ingredients suffice to evaluate (2.9).

By construction, the matrices $G[A]$ solve the pentagon relation



Explicitly, this pentagon reads

$$\begin{aligned}
 & \underset{\substack{\text{X} \\ \text{''}}}{G[A]_{2 \quad 3;''r_2}^{(jk)}} \underset{\substack{\text{X} \\ \text{''}}}{G[A]_{1 \quad 1;''1q_1}^{(ir)}} \\
 & = \underset{\substack{\text{X} \\ \text{p} \quad 1;2;1}}{G[A]_{1 \quad 2;1p_2}^{(ij)}} \underset{\substack{\text{X} \\ \text{''}}}{G[A]_{1 \quad 3;1q_2}^{(pk)}} \underset{\substack{\text{X} \\ \text{''}}}{G_{2p_2;1r_2}^{(ijk)q}} : \quad (2.11)
 \end{aligned}$$

If one prefers the fusing matrix F of C to appear directly, rather than its inverse G , one may rewrite this in the form

$$\begin{aligned}
 & \underset{\substack{\text{X} \\ \text{''}}}{G[A]_{1 \quad 2;1p_2}^{(ij)}} \underset{\substack{\text{X} \\ \text{''}}}{G_{1 \quad 3;1q_2}^{(pk)}} \\
 & = \underset{\substack{\text{X} \\ \text{r} \quad 1;2;''}}{G[A]_{2 \quad 3;''r_2}^{(jk)}} \underset{\substack{\text{X} \\ \text{''}}}{G[A]_{1 \quad 1;''1q_1}^{(ir)}} \underset{\substack{\text{X} \\ \text{''}}}{F_{1r_2;2p_2}^{(ijk)q}} : \quad (2.12)
 \end{aligned}$$

When all morphism spaces involved are one-dimensional, these relations simplify considerably, e.g. (2.11) reads

$$G[A]_{;r}^{(jk)} G[A]_{;q}^{(ir)} = \underset{\substack{\text{X} \\ \text{p}}}{G[A]_{;p}^{(ij)} G[A]_{;q}^{(pk)} G_{p;r}^{(ijk)q}} : \quad (2.13)$$

Remark 2.1 :

(i) The fusing matrices $G[A]$ (or rather, their inverses $F[A]$) also appear in an approach to CFT based on graphs and cells [22,23], where the notation ${}^{(1)}F$ is used. The ${}^{(1)}F$ are required to solve a pentagon relation; the corresponding equation for $G[A]$ is (2.11). In fact, the associativity conditions between the categories C , C_A and ${}_A C_A$ give rise to a number of pentagon relations, called the "Big Pentagon", for the corresponding associators. The associators and the pentagon relations can be visualised using cells (known as 0-cneanu cells) [36,37], and can also be interpreted in terms of a 2-category with two objects, see e.g. [27] for more details.

(ii) As observed for the Cardy case $A = 1$ in [14, 38], and for the general case in [39], the pentagon for $G[A]$ is equivalent to the sewing (or factorisation) constraint [6] for four boundary fields on the upper half plane. If a denotes a boundary field which changes a boundary condition described by the A -module M to M' (looking along the real axis towards $+1$) and has chiral representation label a , the boundary OPE symbolically takes the form

$$a_a = \sum_c c_{abc} a_c; \quad (2.14)$$

where the constants c_{abc} are the OPE coefficients². Factorisation of the correlator of four boundary fields leads to the constraint [6]

$$c_{abf} c_{fcg} = \sum_c c_{bce} c_{aed} F_{ef}^{(abc)d}; \quad (2.15)$$

By relation (2.12), this equation in the unknowns c is solved by

$$c_{abc} = G[A]^{(ab)}_{;c}; \quad (2.16)$$

where again all multiplicity labels are omitted.

And indeed, when evaluating the corresponding ribbon invariant in (4.8) below, one finds the explicit expression (4.12) for the coefficient occurring in the correlator of three boundary fields. This expression implies³ (2.16). We thus arrive at the conclusion that the boundary OPE coefficients are given by the 6j-symbols of the module category C_A .

2.2 Fusing matrices for bimodules

The bimodule category that is needed for the description of the bulk structure constants is of the form⁴ $C \otimes B \otimes \overline{C}^!$. Here \overline{C} denotes the tensor category dual⁵ to C in the sense that if $C = (C; \cdot)$ then $\overline{C} = (C; \cdot^{\text{opp}})$. Denoting the quantities in \overline{C} with a bar, this means that $\overline{U} = U$ and $\overline{U} \otimes \overline{V} = V \otimes U$. The bimodule category B of interest here is the category ${}_A C_A$ of A -bimodules, see definition I.4.5.

For the action of C and \overline{C} on ${}_A C_A$ there are, in each case, two possibilities. Let us start with ${}_B^1 : C \otimes {}_A C_A \rightarrow {}_A C_A$. Given an object U of C and an A -bimodule $X = (X; \cdot_1, \cdot_r)$, we define the bimodules $U \otimes X$ as

$$\begin{aligned} U \otimes^+ X &= (U \otimes X; (\text{id}_U \otimes \text{id}_X), (G_A^{-1} \otimes \text{id}_X); \text{id}_U \otimes \text{id}_X) \quad \text{and} \\ U \otimes^- X &= (U \otimes X; (\text{id}_U \otimes \text{id}_X), (G_{A;U}^{-1} \otimes \text{id}_X); \text{id}_U \otimes \text{id}_X); \end{aligned} \quad (2.17)$$

² With all multiplicity labels and coordinate dependence in place, one obtains an equation of the form (I.3.11).

³ In (4.12) the combination $c_{jik} c_{kk0}$ appears because it describes a three-point correlator, rather than an OPE coefficient.

⁴ As mentioned in section 1.1, we treat here only theories defined on surfaces of types (3) and (4). When one does not include surfaces with boundary, one can also consider heterotic theories, in which case more general bimodule categories $C \otimes B \otimes \overline{D} \otimes B$ occur.

⁵ The dual of a tensor category $(C; \cdot)$ is e.g. defined in section 6.2 of [31], where it was taken to be $(C^{\text{opp}}; \cdot)$ rather than $(C; \cdot^{\text{opp}})$. These two categories are tensor equivalent via the functor ?^{opp} , i.e. by taking the duals of objects and morphisms.

respectively. (In graphical notation, for the U^+ -ribbon passes above the A -ribbon, while for U^- it passes below.) We take the functor \mathbb{B}^1 to be given by U^+ . Similarly we can define bimodules $X \otimes U$ when tensoring with U from the right as

$$\begin{aligned} X^+ U &= (\mathbb{X} - U; _ \ id_U; (_ \ id_U) \ (\mathbf{id}_X \ c_{U,A})) \quad \text{and} \\ X^- U &= (\mathbb{X} - U; _ \ id_U; (_ \ id_U) \ (\mathbf{id}_X \ c_{A,U}^{-1})); \end{aligned} \tag{2.18}$$

respectively. (In graphical notation, again for $\begin{smallmatrix} + \\ \circ \end{smallmatrix}$, U passes above A , while for $\begin{smallmatrix} \circ \\ + \end{smallmatrix}$, it passes below.) We take the functor $\begin{smallmatrix} r \\ B \end{smallmatrix}$ to be given by $\begin{smallmatrix} \circ \\ + \end{smallmatrix}$.

The reason for choosing the actions of C and \bar{C} on ${}_A G_A$ in this particular way is that defect fields are to be labelled by elements of the space $\text{Hom}_{A\text{-}\mathbb{A}}(U^+X^-V; Y)$ of bimodule morphisms between the A -bimodules U^+X^-V and Y . In [I, II] instead the space $\text{Hom}_{A\text{-}\mathbb{A}}(X^-V; Y^+U^-)$ of bimodule morphisms was used. These two spaces are canonically isomorphic; an isomorphism can be given as follows.

Lemma 2.2:

The mapping

$$' : \text{Hom}_{A/\mathbb{A}}(X \otimes V; Y \otimes U) \rightarrow \text{Hom}_{A/\mathbb{A}}(U \otimes X \otimes V; Y) \quad (2.19)$$

given by

$$' (f) \asymp (\alpha_U - \text{id}_Y) \circ (\text{id}_U - [C_Y, U - f]) \quad (2.20)$$

is an isomorphism.

Proof:

That ' \tilde{f} ' commutes with the left and right action of A follows by a straightforward use of the definitions. Further, one readily checks that the map ' $\tilde{\cdot}$ ' acting as

$$\sim(g) = c_{Y,U^-}^{-1} (\text{id}_{U^-} - g) \circ \text{id}_U - \text{id}_X \circ \text{id}_V) \quad (221)$$

for $g \in \text{Hom}_{A/\mathbb{A}}(U, V; Y)$ is left and right inverse to g .

It follows from proposition I.4.6 that the category of A -bimodules is isomorphic to the category of left modules over the algebra $A \otimes A_{\text{op}}$. Since A is a symmetric special Frobenius algebra, so is $A \otimes A_{\text{op}}$. It follows that the category of $A \otimes A_{\text{op}}$ -modules is semisimple, and hence $A \otimes A$ is semisimple, too. Let us choose a set of representatives $\{X_j\}_{j \in \mathbb{K}}$ of isomorphism classes of simple A -bimodules.

The algebra A is called simple if it is a simple bimodule over itself or, equivalently, if $Z(A)_{00} = 1$, see definition 2.26 and remark 2.28(i) of [31] for details. If A is simple, then we choose the representatives of simple modules such that $X_0 = A$.

Further, we choose bases $f_{(i,j)}$, g of the spaces $\text{Hom}_{A\otimes A}(U_i \xrightarrow{+} X, U_j; X)$, with graphical representation

$$\begin{array}{c}
 \text{X} \\
 \vdash \\
 \text{U}_i \quad \text{X} \quad \text{U}_j \\
 \text{---} \\
 \text{U}_i \quad \text{U}_j
 \end{array}
 \stackrel{?}{=} (2.22)$$

For the special case $i = j = 0$ we choose $_{(0,0)} = \text{id}_X$. The number of elements in the basis $f_{(i,j)}$ of $\text{Hom}_{A \otimes A}(U_i \otimes X \otimes U_j; Y)$ is denoted by $Z_{ij}^{X \otimes Y}$; more generally, for any two A -bimodules X and Y we set

$$Z_{ij}^{X \otimes Y} := \dim \text{Hom}_{A \otimes A}(U_i \otimes X \otimes U_j; Y) = \dim \text{Hom}_{A \otimes A}(X \otimes U_j; Y \otimes U_i); \quad (2.23)$$

the second equality follows from lemma 2.2 together with $U_i = U_i$. We denote the basis elements dual to (2.22) by $^{(i,j)} \text{Hom}_{A \otimes A}(X; U_i \otimes X \otimes U_j)$; they obey

$$\begin{aligned} {}_{(i,j)} &= \text{id}_X \quad \text{and} \quad X \otimes \overset{Z_{ij}^{X \otimes Y}}{\underset{2K}{\underset{=1}{\text{X}}}} \\ & \quad {}_{(i,j)} = \text{id}_{U_i} \quad \text{id}_X \quad \text{id}_{U_j} \end{aligned} \quad (2.24)$$

The definition (2.23) of $Z_{ij}^{X \otimes Y}$ is in accordance with the definition via the ribbon invariant (I.5.151), as can be seen by inserting the second identity of (2.24) into the ribbon graph (I.5.151) and using $Z_{00}^{X \otimes Y} = \dim \text{Hom}_{A \otimes A}(X; Y)$. The numbers $Z_{ij}^{X \otimes Y}$ also have a physical interpretation; they describe the torus partition function with the insertion of two parallel defect lines [40, 24]; see section I.5.10 for details.

To motivate the definition of the fusing matrices for $B = {}_A G_A$, let us have a look at the left action of \bar{C} on B . By semisimplicity, the isomorphism $(X \otimes {}_B^r \bar{U}_i) \otimes {}_B^r \bar{U}_j = X \otimes {}_B^r (\bar{U}_i \otimes \bar{U}_j)$ on objects gives rise to an isomorphism

$$\begin{aligned} & \text{Hom}^B(X \otimes {}_B^r \bar{U}_i; X) \quad \text{Hom}^B(X \otimes {}_B^r \bar{U}_j; X) \\ & \stackrel{M}{=} \text{Hom}^B(X \otimes {}_B^r \bar{U}_k; X) \quad \text{Hom}^{\bar{C}}(\bar{U}_i \otimes \bar{U}_j; \bar{U}_k) \end{aligned} \quad (2.25)$$

of morphism spaces. By definition, the space $\text{Hom}^{\bar{C}}(\bar{U}_i \otimes \bar{U}_j; \bar{U}_k)$ of morphisms in \bar{C} is equal to the morphism space $\text{Hom}^C(U_j \otimes U_i; U_k)$ in C , while $\text{Hom}^B(X \otimes {}_B^r \bar{U}_i; X) = \text{Hom}_{A \otimes A}(X \otimes U_i; X)$ etc. We would still like to describe the isomorphism (2.25) with the help of the graphical representation of morphisms in the ribbon category C . To this end we need a visualisation for morphisms in \bar{C} . A natural possibility is to represent them graphically by coupons that face the reader with their back side. Thus, using dashed lines for ribbons with back side facing the reader (see the beginning of section II.3 for conventions), we have

=

(2.26)

for $f \in \text{Hom}^{\bar{C}}(\bar{U} \otimes \bar{V}; \bar{W}) = \text{Hom}^C(V \otimes U; W)$, where on the left hand side the coupon labelled by f is showing the black side to the reader while on the right hand side it is showing its white side.

After these preliminaries we are ready to give the definition of the fusing matrices $F[\mathbb{A} \mathbb{A}]$ of the bimodule category $\mathbb{A} \mathbb{C}_{\mathbb{A}}$. We have

$$\begin{array}{c}
 \text{Diagram: } \text{A vertical blue line labeled } X \text{ with a green loop } U_i \text{ attached to the left, a green loop } U_j \text{ attached to the right, and a green loop } U_k \text{ attached to the right. A green dashed loop } U_1 \text{ is attached to the right. Two green squares are at the top, with a green line } X \text{ connecting them.} \\
 = \\
 \text{Equation: } X = \sum_{q_1, q_2} \frac{z_{X^{q_2} X}^{X^{q_1} X}}{q_1 q_2 2 \mathbb{I}} = \sum_{i=1}^{N_{X^{q_1} X}} \sum_{j=1}^{N_{X^{q_2} X}} F[\mathbb{A} \mathbb{A}]^{(ij, kl)}_{q_1 q_2} \frac{U_{q_1}^{(i)} U_{q_2}^{(j)}}{U_i U_j X U_k U_1} \\
 \text{Diagram: } \text{A vertical blue line labeled } X \text{ with a green loop } U_i \text{ attached to the left, a green loop } U_j \text{ attached to the right, and a green loop } U_k \text{ attached to the right. Two green squares are at the top, with a green line } X \text{ connecting them. A green dashed loop } U_1 \text{ is attached to the right.} \\
 \end{array} \quad (2.27)$$

Note that this encodes both the left action of \mathbb{C} and the right action of \mathbb{C} ; the individual actions can be extracted by setting $i = j = 0$ or $k = l = 0$, respectively.

An expression for the bimodule fusing matrix $F[\mathbb{A} \mathbb{A}]$ is obtained from (2.27) by composing with the dual basis. One finds

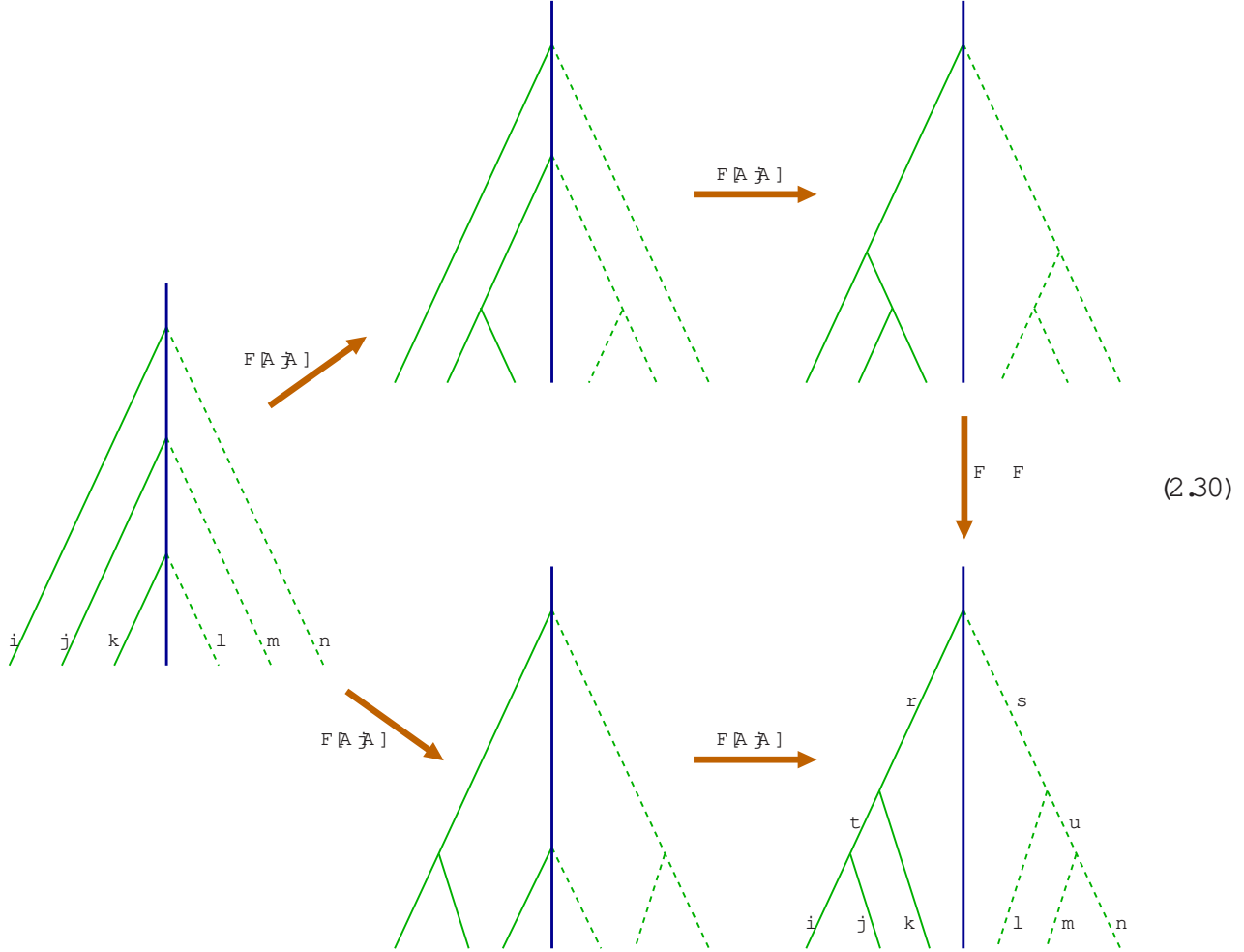
$$\begin{array}{c}
 \text{Diagram: } \text{A vertical blue line labeled } X \text{ with a green loop } U_i \text{ attached to the left, a green loop } U_j \text{ attached to the right, and a green loop } U_k \text{ attached to the right. Two green squares are at the top, with a green line } X \text{ connecting them.} \\
 = \\
 \text{Diagram: } \text{A vertical blue line labeled } X \text{ with a green loop } U_i \text{ attached to the left, a green loop } U_j \text{ attached to the right, and a green loop } U_k \text{ attached to the right. Two green squares are at the top, with a green line } X \text{ connecting them. A green dashed loop } U_1 \text{ is attached to the right.} \\
 = \\
 \text{Diagram: } \text{A vertical blue line labeled } X \text{ with a green loop } U_i \text{ attached to the left, a green loop } U_j \text{ attached to the right, and a green loop } U_k \text{ attached to the right. Two green squares are at the top, with a green line } X \text{ connecting them. A green dashed loop } U_1 \text{ is attached to the right.} \\
 \end{array} \quad (2.28)$$

Evaluating this expression is again a linear problem, but it is more complicated than the procedure for evaluating (2.9). First one must find all simple \mathbb{A} -bimodules. By proposition I.4.6, this is the same as finding all simple $\mathbb{A} \mathbb{A}_{\text{op}}$ -bimodules, which (via the method of induced modules) is a finite, linear problem. Next, the subspaces $\text{Hom}_{\mathbb{A} \mathbb{A}}(U_i \xrightarrow{+} X \xleftarrow{-} U_j; Y)$ of $\text{Hom}(U_i \xrightarrow{+} X \xleftarrow{-} U_j; Y)$ can be determined as images of the projection operators

$$\begin{array}{c}
 \text{Diagram: } \text{A vertical blue line labeled } X \text{ with a green loop } U_i \text{ attached to the left and a green loop } U_j \text{ attached to the right. A yellow box labeled } f \text{ is at the top. A green line } Y \text{ connects the top of the blue line to the yellow box.} \\
 = \\
 \text{Equation: } P(f) = \sum_{q_1, q_2} \frac{z_{X^{q_2} X}^{X^{q_1} X}}{q_1 q_2 2 \mathbb{I}} = \sum_{i=1}^{N_{X^{q_1} X}} \sum_{j=1}^{N_{X^{q_2} X}} P(f)_{q_1 q_2}^{(ij)} \frac{U_{q_1}^{(i)} U_{q_2}^{(j)}}{U_i U_j X U_i U_j} \\
 \end{array} \quad (2.29)$$

for $f \in \text{Hom}(U_i \otimes U_j; \mathbb{Y})$. This is a linear problem, after the solution of which one has all the ingredients at hand that are needed to evaluate (2.28).

By construction, the $F[A \bar{A}]$ satisfy a pentagon relation; schematically, this relation looks like



and explicitly it reads

$$\begin{aligned}
 & X \\
 & F[A \bar{A}]_{2 \quad 3; \quad 1 \quad 1}^{(ij \quad m \quad n)} F[A \bar{A}]_{1 \quad 1; \quad 1 \quad 2}^{(tk \quad lu)} \\
 & = \underset{pq \quad 1; \quad 2; \quad 3; \quad 2; \quad 3}{X} \quad F[A \bar{A}]_{1 \quad 2; \quad 1 \quad 3}^{(jk \quad lm)} F[A \bar{A}]_{1 \quad 3; \quad 1 \quad 2}^{(ip \quad qn)} F_{2 \quad p \quad 2; \quad 1 \quad t \quad 2}^{(ijk) \quad r} F_{3 \quad q \quad 3; \quad 1 \quad u \quad 2}^{(nm) \quad s} \quad (2.31)
 \end{aligned}$$

Remark 2.3 :

(i) In remark 2.1 (ii) we have seen that the boundary OPE is given by the 6j-symbols of the module category \mathcal{C}_A . In fact, similar considerations apply to bulk and defect fields.

Let \mathcal{A} be a bulk field with chiral/antichiral representation labels l, r . Omitting all position dependence and multiplicity indices, the OPE of two bulk fields can symbolically be written as

$$= \underset{C}{X} : \quad (2.32)$$

The OPE coe cients C must solve a factorisation constraint coming from the fourpoint correlator on the sphere [5,6,41],

$$C' C = \overset{X}{\underset{''}{C}} C'' F_{1,1}^{(1,1,1)} F_{r,r}^{(r,r,r)}; \quad (2.33)$$

where again all multiplicity indices and summations are omitted. If we identify

$$C = F[A]^{(1,1,0,r,r)}; \quad (2.34)$$

then (2.33) is equivalent to the pentagon relation (2.31) for the $F[A]$ -matrices. Recall that the bimodule index 0 refers to the algebra A itself (we take A to be simple).

In the TFT approach, the factorisation constraints hold by construction, and indeed the ribbon invariant (4.28) for the correlator of three bulk fields on the sphere (to be constructed in section 4.4 below) leads to the coe cient (4.34), which implies (2.34). Note that in (4.34) two factors $F[A]$ appear because this equation describes the coe cient for a three-point correlator, which is a product of two OPE coe cients.

Let us now turn to defect fields. Denote by X a defect field which changes a defect described by a bimodule X into a defect described by X . One can think of a bulk field as a special defect field which changes the invisible defect (labelled by A itself) to the invisible defect, i.e. with X set to zero. One can convince oneself that the OPE-coe cients of defect fields have to ful l a factorisation condition similar to (2.33) and accordingly we would expect that these OPE-coe cients are also given by matrix elements of $F[A]$. As before, this does indeed result from the TFT-computation, see (4.42) below. Thus, just like is the case of boundary fields, the OPE coe cients of defect fields can be seen as the coe cients of a suitable associator morphism.

(ii) It is also worth recalling a well-known geometric interpretation of the pentagon identity for the F -matrices (see e.g. [42]). This uses a description of the 6j-symbols F of a semisimple tensor category as tetrahedra, with edges labelled by simple objects U_i and faces by morphisms H on $(U_i, U_j; U_k)$, i.e. schematically

$$F = \begin{array}{c} \text{Diagram of a double tetrahedron: two tetrahedra sharing a common face. Arrows on edges indicate orientation. A central dashed edge connects vertices not on the common face.} \\ \end{array} \quad (2.35)$$

In this description, the pentagon identity corresponds to the equality between two ways to obtain the body of a 'double tetrahedron': first, by gluing two tetrahedra along a common face, and second, by gluing three tetrahedra along an edge common to all three of them (namely the edge that, in the first description, connects the two vertices not belonging to the distinguished face) and along three faces each of which is common to two of the tetrahedra. In the resulting equation, the labels of the common faces and the internal edge are to be summed over.

To obtain an analogous interpretation of the pentagon relation (2.31) for bimodules, one

can represent the $F[A \otimes A]$ as prisms

$$F[A \otimes A] = \begin{array}{c} \text{Diagram of a double prism} \\ \text{with two triangular faces and a central quadrangle.} \end{array} \quad (2.36)$$

in which the edges of the two triangular faces are labelled by simple objects of C and the remaining edges by simple A -bimodules. The pentagon (2.31) then describes again the equality between two ways to obtain a certain geometric body, this time a 'double prism': on one side (two $F[A \otimes A]$) two prisms are glued along a common quadrangle; on the other side, they are instead glued along a quadrangle of which two edges are those edges of the original outer quadrangles that were not involved in the previous gluing; at the remaining two edges the quadrangle must touch triangles, and this is achieved by gluing a tetrahedron to each of the original triangles. Again, the labels of common faces and internal edges are to be summed over. Pictorially,

$$\begin{array}{c} \text{Diagram of two prisms glued along a common quadrangle} \\ = \\ \text{Diagram of a double prism with a central tetrahedron} \end{array} \quad (2.37)$$

2.3 Expressions in a basis

As already pointed out, the fusing matrices $G[A]$ and $F[A \otimes A]$ are completely determined by the modular tensor category C , the symmetric special Frobenius algebra A , and a choice of bases in the relevant morphism spaces. While the explicit expressions are not very illuminating, we still quickly go through the calculations, because later on we will need some of the quantities entering these computations.

We can describe simple subobjects of an object V of C by bases $b_{(i;)}^V, g$ of the morphism spaces $\text{Hom}(U_i; V)$ and the dual bases $b_V^{(i;)} g$ of $\text{Hom}(V; U_i)$, satisfying $b_V^{(j;)} b_{(i;)}^V = \delta_{ij} \text{id}_{U_i}$ and the completeness property $\sum_{i \in I} b_{(i;)}^V b_V^{(i;)} = \text{id}_V$. Their graphical notation is

$$\begin{array}{ccc} b_{(i;)}^V = : \begin{array}{c} V \\ \uparrow \\ U_i \end{array} : & ; & b_V^{(j;)} = : \begin{array}{c} U_j \\ \downarrow \\ V \end{array} : \end{array} \quad (2.38)$$

For modules, this amounts to the choice of morphisms introduced in (I.4.21). For bimodules we take analogously $b_{(i;)}^X, 2 \text{Hom}(U_i; X)$ and $b_X^{(i;)} 2 \text{Hom}(X; U_i)$. In terms of these embedding and

restriction morphisms we can now expand the morphisms $s_{(k)}$ and $s_{(i,j)}$ described before, as well as their duals. We choose the conventions

$$\begin{array}{c}
 \text{Diagram: } M \text{ (green vertical line)} \otimes M \text{ (purple vertical line)} \xrightarrow{\text{green box}} M \text{ (purple vertical line)} \otimes U_k \text{ (green curved line)} \\
 \text{Label: } (k) \\
 \text{Equation: } X \otimes \text{hU}_X^M \xrightarrow{\text{green box}} \text{hU}_X^M \otimes \text{iN}_{X^M}^n \xrightarrow{\text{green box}} [s_{(k)}]_{1,2}^{m,n} = 1
 \end{array}
 \quad
 \begin{array}{c}
 \text{Diagram: } M \text{ (purple vertical line)} \otimes M \text{ (green vertical line)} \xrightarrow{\text{green box}} M \text{ (purple vertical line)} \otimes U_k \text{ (green curved line)} \\
 \text{Label: } (k) \\
 \text{Equation: } X \otimes \text{hU}_X^M \xrightarrow{\text{green box}} \text{hU}_X^M \otimes \text{iN}_{X^M}^n \xrightarrow{\text{green box}} [s_{(k)}]_{1,2}^{m,n} = 1
 \end{array}
 \quad
 \begin{array}{c}
 \text{Diagram: } M \text{ (purple vertical line)} \otimes M \text{ (green vertical line)} \xrightarrow{\text{green box}} M \text{ (purple vertical line)} \otimes U_k \text{ (green curved line)} \\
 \text{Label: } (k) \\
 \text{Equation: } X \otimes \text{hU}_X^M \xrightarrow{\text{green box}} \text{hU}_X^M \otimes \text{iN}_{X^M}^n \xrightarrow{\text{green box}} [s_{(k)}]_{1,2}^{m,n} = 1
 \end{array}
 \quad (2.39)$$

for the module basis; the expansion coefficients $[s_{(k)}]_{1,2}^{m,n}$ are complex numbers. Analogously, for bimodules we choose

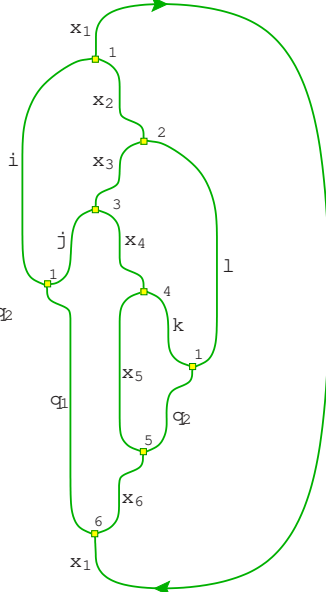
$$\begin{array}{c}
 \text{Diagram: } X \text{ (blue vertical line)} \otimes U_i \text{ (green curved line)} \otimes X \text{ (blue vertical line)} \otimes U_j \text{ (green curved line)} \\
 \text{Label: } (i,j) \\
 \text{Equation: } X \otimes X \xrightarrow{\text{blue box}} \text{hU}_X^X \xrightarrow{\text{blue box}} [s_{(i,j)}]_{1,2;1,2}^{m,n} = 1
 \end{array}
 \quad
 \begin{array}{c}
 \text{Diagram: } X \text{ (blue vertical line)} \otimes U_i \text{ (green curved line)} \otimes X \text{ (blue vertical line)} \otimes U_j \text{ (green curved line)} \\
 \text{Label: } (i,j) \\
 \text{Equation: } X \otimes X \xrightarrow{\text{blue box}} \text{hU}_X^X \xrightarrow{\text{blue box}} [s_{(i,j)}]_{1,2;1,2}^{m,n} = 1
 \end{array}
 \quad
 \begin{array}{c}
 \text{Diagram: } X \text{ (blue vertical line)} \otimes U_i \text{ (green curved line)} \otimes X \text{ (blue vertical line)} \otimes U_j \text{ (green curved line)} \\
 \text{Label: } (i,j) \\
 \text{Equation: } X \otimes X \xrightarrow{\text{blue box}} \text{hU}_X^X \xrightarrow{\text{blue box}} [s_{(i,j)}]_{1,2;1,2}^{m,n} = 1
 \end{array}
 \quad (2.40)$$

Substituting the expansion (2.39) into the ribbon invariant (2.9) for $G[A]$ and taking the trace

on both sides of (2.9) immediately leads to

$$G[A]^{(ij)}_{;k} = \frac{X}{\dim(U_n)} \frac{X}{\dim(M_-)} \left[\begin{smallmatrix} (i) & \mathfrak{m} & r \\ & 2 & 3 & 2 \\ & 1 & 2 & 3 & 4 \end{smallmatrix} \right] \left[\begin{smallmatrix} (j) & \mathfrak{m} & n \\ & 3 & 1 & 3 \\ & 1 & 2 & 1 & 2 \end{smallmatrix} \right] \left[\begin{smallmatrix} (k) & \mathfrak{m} & n \\ & 2 & 1 & 1 \\ & 1 & 2 & 1 & k \end{smallmatrix} \right] G^{(mij)n}_{n_2 r n_3; n_1 k} : \quad (2.41)$$

For the fusion matrices of the bimodule category one must substitute (2.40) into (2.28). Using also the braiding relation (I2.41), this results in

$$F[A]^{(ij)kl}_{;q_1 q_2 1 2} = \frac{1}{\dim(X_-)} \left[\begin{smallmatrix} X & X & X \\ x_1, \dots, x_6 & x_1, \dots, x_6 & x_1, \dots, x_6 \end{smallmatrix} \right] \left[\begin{smallmatrix} (q_1 q_2) & X \\ x_5, x_4, x_3 & x_3, x_2, x_1 \\ (j, k) & (i, l) \end{smallmatrix} \right] R^{(lk)q_2}_{1 2} : \quad (2.42)$$


Applying the fusing relation (I2.40) first to the vertex labelled x_3 and then to the vertex labelled x_4 finally yields

$$F[A]^{(ij)kl}_{;q_1 q_2 1 2} = \frac{X}{\dim(U_{n_1})} \frac{X}{\dim(X_-)} \left[\begin{smallmatrix} X & X \\ x_1, \dots, x_6 & x_1, \dots, x_6 \end{smallmatrix} \right] \left[\begin{smallmatrix} (q_1 q_2) & X \\ x_5, x_4, x_3 & x_3, x_2, x_1 \\ (j, k) & (i, l) \end{smallmatrix} \right] R^{(lk)q_2}_{1 2} G^{(jn_4 l) n_2}_{n_3 n_3; 2 n_6} G^{(n_5 k l) n_6}_{4 n_4 3; 5 q_2 1} F^{(ij n_6) n_1}_{1 n_2 2; 1 q_1 6} : \quad (2.43)$$

In writing the expansions (2.39) and (2.40), as well as the expressions (2.41) and (2.43) for the fusion matrices, we have included all multiplicity indices. In the Cardy case $A = 1$ treated below, as well as later on in section 4.8, we make the simplifying assumption that the fusion rules in C obey $N_{ij}^k \geq 0$ so as to somewhat reduce the notational burden.

2.4 Example: The Cardy case

Let us now work out the fusion matrices for the module and bimodule categories in the case $A = 1$. This choice for the algebra A corresponds to having the charge conjugation modular invariant as the partition function on the torus. As already mentioned, for further simplification we assume in the sequel that the fusion rules of the modular tensor category C satisfy $N_{ij}^k \geq 0$; this allows us to suppress many of the multiplicity labels.

The simple 1-modules are just the simple objects of C , so that $C_A = C$ as categories. We choose the representatives of simple modules as $M = U$ with $2 I$. Similarly, for the bimodules we have ${}_A C_A = C$, this time even as tensor categories, and we choose the representatives of simple bimodules as $X = U$, $2 I$. Note that we continue to use greek letters to label simple modules and bimodules to avoid confusion, even though now the three index sets I , J and K are identical.

Next we must specify the basis elements (k) and (i, j) that we will use. We make the choices

$$\begin{aligned}
 (k) &= k; \\
 \text{and} & \\
 (i_j) &= t_j^{-1} \underset{ij}{\text{;}} \quad (2.44)
 \end{aligned}$$

where the (non-zero) constants t_k and t_{ij} can be chosen at will; later on they will serve as normalisations of the bulk, boundary and defect fields. The phases t_j appearing in (2.44) have been defined in (II.3.43). If \mathcal{C} is the representation category of a conformal vertex algebra we take $t_j = \exp(i\vartheta_j)$ with ϑ_j the conformal highest weight of the representation labelled by j . The phases t_j are convenient because they will lead to simpler expressions for the bulk two-point function on the sphere and for the bulk one-point function on the disk.

Because of $\text{Hom}_A(M \otimes_{U_k} M) = \text{Hom}(U \otimes_{U_k} U, U)$, there is no need for a multiplicity label in the first formula in (2.44). In contrast, the dimension of the morphism space $\text{Hom}_{A \otimes A}(U_i \otimes X \otimes U_j, X) = \text{Hom}(U_i \otimes U \otimes U_j, U)$ can be larger than one, and accordingly the basis elements $_{(i,j)}$ are labelled by those simple objects U that occur in the fusion $U_i \otimes U_j$ and for which $N_i \neq 0$. In the notation introduced in (2.39) and (2.40) the basis choice (2.44) reads

$$[\begin{smallmatrix} & & m \\ & & n \end{smallmatrix}]^m n = \begin{smallmatrix} & & m \\ & & n \end{smallmatrix} ; \quad \text{and} \quad [\begin{smallmatrix} & & x \\ i & j & \end{smallmatrix}]^{xyz} = t_j^{-1} \begin{smallmatrix} & & j \\ i & j & \end{smallmatrix} x y z : \quad (2.45)$$

The dot ' ' stands for a multiplicity label that can take only a single value, the corresponding morphism space being one-dimensional.

We also need the duals of the bases (2.44). One easily checks that these are given by

$$\begin{array}{c}
 \text{Diagram 1:} \\
 \text{A green line with a loop. The top-left part is labeled } U, \text{ the top-right part is labeled } U_k, \text{ and the bottom part is labeled } U. \text{ A yellow dot is at the bottom-left corner of the loop.} \\
 \\
 \text{Diagram 2:} \\
 \text{A green line with a loop. The top-left part is labeled } U_i, \text{ the top-right part is labeled } U, \text{ the top-right loop is labeled } U_j, \text{ and the bottom part is labeled } U. \text{ A yellow dot is at the bottom-left corner of the bottom line.} \\
 \\
 \text{and} \\
 \\
 \text{Diagram 3:} \\
 \text{A green line with a loop. The top-left part is labeled } (i-j), \text{ the top-right part is labeled } U_j, \text{ and the bottom part is labeled } U_{ij}. \text{ A yellow dot is at the bottom-left corner of the bottom line.} \\
 \\
 \text{Diagram 4:} \\
 \text{A green line with a loop. The top-left part is labeled } U_i, \text{ the top-right part is labeled } U, \text{ the top-right loop is labeled } U_j, \text{ and the bottom part is labeled } U. \text{ A yellow dot is at the bottom-left corner of the bottom line.} \\
 \\
 \text{Equation:} \\
 (k) = \frac{1}{k} ; \quad \text{and} \quad (i-j) = \frac{U_j}{ij} ; \quad (2.46)
 \end{array}$$

Substituting the choice of basis (2.44) into (2.9) immediately yields

$$G_{\{k\}}^{(ij)} = \frac{\begin{matrix} ; & ; \\ j & i \\ ; & ; \end{matrix}}{\begin{matrix} k \end{matrix}} G_{k}^{(ij)} \quad (2.47)$$

for the fusion matrices of G_A .

For the fusion matrices of the bimodule category we deduce from (2.28) that

Similarly to the calculation in (2.42), applying the fusion relation (I.2.40) first to the vertex for $H \circ_m (U_j \otimes U_k; U)$ and then to the one for $H \circ_m (U_i \otimes U_k; U)$ results in the expression

$$F_{[l][k]}^{(ij)} = \frac{t_l^{ij} t_k^{ij}}{t_l t_k} R^{(lk)} q \frac{t_q}{t_l t_k} G^{(j-1)} G^{(k-1)} F_p^{(ij)} : \quad (2.49)$$

3 Ribbon graph representation ofeld insertions

In this section we present the ribbon graph representation for field insertions on boundaries, in the bulk and on defect lines. This will be used in section 4 to express structure constants as invariants of ribbon graphs in three-manifolds.

The ribbon graph representations will be given explicitly only for the case of unoriented world sheets. Recall from [II] that in this case the relevant algebraic structure to describe the full CFT is a J and l algebra.

It is then straightforward to obtain the oriented case as well. Of course, given an oriented world sheet, one can just forget the orientation to obtain an unoriented world sheet, for which one can apply the construction below. However, this is not the correct procedure to use, since in the two cases different algebraic structures are relevant:

oriented world sheets	!	symmetric special Frobenius algebra
unoriented world sheets	!	Jordan algebra

Thus for oriented world sheets one must formulate the construction of the ribbon graphs in a way that is applicable for any symmetric special Frobenius algebra, not just for those admitting a reversion. This can be done as follows.

First, as already emphasised, instead of a Jandlalgebra, just a symmetric special Frobenius algebra is to be used. Second, whenever in the unoriented case an orientation or_1 of a boundary component, respectively or_2 of a surface, enters the construction, then in the corresponding oriented case a canonical choice is provided by the orientation of the world sheet. In the unoriented case there are equivalence relations linking the two possible choices for $or_{1,2}$, and this is in fact the only place where the reversion of the Jandlalgebra enters. In the oriented case these equivalence relations are not needed and hence only the symmetric special Frobenius structure is used.

For example, recall from section II:3 that in the unoriented case boundary conditions are labelled by equivalence classes $(M; or_1)$, where M is a left A -module and or_1 is an orientation of the boundary component. The equivalence relation (II:3.1) is that $(M; or_1) \sim (M^0; or_1^0)$ if either $or_1^0 = or_1$ and $M^0 = M$ or if $or_1^0 = -or_1$ and $M^0 = M$, where M^0 is the module conjugate to M (see section II:2.3). To obtain the prescription in the oriented case, we use the orientation or_{ex} of the boundary that is induced by the world sheet orientation or_x to select the pair $(M; or_{\text{ex}})$. The second alternative in the equivalence relation is then obsolete.

3.1 A note on conventions

The construction of the ribbon graph described in this section departs slightly from the one used in [I] and [II], resulting from a number of choices of conventions that have to be made. However, in the absence of field insertions the final result, i.e. the ribbon graph embedded in the connecting manifold, is still the same as in [I, II]. To see this let us summarise the conventions we choose and point out how they differ from those in [I, II].

Category of three-dimensional cobordisms

Recall from the summary in sections I:2.3 and I:2.4 that a three-dimensional topological field theory furnishes a functor $(\mathbb{Z}; H)$ from the cobordism category 3-cobord (\mathcal{C}) to the category of finite-dimensional complex vector spaces; such a functor can be constructed from any modular tensor category \mathcal{C} . It turns out to be convenient to give a definition of the objects and morphisms of 3-cobord (\mathcal{C}) slightly different from the one used in section I:2.4.

Objects of 3-cobord are extended surfaces and morphisms of 3-cobord are cobordisms between extended surfaces. An extended surface E consists of the following data:

- A compact oriented two-dimensional manifold without boundary, also denoted by E .
- A finite set of marked points $\{p_i\}$ that is, of quadruples $(p_i; [\gamma_i]; V_i; \gamma_i)$, where the $p_i \in E$ are mutually distinct points of the surface E and $[\gamma_i]$ is a germ of arcs⁶ $\gamma_i: [\gamma_i; \gamma_i] \rightarrow E$ with $\gamma_i(0) = p_i$. Furthermore, $V_i \in \text{Ob}(\mathcal{C})$, and γ_i is a sign.
- A Lagrangian subspace $H_1(E; \mathbb{R})$.

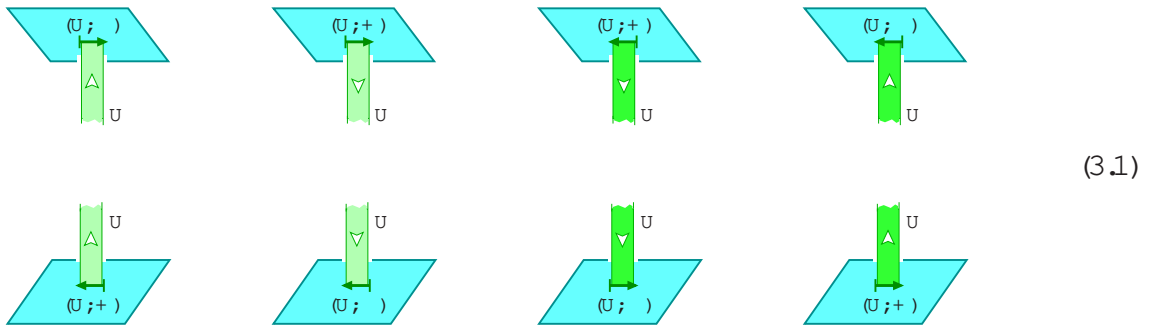
A morphism $E \rightarrow E'$ is a cobordism M , consisting of the following data:

⁶ By a germ of arcs we mean an equivalence class $[\gamma]$ of continuous embeddings of intervals $[\gamma; \gamma] \subset \mathbb{R}$ into the extended surface E . Two embeddings $\gamma: [\gamma; \gamma] \rightarrow E$ and $\gamma': [\gamma'; \gamma'] \rightarrow E$ are equivalent if there is a positive $\gamma < \gamma'$ such that γ and γ' are equal when restricted to the interval $[\gamma; \gamma']$.

- A compact oriented three-manifold, also denoted by M , such that $\partial M = (\mathbb{E})^t E^0$. Here E is obtained from \mathbb{E} by reversing its 2-orientation and replacing any marked point $(p; []; U; ")$ by $(p; [\sim]; U; ")$ with $\sim(t) = -t$, see section I2.4. The boundary ∂M of a cobordism is oriented according to the inward pointing normal.
- A ribbon graph R inside M such that for each marked point $(p; []; U; ")$ of $(\mathbb{E})^t E^0$ there is a ribbon ending on $(\mathbb{E})^t E^0$ in the following way. Let $\iota : [0; 1] \rightarrow [\frac{1}{10}; \frac{1}{10}] \subset M$ be the parametrisation⁷ of a ribbon S embedded in M and labelled by $U \in \text{Obj}(\mathcal{C})$. If $" = +1$, then the core of S must point away from ∂M and the end of S must induce the germ $[]$, i.e. $\iota(0; 0) = p$ and $\iota'(0; t) = [(t)]$. If $" = -1$, then the core of S must point towards ∂M , and $\iota(1; 0) = p$ as well as $\iota'(1; t) = [(t)]$, the presence of the minus sign implying that the orientation of the arc is reversed.

The difference to the definition used in section I2.4 is that we do not take a surface with embedded arcs, but rather with germs of arcs.⁸ The reason for using this definition of extended surface will become clear in section 5.3 where we assign a germ of arcs to a germ of local coordinates.

Note also that the allowed ways for a ribbon to end on an arc-germ of an extended surface depend on the orientations of arc, ribbon-surface and ribbon-core, but not on the orientation of the three-manifold M or of the extended surface \mathbb{E} . The two allowed possibilities are (looked at from 'above' and 'below' \mathbb{E} , as well as from 'in front of' and 'behind' the ribbon) the following:



(For instance, the first picture in the first row is the same as the fourth picture in the first row, as well as the second and third picture in the second row.)

Ribbon graph embedded in the connecting manifold

In the TFT description of correlators for oriented world sheets, we have the following conventions:

⁷ By a parametrisation of a ribbon S we mean the following. S has a 2-orientation of its surface and a 1-orientation of its core. The rectangle $[0; 1] \times [\frac{1}{10}; \frac{1}{10}]$ carries a natural 2-orientation as a subset of \mathbb{R}^2 , and the interval $[0; 1]$ along carries a natural 1-orientation as a subset of the x -axis. A parametrisation ι of S is required to preserve both of these orientations.

⁸ This convention should be compared to those of [19], which uses the arcs themselves, and of [20], which uses tangential vectors at the insertion points p . The present convention is a compromise between the two. Only the behaviour in an arbitrarily small neighbourhood of p is relevant, but it does not need a differential structure on \mathbb{E} .

- The correlator for a world sheet X is described by a cobordism $;^M \dagger \hat{X}$, where \hat{X} is the double of X . In particular, \hat{X} is the outgoing part of the boundary ∂M_X .
- Field insertions on the world sheet X lead to marked points on the double \hat{X} . For the ribbon graph inside the cobordism $;^M \dagger \hat{X}$ we take all ribbons ending on ∂M_X to have cores pointing away from the boundary, i.e. $= +1$ for all marked points on \hat{X} .
- The non-negative integers (compare formulas (I5.30) and (I5.65), and lemma 2.2)

$$Z(A)_{ij} = \dim \text{Hom}_{A \otimes A} ({}_{\text{A}}(U_j); {}^{+}_{\text{A}}(U_i)) = \dim \text{Hom}_{A \otimes A} (U_i \otimes A \otimes U_j; A); \quad (3.2)$$

with ${}_{\text{A}}(U)$ denoting -induced ⁹ bimodules, count the number of linearly independent primary bulk fields ${}_{ij}(z; z)$ that have chiral representation label i and anti-chiral representation label j .

- Boundary conditions are labelled by left A -modules.

As a consequence (compare (I5.30) or (3.24) below), when constructing the ribbon graph in M_X for an oriented world sheet X , the ribbons embedded in X must be inserted in such a manner that their 'white' side faces the boundary of M_X which has the same orientation as X . In particular, the orientation of the ribbon-surfaces is opposite to that of the world sheet X .

This clashes with the prescription given in section I5.1, according to which orientation of the world sheet and the ribbons agree. The reason is that in [I] implicitly, the boundary of a cobordism was taken to be oriented according to the outward pointing normal. However due to the conventions above we should use the inward pointing normal.

It is not difficult to convince oneself that all pictures and formulas in [I] and [II] remain unchanged provided that

- { one uses the inward pointing normal to orient the boundary of a cobordism, and that
- { the prescription in sections I5 and II3.1 is modified such that ribbons embedded in $X \subset M_X$ have surface orientation opposite to the (local) orientation of X , and similarly their core has opposite orientation to ∂X if they lie on the world sheet boundary.

From hereon we use this modified prescription both in the oriented and in the unoriented case.

3.2 Boundary fields

A connected component b of the boundary ∂X of the world sheet has the topology of a circle. On b there may be several insertions of boundary fields, and accordingly the intervals between the field insertions may be labelled by different boundary conditions. Below we will see that the configurations of fields and boundary conditions on such a boundary component are again labelled by equivalence classes, and that this labelling generalises the one for boundaries without field insertions.

In the sequel we say that two curves γ and γ' are aligned in a point p of the world sheet if there exist parametrizations $\gamma^0(t)$ of γ and $\gamma'^0(t)$ of γ' such that $\gamma^0(0) = p = \gamma'^0(0)$ and $[\gamma^0] = [\gamma'^0]$.

⁹ For the notion of -induction , which is due to [43], see e.g. definition 2.21 of [31]. The definition, as well as a list of references, is also given in section I5.4 where, however, the notation $\langle \rangle$ is used in place of ${}_{\text{A}}$.

Labelling of boundary insertions

A boundary *eld* is a collection

$$= (M; N; V; ; p; []) \quad (3.3)$$

of the following data: $M; N$ are left A -modules, V is an object of C , the morphism ϕ is an element of $\text{Hom}_A(M \rightarrow V; N)$, $p \in \partial X$ is a point on the boundary of the world sheet X , and finally $[]$ is an arc germ such that $(0) = p$ and that ϕ is aligned to ∂X in p .

Denote by $b([1]; \dots; [n])$ a connected component of ∂X together with n arc germs $[k]$ such that $[k]$ is aligned to ∂X in $p_k(0)$. The points $p_k(0)$ mark the insertion points of the boundary elds. A boundary component $b([1]; \dots; [n])$ with n boundary eld insertions is labelled by equivalence classes of tuples

$$(M_1; \dots; M_{n^0}; \phi_1; \dots; \phi_{n^0}; \text{or}_1) \quad (3.4)$$

subject to the following conditions.

- or_1 is an orientation of the boundary circle b .
- The points $p_k = p_k(0)$ are ordered such that when passing along the boundary circle b opposite to the direction given by or_1 , one passes from p_k to p_{k+1} . (Here and below it is understood that $p_0 = p_n$ and $p_{n+1} = p_1$, and analogously for M_k and ϕ_k .)
- The $M_1; \dots; M_{n^0}$ are left A -modules. M_k labels the boundary condition on the stretch of boundary between p_{k-1} and p_k . Thus if there are no eld insertions, then $n^0 = 1$, and otherwise $n^0 = n$.
- The $\phi_1; \dots; \phi_{n^0}$ are boundary elds with defining data

$$_k = (M_k; M_{k+1}; V_k; \phi_k; p_k; [k]) : \quad (3.5)$$

To define the equivalence relation we need

Definition 3.1 :

Let A be a Jandl algebra in C . Given an object V of C and two left A -modules M and N , $s_{M, N, V}$ is the map $s: \text{Hom}(M \rightarrow V; N) \rightarrow \text{Hom}(N \rightarrow V; M)$ defined by

$$s(\phi) := \begin{array}{c} \text{Diagram showing a boundary component } b \text{ with boundary condition } M \rightarrow V. \\ \text{The boundary } b \text{ is a closed loop with an insertion point } p_k \text{ marked by a yellow square.} \\ \text{The boundary condition } M \rightarrow V \text{ is represented by a green line segment connecting the boundary to the point } p_k. \\ \text{The map } s(\phi) \text{ is defined by mapping the boundary condition } M \rightarrow V \text{ to the boundary condition } N \rightarrow V. \end{array} \quad (3.6)$$

for $\phi \in \text{Hom}(M \rightarrow V; N)$.

Lemma 3.2 :

Let A and s be as in definition 3.1. If $\mathbb{2}\text{Hom}_A(M \rightarrow V; N \rightarrow V; M \rightarrow N)$, then $s(\mathbb{2}\text{Hom}_A(M \rightarrow V; N \rightarrow V; M \rightarrow N))$.

Proof:

The assertion follows by direct computation from the defining properties of conjugate left modules, as given in definition II.2.6. \square

We can now formulate the equivalence relation on labellings (3.4) of a boundary component b with (or without) end insertions. Consider two tuples

$$(M_1; \dots; M_{n^0}; \dots; M_n; \text{or}_1) \quad \text{and} \quad (M_1^0; \dots; M_{n^0}^0; \dots; M_n^0; \text{or}_1^0); \quad (3.7)$$

where $M_k = (M_k; M_{k+1}; V_k; p_k; [k])$ and $M_k^0 = (M_k^0; M_{k+1}^0; V_k^0; p_k^0; [k])$. We assume that the numbering of boundary insertions is done such that either $p_k = p_k^0$ or $p_k = p_{n-k}^0$ (otherwise the numbering must be shifted appropriately).

Definition 3.3 :

The set of labels for the boundary component $b([1]; \dots; [n])$ is the set

$$B(b([1]; \dots; [n])) := \{M_1; \dots; M_{n^0}; \dots; M_n; \text{or}_1\} = \quad (3.8)$$

of equivalence classes with respect to the following equivalence relation : The two tuples (3.7) are equivalent if one of the following two conditions is satisfied:

(i) We have $\text{or}_1^0 = \text{or}_1$, $V_k^0 = V_k$, $p_k^0 = p_k$, $[k^0] = [k]$, and for $k = 1; \dots; n^0$ there exist isomorphism $s'_k \in \mathbb{2}\text{Hom}_A(M_k^0; M_k)$ such that

$$s'_k = \begin{pmatrix} & & 0 \\ & & k \\ & & (k^{-1} & \text{id}_{V_k}) \end{pmatrix}; \quad (3.9)$$

(ii) $\text{or}_1^0 = -\text{or}_1$, $V_k^0 = V_{n-k}$, $p_k^0 = p_{n-k}$, $[k^0] = [n-k]$, and for $k = 1; \dots; n^0$ there exist isomorphism $s'_k \in \mathbb{2}\text{Hom}_A(M_k^0; M_{n^0-k+1})$ such that

$$s'_k = \begin{cases} \begin{pmatrix} & & 0 \\ & & k \\ & & (k^{-1} & \text{id}_{V_k^0}) \end{pmatrix} & \text{if } \text{or}_1^0 = \text{or}([k^0]); \\ \begin{pmatrix} & & 0 \\ & & k \\ & & (k^{-1} & V_k^0) \end{pmatrix} & \text{if } \text{or}_1^0 = -\text{or}([k^0]); \end{cases} \quad (3.10)$$

where $\text{or}([k^0])$ denotes the local orientation of b induced by the arc-germ $[k^0]$.

Marked points on the double

Every boundary end insertion $= (M; N; V; p; [])$ on X gives rise to one marked point on the double \hat{X} . This marked point is given by

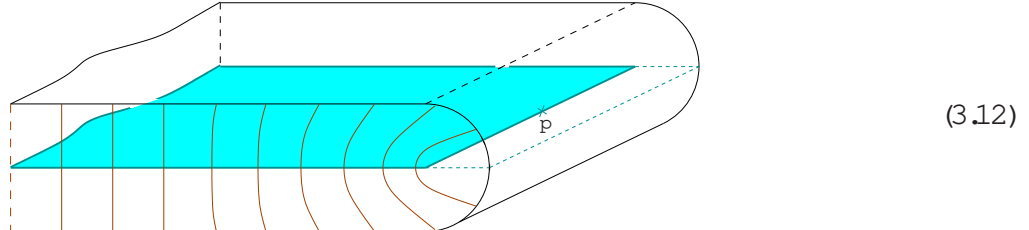
$$(p; [\sim]; V; +) \quad (3.11)$$

with $p = [p; \text{or}_2(p)]$. Recall from (1.1) that \hat{X} is the orientation bundle over X with the two orientations identified over the boundary ∂X . To obtain the germ $[\sim]$, first choose a representative of $[]$. Since $[]$ is aligned with ∂X at p , by definition there exists a $\epsilon > 0$ such that $:[\sim; \sim]! \partial X$. A representative $\sim : [\sim; \sim]! \hat{X}$ of $[\sim]$ is then given by $\sim(t) = [t(t); \text{or}_2]$.

Given a labelling $B \in B(b([1]; \dots; [n]))$, one can verify that the set of marked points on \hat{X} obtained in the way described above is indeed independent of the choice of representative of B .

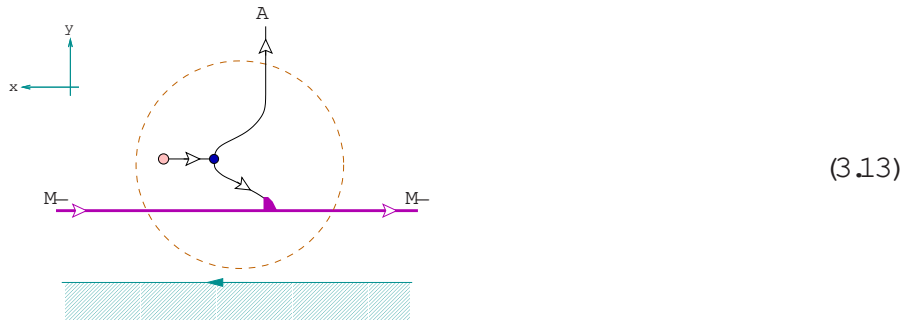
Ribbon graph embedded in the connecting manifold

Note that in a small neighbourhood of a point p on the boundary of the world sheet X , the connecting manifold M_X from (II.3.8) looks as follows:



Indicated are also the intervals $[1;1]$, which according to the identification rule of the general prescription degenerate into an interval $[0;1]$ above each boundary point. The ribbon graph representation of the boundary component $b([1]; \dots; [n])$ labelled by an equivalence class $B = [M_1; \dots; M_{n^0}; 1; \dots; n; \text{or}_1]$ in $B(b([1]; \dots; [n]))$ is now constructed as follows.

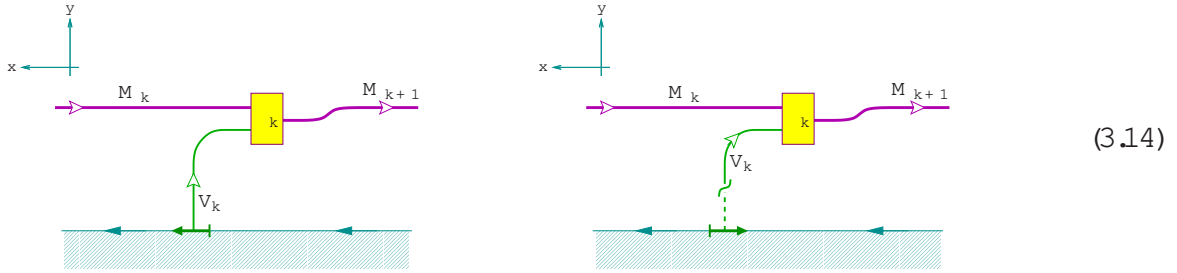
- Choose a representative $(M_1; \dots; M_{n^0}; 1; \dots; n; \text{or}_1)$ of the equivalence class B { Choice # 1 }.
- Choose a dual triangulation of X such that the insertion points of b lie on edges of the triangulation { Choice # 2 }.
- The orientation or_1 of the boundary circle b together with the inward pointing normal induces an orientation of its neighbourhood in the world sheet X . This fixes a local orientation of X close to b , which agrees with both the bulk and the boundary orientation of the upper half plane.
- At each vertex of the triangulation which lies on the boundary b place the element¹⁰



in such a way that the orientation of bulk and boundary agree with that around the vertex.

¹⁰ Note that the orientations in this picture are opposite to those in (II.3.12). This is due to the change in convention explained in section 3.1.

- At each insertion point $p_k = (M_k; M_{k+1}; V_k; p_k; [k])$ place one of the two elements

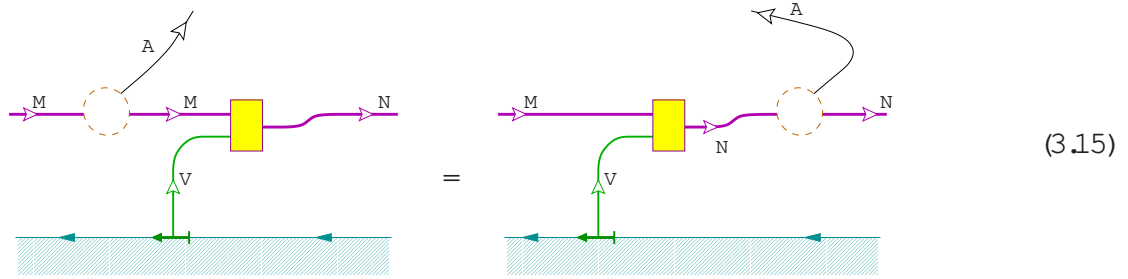


depending on the orientation of the arc-germ $[k]$ relative to that of the boundary (recall also the convention in (3.1)). Shown in (3.14) is a horizontal section of the connecting manifold (3.12). Correspondingly the lower boundary in (3.14) is that of M_x while the ribbons M_k and M_{k+1} are placed on the boundary of X as embedded in M_x . The arrow on the boundary in (3.14) indicates the orientation of ∂X (transported to ∂M_x along the preferred intervals). The ribbon graph must be placed in the plane of the world sheet X (embedded in M_x) in such a way that the bulk and boundary orientation of (3.14) agree with the local orientations at the insertion point $p_k \in X$.

The prescription involves two choices, and we proceed to show that different choices lead to equivalent ribbon graphs.

- Choice # 2:

As in sections I:5.1 and II:3.1, independence of the triangulation follows from the identities (I:5.11) and (I:5.12). However, if there are old insertions on the boundary we need an additional move to relate any one dual triangulation to any other dual triangulation. It consists of taking a vertex of the triangulation past a boundary insertion,



together with a similar identity for an insertion of (3.14b). The dashed circle in (3.15) represents the piece of ribbon graph inside the dashed circle in (3.13). This identity is a direct consequence of the fact that the morphism $\text{in} = (M; N; V; p; [])$ is an intertwiner of A -modules, $2\text{Hom}_A(M \otimes V; N)$.

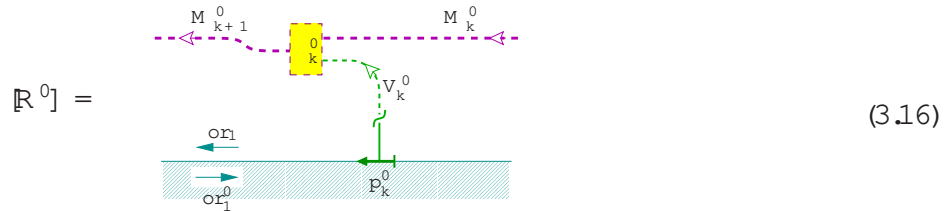
- Choice # 1:

Denote by $R = (M_1; \dots; M_n; \text{or}_1; \dots; \text{or}_n)$ and $R^0 = (M_1^0; \dots; M_n^0; \text{or}_1^0; \dots; \text{or}_n^0)$ two representatives of B . We will apply the above construction to the representative R^0 and show that the resulting ribbon graph can be turned into the one obtained from R . According to definition 3.3 we must consider two cases.

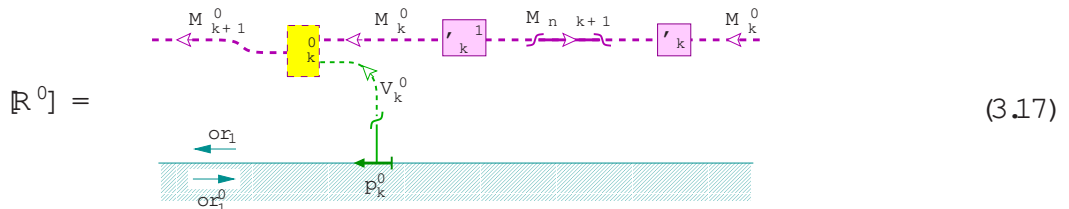
(i) $\text{or}_1^0 = \text{or}_1$. Then also $V_k^0 = V_k$, $p_k^0 = p_k$ and $[k]^0 = [k]$, and there exists a choice of isomorphisms $s_k \in 2\text{Hom}_A(M_k^0; M_k)$ fulfilling (3.9). Starting with the ribbon graph constructed from

R^0 , we insert on each ribbon M_k^0 the identity morphism in the form $\text{id}_{M_k^0} = '_{k+1} '_k$, in such a way that $'_{k+1}$ comes next to the $\text{eld insertion } '_{k+1}^0$. Then we move the morphism $'_k$ to the other end of the M_k^0 -ribbon. As in (II:3.17), $'_k$ can be taken past vertices of the triangulation, which may lie on the boundary interval labelled by M_k^0 . After these manipulations, every $\text{eld insertion } '_{k+1}^0$ comes with the morphism $'_{k+1}$ to one side and with $'_{k+1}$ to the other. In other words, for each k the morphism $'_{k+1}^0$ appearing in $'_{k+1}^0$ is replaced by $'_{k+1} '_{k+1}^0 ('_k '_{k+1}^0 \text{id}_{V_k})$. We thus remain with the ribbon graph constructed from R^0 .

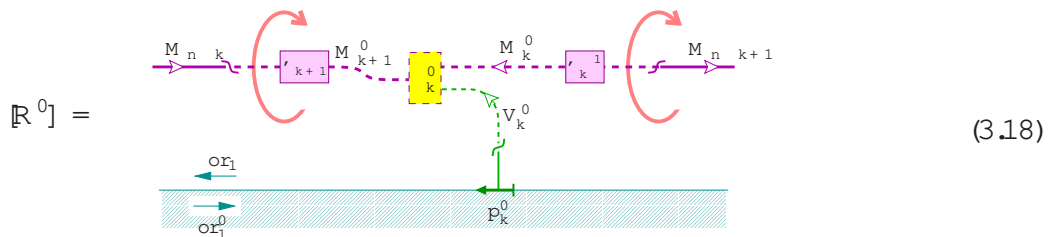
(ii) $\text{or}_1^0 = -\text{or}_1$. Then also $V_k^0 = V_{n-k}$, $p_k^0 = p_{n-k}$ and $[_{k+1}^0] = [_{n-k}]$, and there exist isomorphisms $'_k \text{Hom}_A(M_k^0; M_{n-k+1}^0)$, for $k = 1, \dots, n^0$, fulfilling (3.10). We shall demonstrate the equivalence of ribbon graphs in some detail for the second case in (3.10); the first case can be seen similarly. Around the $\text{eld insertion } '_{k+1}^0$ the ribbon graph obtained from R^0 , which we denote by $[R^0]$, looks as follows:



The two opposite orientations of the boundary are indicated. We are facing the black side of the ribbons because in order to make the local orientations of (3.16) induced by or_1^0 agree with those in (3.14b), the element (3.14b) must be turned 'upside down' before it is inserted. As in case (i) we insert $\text{id}_{M_1^0} = '_{1+1} '_1$ on each M_1^0 , close to $'_1^0$. After applying in addition a half-twist and using that, by definition, $M_- = M_-$ as an object, this leads to

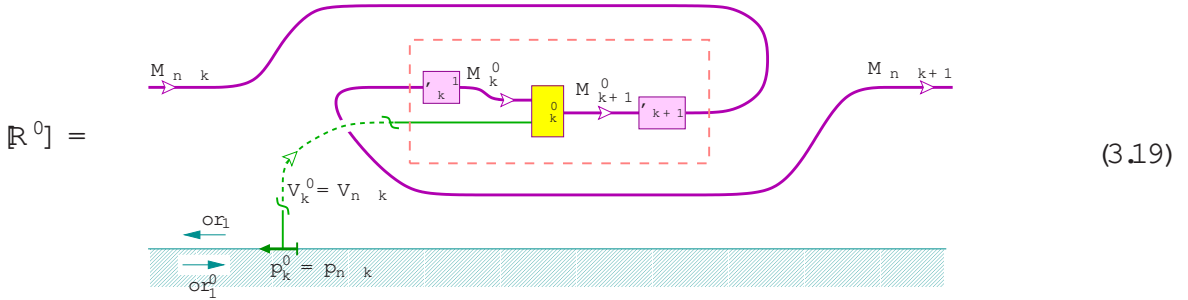


By a reasoning similar to that of (II:3.18) this specific combination of half-twist and $'_k$ can be taken past vertices of the triangulation that lie on the boundary, i.e. past locations at which A-ribbons arriving from the bulk are attached to the module-ribbons on the boundary. Taking all of the $'_1$ to the neighbouring eld insertion leads to a ribbon graph which close to $'_k^0$ looks as



The morphism $'_{k+1}^0$ has arrived from the insertion $'_{k+1}^0$ which is not visible in the section of the full ribbon graph $[R^0]$ that we display. Next rotate the coupons labelled by $'_{k+1}$, $'_k^0$ and

σ_k^{-1} by 180° in the manner already indicated in figure (3.18), and deform the resulting ribbon graph slightly,



By the second alternative in (3.10), the morphism in the dashed box is equal to $s_{(n-k)}$. After replacing the dashed box by the explicit form of $s_{(n-k)}$ in (3.6), the ribbon graph can be deformed so as to obtain the ribbon graph constructed from the representative R of B .

We have thus established that the ribbon graph that is obtained by our prescription for a boundary component $b([1]; \dots; [n])$ labelled by an equivalence class in $B(b([1]; \dots; [n]))$ is independent of the choices involved.

3.3 Bulk fields

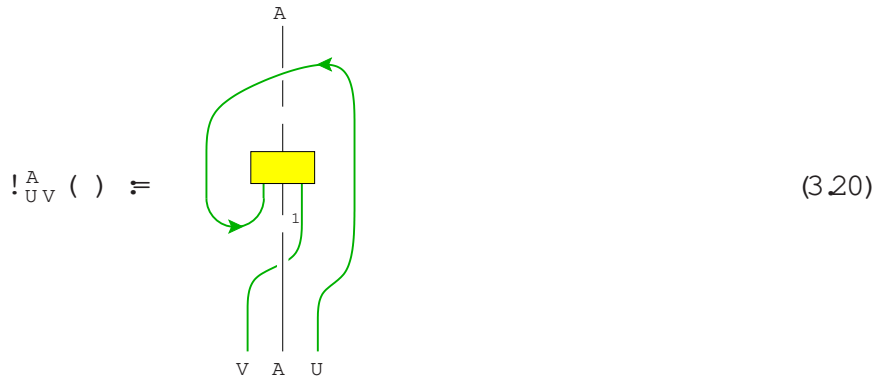
A bulk field insertion is described by a point p in the interior of X , together with an arc-germ $[]$ at p and a label $[]$. The set of labels for bulk insertions at $[]$ will be denoted by $D([])$. Similarly as for boundary fields, this set consists of equivalence classes of certain tuples.

Labelling of bulk fields

The equivalence relation will be formulated in terms of a linear map $!_{U,V}^A$ that is defined as follows.

Definition 3.4 :

For A a J-algebra in C , the morphism $!_{U,V}^A : \text{Hom}(U \otimes A \otimes V; A) \rightarrow \text{Hom}(V \otimes A \otimes U; A)$ is defined by



for $\text{Hom}(U \otimes A \otimes V; A)$.

Some properties of the map $!_{U,V}^A$ that will be needed below are listed in the following lemma.

Lemma 3.5 :

With A and $!_{UV}^A$ as in definition 3.4, we have:

- (i) For any $2\text{Hom}(U \otimes A \otimes V; A)$ one has $!_{VU}^A \circ !_{UV}^A(\cdot) = \cdot$.
- (ii) If $2\text{Hom}_{A\text{-}\mathcal{A}}(U \otimes A \otimes V; A)$, then $!_{UV}^A(\cdot) \in 2\text{Hom}_{A\text{-}\mathcal{A}}(V \otimes A \otimes U; A)$.

Proof:

(i) Writing out the ribbon graph for the morphism $!_{VU}^A \circ !_{UV}^A(\cdot)$ and using $\circ = \circ_A$, one can deform the resulting ribbon graph (which amounts to using that C is sovereign) so as to be left with the graph for \cdot .

(ii) One must verify that the morphism $!_{UV}^A(\cdot)$ commutes with the left and right action of A if it itself does. This can be done by a straightforward computation using the definitions (2.17) and (2.18) of the left and right action of A as well as the defining properties (II.2.6) of the reversion on A . X

Definition 3.6 :

Let $[\cdot]$ be an arc-germ around a point $p = (0)$ in the interior of X . The possible bulk fields that can be inserted at p are labelled by equivalence classes

$$D([\cdot]) = \{ (i; j; \cdot; p; [\cdot]; \text{or}_2(p)) = : \quad (3.21)$$

Here $i, j \in I$ label simple objects, \cdot is a morphism in $\text{Hom}_{A\text{-}\mathcal{A}}(U_i \otimes A \otimes U_j; A)$, the insertion point p is at (0) , and $\text{or}_2(p)$ is a local orientation of the world sheet X around at p . The equivalence relation is defined as

$$i; j; \cdot; p; [\cdot]; \text{or}_2(p) \sim j; i; !_{U_i U_j}^A(\cdot); p; [\cdot]; \text{or}_2(p) : \quad (3.22)$$

Marked points on the double

Each bulk field insertion $[\cdot]$ on the world sheet X gives rise to two marked points on the double \hat{X} . If $i; j; \cdot; p; [\cdot]; \text{or}_2(p)$ is a representative of $[\cdot]$, then these two points are

$$(p_i; \tilde{\gamma}_i; U_i; +) \quad \text{and} \quad (p_j; \tilde{\gamma}_j; U_j; +) ; \quad (3.23)$$

the terms appearing in these tuples are given by $p_i = [p; \text{or}_2(p)]$, $p_j = [p; \text{or}_2(p)]$, as well as $\tilde{\gamma}_i(t) = [\gamma_i(t); \text{or}_2(\gamma_i(t))]$ and $\tilde{\gamma}_j(t) = [\gamma_j(t); \text{or}_2(\gamma_j(t))]$. Here $\text{or}_2(\gamma_i(t))$ is obtained by the extension of $\text{or}_2(p)$ to a neighbourhood of p .

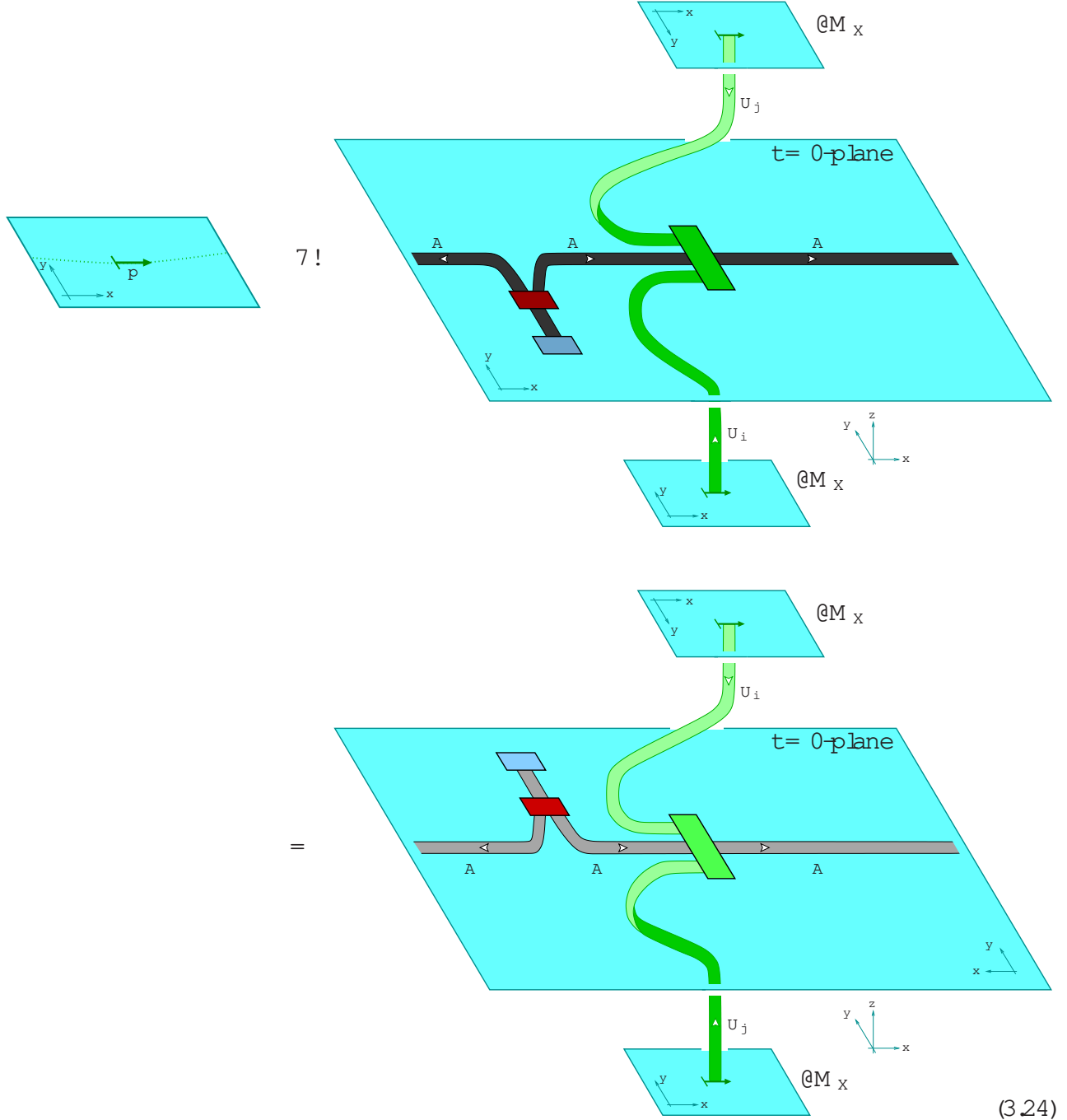
Just like in the case of boundary fields, one verifies that the marked points (3.23) on \hat{X} are independent of the choice of representative of $[\cdot]$.

Ribbon graph embedded in the connecting manifold

The ribbon graph representation of a bulk field $[\cdot]$ is constructed as follows.

- Choose a representative $(i; j; \cdot; p; [\cdot]; \text{or}_2(p))$ of $[\cdot]$ { Choice # 1 }.
- Choose a dual triangulation of X such that the insertion point p lies on an edge and such that the arc \cdot is aligned with this edge at $p = (0)$ { Choice # 2 }.

- The bulk insertion is treated as a two-valent vertex that is to be included in the dual triangulation. Locally around the insertion point p , the world sheet has the orientation or_2 . In M_X place the following ribbon graph:



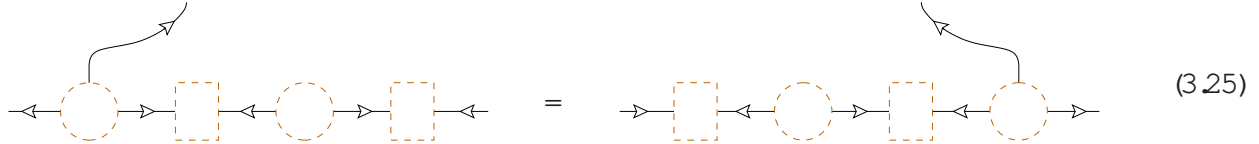
In this figure we display the ribbon graph twice, once looked upon from 'above' the connecting manifold and once looked at from 'below'. In any case, the orientation of the A-ribbons is opposite to that of the world sheet and their white side faces the insertion point of the chiral field label U_i . The ribbon graph (3.24) must be placed in M_X in such a manner that the embedding respects the orientation of the three-manifold M_X , the local orientation or_2 of the world sheet X , as well as the orientation of the arcs on the boundary of M_X . There is

precisely one way to do this; no further choice needs to be made.

We proceed to establish independence of the two choices.

■ Choice # 2:

Independence of the dual triangulation follows from the identities (I.5.11) together with a move that allows to take three-valent vertices of the triangulation past the two-valent vertex formed by the bulk field insertion



and together with similar identities for different local orientations and for situations where the A-ribbon arrives from the other side. The empty dashed circle in picture (3.25) stands for the element (II.3.11), the dashed rectangular box for (II.3.13), and the dashed circle with inscribed for the element (3.24). Analogously as for (I.5.11) and (I.5.12),¹¹ the equality follows in a straightforward way upon substituting the definitions and using that the morphism is an intertwiner of A-bimodules.

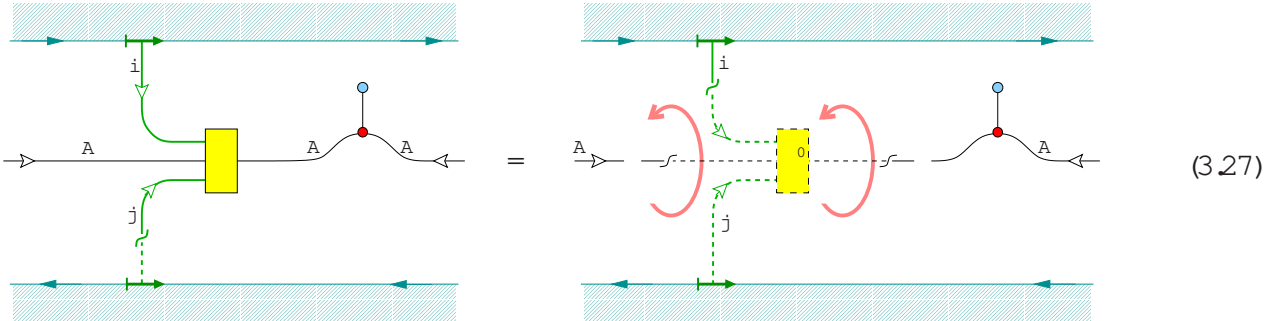
■ Choice # 1:

Let $(i; j; \mathbb{1}; p; [\mathbb{1}]; \text{or}_2)$ and $(j; i; \mathbb{0}; p; [\mathbb{1}]; \text{or}_2)$ be the two representatives of $[\mathbb{1}]$, i.e. we have $\mathbb{0} = !_{U_i U_j}^A(\mathbb{1})$. We must show that



The dashed boxes stand for (II.3.13) and (II.3.14), respectively, while the dashed circle with or inscribed stands for the element (3.24), inserted with the appropriate orientation.

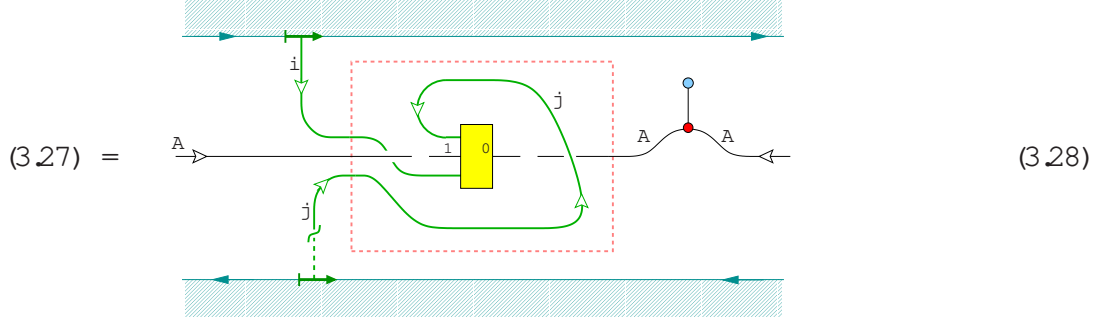
To facilitate drawing, let us rotate the middle plane of (3.24) into the paper plane and use the blackboard framing convention. Equation (3.26) then looks as follows.



In the right figure one must insert the element (3.24) 'upside down' because the local orientation of the world sheet is inverted with respect to the left figure. As compared to (3.26), on both sides of the equation one coproduct has been removed against one product using the Frobenius

¹¹ For detailed derivations, see [V].

property. In the right figure of (3.27) the central part of the ribbon graph can be rotated by 180° as indicated. Using also $U_A^{-1} = U_A^{-1}$ this leads to



Comparing with (3.20) we see that the part of the ribbon graph inside the dashed box amounts to the morphism

$$[\text{dashed box}] = !_{U_j U_i}^A ({}^0) = ; \quad (3.29)$$

where the last equality follows from the equivalence relation for bulk labels which forces ${}^0 = !_{U_i U_j}^A ({}^0)$, together with lemma 3.5. Thus (3.28) is equal to the left hand side of (3.27), establishing the claimed equality between the left hand side and the right hand side of (3.27).

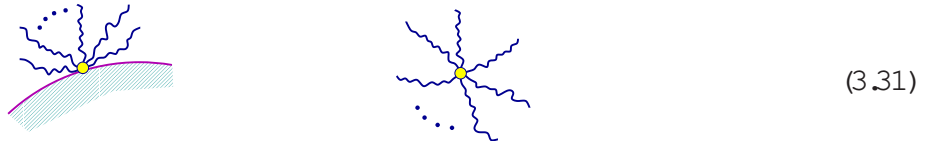
This finishes the demonstration that the ribbon graph for a bulk field insertion is independent of the choices involved in its construction.

3.4 Defect fields

Together with the defect fields treated in this section, the three types of fields we consider are



Note, however, that this is not the most general way to treat defects. In fact, upon forming operator products, the first two kinds of fields in (3.30) close amongst each other. But once we include also the defect field, we can generate the following more general class of fields by taking operator products,



i.e. a boundary field with several defect lines attached and a defect field with more than two defect lines ending on it. For example, a field of the first kind can be obtained by taking the operator product of a boundary field and a defect field of the types listed in (3.30). While fields of the type (3.31) and their operator products can be treated in the TFT-formalism in a natural way, in this paper we will nonetheless only consider fields of the types (3.30).

Labelling of defect elds

Recall from section II:3.8 that a circular defect d without eld insertions and with orientable neighbourhood is labelled by equivalence classes of triples $[X; \text{or}_1; \text{or}_2]$, where X is an A -bimodule, or_1 is an orientation of the defect circle and or_2 is an orientation of its neighbourhood. The equivalence relation is given in (II:3.150).

In order to describe the labelling of a defect circle with eld insertions $d([1]; \dots; [n])$ we first need the following definition.

Definition 3.7 :

The linear maps

$$\begin{aligned} u : \text{Hom}(U_i \otimes X \otimes U_j; Y) &\rightarrow \text{Hom}(U_j \otimes X \otimes U_i; Y) \\ \alpha : \text{Hom}(U_i \otimes X \otimes U_j; Y) &\rightarrow \text{Hom}(U_i \otimes Y \otimes U_j; X) \end{aligned} \quad (3.32)$$

are defined by

$$\begin{aligned} u(\#) &= \text{Diagram showing a green loop with a yellow box labeled '#'. The loop is attached to a vertical blue line labeled 'Y' at the top. The blue line is labeled 'U_j' at the bottom left and 'U_i' at the bottom right. The green loop is labeled 'X' at the bottom center.} \\ \text{and} \quad \alpha(\#) &= \text{Diagram showing a blue line labeled 'X' at the top. The line is labeled 'U_i' at the bottom left and 'U_j' at the bottom right. A green loop with a yellow box labeled '#' is attached to the blue line.} \end{aligned} \quad (3.33)$$

for $\# \in \text{Hom}(U_i \otimes X \otimes U_j; Y)$.

The maps u and α will enter into the formulation of the equivalence relation for defect labels. This also requires the following lemma, which can be verified by direct calculation.

Lemma 3.8 :

Let A be an algebra and let $X; Y$ be A -bimodules. Then α restricts to an isomorphism

$$\alpha : \text{Hom}_{A \otimes A}(U_i \otimes X \otimes U_j; Y) \rightarrow \text{Hom}_{A \otimes A}(U_i \otimes Y \otimes U_j; X) : \quad (3.34)$$

If A is a Jandl algebra, then in addition u restricts to an isomorphism

$$u : \text{Hom}_{A \otimes A}(U_i \otimes X \otimes U_j; Y) \rightarrow \text{Hom}_{A \otimes A}(U_j \otimes X^s \otimes U_i; Y^s) : \quad (3.35)$$

Here $X^s; Y^s$ and $X^s; Y^s$ denote two of the three duals one has for the bimodules $X; Y$, as defined in (II:2.40).

After these preliminaries we turn to the description of defect labels. Let A be a Jandl algebra. A defect eld is a collection of data

$$= X; \text{or}_2(X); Y; \text{or}_2(Y); i; j; \#; p; []; \text{or}_2(p) : \quad (3.36)$$

Here $i, j \in I$, X, Y are A -bundles, and $or_2(X)$ and $or_2(Y)$ are local orientations of the world sheet on a neighbourhood of the defect line labelled by X and Y , respectively; $\#$ is a morphism

$$\# : \text{Hom}_{A\text{-}\mathcal{A}}(U_i \rightarrow U_j; Z^0); \quad (3.37)$$

where

$$Z = \begin{cases} X & \text{if } or_2(X) = or_2(p); \\ X^s & \text{if } or_2(X) = -or_2(p) \end{cases} \quad \text{and} \quad Z^0 = \begin{cases} Y & \text{if } or_2(Y) = or_2(p); \\ Y^s & \text{if } or_2(Y) = -or_2(p); \end{cases} \quad (3.38)$$

Finally $p = (0)$ is the insertion point of the defect eld , and $[\cdot]$ is a germ of arcs aligned with the defect line at p .

A defect circle $d([1]; \dots; [n])$ on the world sheet is labelled by equivalence classes of tuples

$$X_1; or_2(X_1); \dots; X_{n^0}; or_2(X_{n^0}); \dots; [1]; \dots; [n]; or_1(d); \quad (3.39)$$

subject to the following conditions.

- $or_1(d)$ is an orientation of the defect circle d .
- The points $p_k = [k](0)$ are ordered such that when passing along the defect circle d in the direction opposite to $or_1(d)$, one passes from p_k to p_{k+1} . Here and below it is understood that $p_0 = p_n$ and $p_{n+1} = p_1$, and similarly for X_k and $[k]$.
- The $X_1; \dots; X_{n^0}$ are A -bundles. X_k labels the defect interval between p_{k-1} and p_k . Thus if there are no eld insertions, then $n^0 = 1$, and otherwise $n^0 = n$.
- $or_2(X_k)$ a local orientation¹² of the world sheet on a neighbourhood of the defect interval between p_{k-1} and p_k .
- $[k]$ is a defect eld with defining data

$$[k] = X_k; or_2(X_k); X_{k+1}; or_2(X_{k+1}); i_k; j_k; \#_k; p_k; [k]; or_2(p_k); \quad (3.40)$$

Because of the large number of orientations entering the labelling of a defect circle, the equivalence relation on the tuples (3.39) becomes somewhat technical; we include it merely for completeness of the presentation.

The relation is conveniently formulated in terms of five basic relations. The full equivalence class is obtained by completing the relations generated by the basic relations with respect to transitivity and reflexivity. Consider the two tuples

$$\begin{aligned} T &= X_1; or_2(X_1); \dots; X_{n^0}; or_2(X_{n^0}); \dots; [1]; \dots; [n]; or_1(d); \\ T^0 &= X_1^0; or_2^0(X_1^0); \dots; X_{n^0}^0; or_2^0(X_{n^0}^0); \dots; [1]^0; \dots; [n]^0; or_1^0(d); \end{aligned} \quad (3.41)$$

The basic relations are:

¹² If the neighbourhood of the whole defect circle is non-orientable we require that there is at least one eld insertion. This eld insertion can transform like an identity eld , though, in which case correlators are independent of the insertion point of this eld (recall the corresponding discussion in the second half of section II.3.8).

■ Relation 1: Shift of labels.

The tuples T and T^0 are equivalent if their data are related by $or_1^0(d) = or_1(d)$ and, for every k , $X_k^0 = X_{k+1}$, $or_2^0(X_k^0) = or_2(X_{k+1})$ and $i_k^0 = i_{k+1}$.

■ Relation 2: Reverse orientation of the defect circle, $or_1^0(d) = or_1(d)$.

Suppose $or_1^0(d) = or_1(d)$. Then T and T^0 are equivalent if the following conditions hold. First, the ordering of the points is reversed in both labellings, $[k^0] = [n_k]$. Second, the bimodules labelling the defect intervals are related by $X_k = (X_{n-k+1}^0)^v$. Finally, the defect elds i_k are related to the elds

$$i_k^0 = X_n^0; or_2^0(X_n^0); X_{n-k+1}^0; or_2^0(X_{n-k+1}^0); i_k^0; j_k^0; \#_k^0; p_k^0; [k^0]; or_2^0(p_k^0) \quad (3.42)$$

via

$$i_k^0 = (X_{n-k+1}^0)^v; or_2^0(X_{n-k+1}^0); (X_{n-k}^0)^v; or_2^0(X_{n-k}^0); \\ i_{n-k}^0; j_{n-k}^0; \sim \alpha(\#_{n-k}^0) (\sim); p_{n-k}^0; [n-k]; or_2^0(p_{n-k}^0); \quad (3.43)$$

where α is the map defined in (3.33), and

$$\begin{aligned} & \stackrel{8}{\sim} \stackrel{8}{=} \stackrel{8}{\sim} \\ & \stackrel{8}{\sim} \stackrel{8}{=} \stackrel{8}{\sim} \stackrel{8}{=} \stackrel{8}{\sim} \end{aligned} \quad (3.44)$$

For the next relations, select any $k_0 \in \{1, 2, \dots, n\}$.

■ Relation 3: Isomorphism of bimodules, $X_{k_0}^0 = X_{k_0}$.

The tuples T and T^0 are equivalent if all data of T^0 coincide with the corresponding data of T , possibly with the exception of $X_{k_0}^0$, $i_{k_0}^0$ and $\#_{k_0}^0$. In the latter case we require the existence of an isomorphism $\iota \in \text{Hom}_{\mathcal{A}}(X_{k_0}^0; X_{k_0})$ such that

$$\#_{k_0-1}^0 = \iota^{-1} \#_{k_0-1} \quad \text{and} \quad \#_{k_0}^0 = \#_{k_0} (\text{id}_{i_{k_0}} \circ \iota \circ \text{id}_{j_{k_0}}); \quad (3.45)$$

where $\#^0$ and $\#$ are the morphisms in the defining data of T^0 and T .

■ Relation 4: Reverse orientation at a field insertion, $or_2^0(p_{k_0}) = or_2(p_{k_0})$.

The tuples T and T^0 are equivalent if all data of T^0 and T agree, with the exception of $i_{k_0}^0$, for which it is instead required that if

$$i_{k_0}^0 = X_{k_0}; or_2(X_{k_0}); X_{k_0+1}; or_2(X_{k_0+1}); i_{k_0}; j_{k_0}; \#_{k_0}; p_{k_0}; [k_0]; or_2(p_{k_0}); \quad (3.46)$$

then $i_{k_0}^0$ is given by

$$i_{k_0}^0 = X_{k_0}; or_2(X_{k_0}); X_{k_0+1}; or_2(X_{k_0+1}); \\ j_{k_0}; i_{k_0}; \sim u(\#_{k_0}) (\sim); p_{k_0}; [k_0]; or_2(p_{k_0}); \quad (3.47)$$

where u is the map defined in (3.33), and

$$\begin{aligned}
 &= \begin{cases} u_{j_{k_0}}^1 & \text{if } \text{or}_1(x_{k_0}) = \text{or}_1(d); \\ \text{id}_{U_{j_{k_0}}} & \text{if } \text{or}_1(x_{k_0}) = \text{or}_1(d); \end{cases} & = \begin{cases} \text{id}_{X_{k_0}} & \text{if } \text{or}_2(p_{k_0}) = \text{or}_2(x_{k_0}); \\ x_{k_0} & \text{if } \text{or}_2(p_{k_0}) = \text{or}_2(x_{k_0}); \end{cases} \\
 &\sim = \begin{cases} u_{i_{k_0}}^1 & \text{if } \text{or}_1(x_{k_0}) = \text{or}_1(d); \\ \text{id}_{U_{i_{k_0}}} & \text{if } \text{or}_1(x_{k_0}) = \text{or}_1(d); \end{cases} & \sim = \begin{cases} \text{id}_{X_{k_0+1}} & \text{if } \text{or}_2(p_{k_0}) = \text{or}_2(x_{k_0+1}); \\ x_{k_0+1}^1 & \text{if } \text{or}_2(p_{k_0}) = \text{or}_2(x_{k_0+1}); \end{cases} \quad (3.48)
 \end{aligned}$$

■ Relation 5: Reverse orientation at a defect segment, $\text{or}_2^0(x_{k_0}^0) = -\text{or}_2(x_{k_0})$.

The tuples T and T^0 are equivalent if all data of T^0 and T agree, with the exception of X_{k_0} and $\text{or}_2(x_{k_0})$, as well as x_{k_0-1} and x_{k_0} . For the latter we demand

$$(x_{k_0}^0)^s = x_{k_0} \quad \text{and} \quad \text{or}_2^0(x_{k_0}^0) = -\text{or}_2(x_{k_0}); \quad (3.49)$$

as well as

$$\begin{aligned}
 x_{k_0-1} &= x_{k_0-1}^0; \text{or}_2^0(x_{k_0-1}^0); (x_{k_0}^0)^s; \text{or}_2^0(x_{k_0}^0); \\
 &\quad i_{k_0-1}^0; j_{k_0-1}^0; \sim \#_{k_0-1}^0; p_{k_0-1}^0; [x_{k_0-1}^0]; \text{or}_2^0(p_{k_0-1}^0); \\
 x_{k_0} &= (x_{k_0}^0)^s; \text{or}_2^0(x_{k_0}^0); x_{k_0+1}^0; \text{or}_2^0(x_{k_0+1}^0); \\
 &\quad i_{k_0}^0; j_{k_0}^0; \#_{k_0}^0; (\text{id}_{U_{i_{k_0}^0}}; \text{id}_{U_{j_{k_0}^0}}); p_{k_0}^0; [x_{k_0}^0]; \text{or}_2^0(p_{k_0}^0); \quad (3.50)
 \end{aligned}$$

where

$$= \begin{cases} \text{id}_{X_{k_0}^0} & \text{if } \text{or}_2(p_{k_0}) = \text{or}_2(x_{k_0}); \\ x_{k_0}^0 & \text{if } \text{or}_2(p_{k_0}) = -\text{or}_2(x_{k_0}); \end{cases} \quad \sim = \begin{cases} \text{id}_{X_{k_0-1}^0} & \text{if } \text{or}_2(p_{k_0-1}) = \text{or}_2(x_{k_0}); \\ x_{k_0-1}^0 & \text{if } \text{or}_2(p_{k_0-1}) = -\text{or}_2(x_{k_0}); \end{cases} \quad (3.51)$$

The set of labels for the defect circle $d([1]; \dots; [n])$ is given by the equivalence classes

$$D(d([1]; \dots; [n])) = X_1; \text{or}_2(x_1); \dots; X_n; \text{or}_2(x_n); \sim_1; \dots; \sim_n; \text{or}_1(d) = ; \quad (3.52)$$

where \sim is the equivalence relation generated by the five basic relations given above.

Marked points on the double

For a defect insertion on the world sheet X the marked points on the double \hat{X} are the same as for bulk fields. Each insertion

$$= X; \text{or}_2(x); Y; \text{or}_2(y); i; j; \#; p; []; \text{or}_2(p) \quad (3.53)$$

on the world sheet X gives rise to two marked points

$$(p_i; \sim_i; U_i; +) \quad \text{and} \quad (p_j; \sim_j; U_j; +) \quad (3.54)$$

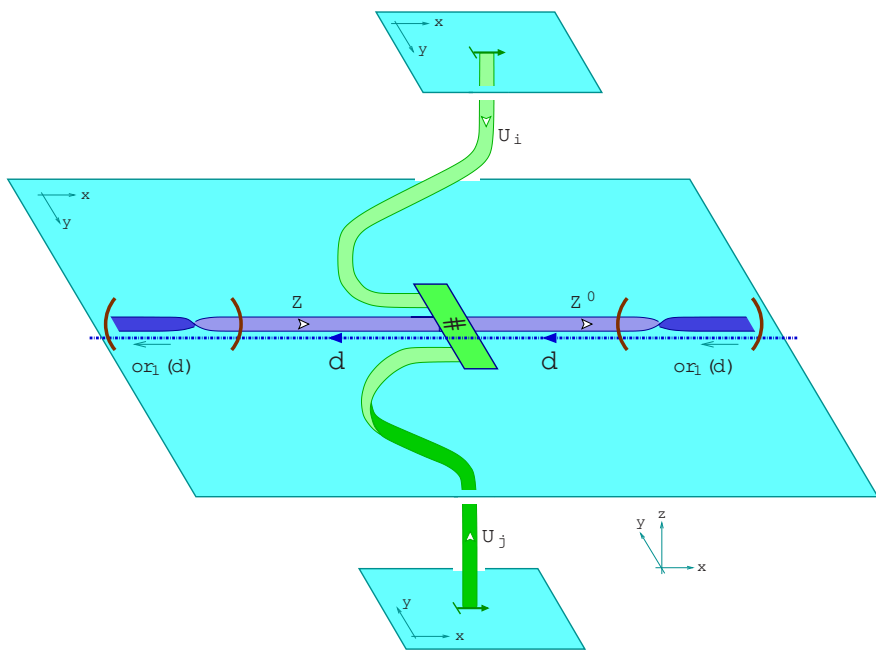
on the double \hat{X} . Here again $p_i = [p; \text{or}_2(p)]$, $p_j = [p; -\text{or}_2(p)]$, as well as $\sim_i(t) = [t; \text{or}_2(-t)]$ and $\sim_j(t) = [t; \text{or}_2(t)]$.

Ribbon graph embedded in the connecting manifold

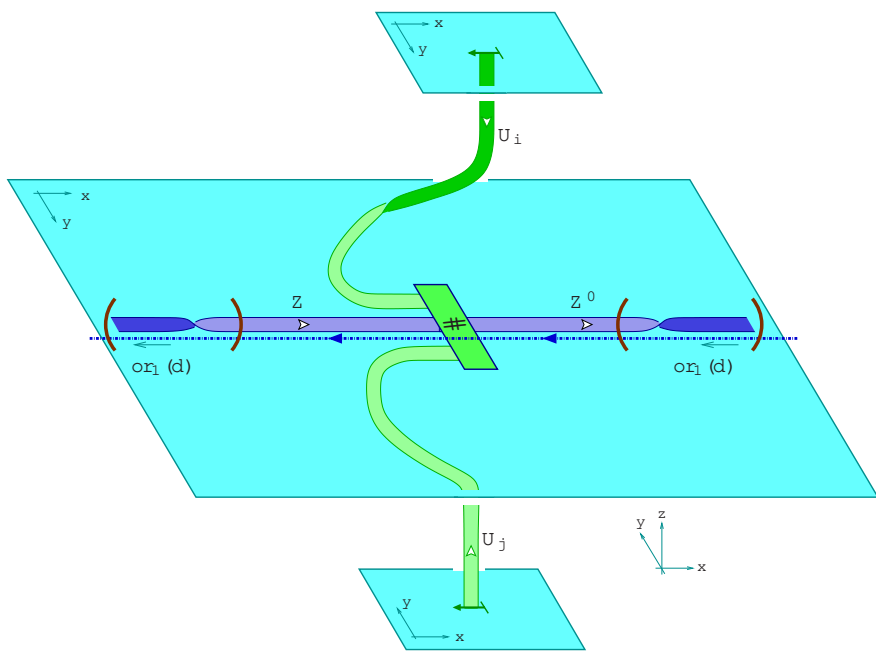
The ribbon graph representation of a defect circle $d([1]; \dots; [n])$ labelled by an equivalence class $D \in \mathcal{D}(d([1]; \dots; [n]))$ is constructed as follows.

- Choose a representative $X_1; \text{or}_2(X_1); \dots; X_n; \text{or}_2(X_n); [1]; \dots; [n]; \text{or}_1(d)$ of D { Choice # 1 }.
- Choose a dual triangulation of X which contains the defect circle as a subset, such that each defect insertion lies on an edge of the dual triangulation { Choice # 2 }.
- At each insertion of a defect $\text{eld} = X_i; \text{or}_2(X_i); Y_i; \text{or}_2(Y_i); i; j; \#; p; []; \text{or}_2(p)$ place { depending on the various orientations { one of the following eight ribbon graphs:

Cases (1) { (4) :



Cases (5) { (8) :



(3.55)

Here in all cases the coupon labelled by $\#$ is placed in such a way that its orientation is opposite to $\text{or}_2(p)$. The bimodule ribbons are always placed such that the orientation of their cores is opposite to $\text{or}_1(d)$. The bimodules Z and Z^0 are related to X and Y as in (3.38). In cases (1) { (4) the orientation of the arc-germ $[\cdot]$ is equal to $\text{or}_1(d)$. Those parts of the ribbon graphs that we have put in brackets are to be inserted only if $\text{or}_2(X) = \text{or}_2(p)$ and $\text{or}_2(Y) = \text{or}_2(p)$, respectively. In cases (5) { (8) the orientation of the arc-germ $[\cdot]$ is equal to $+\text{or}_1(d)$; the parts of the ribbon graph in brackets are to be understood in the same way as in cases (1) { (4).

We only briefly sketch how to establish independence of these choices.

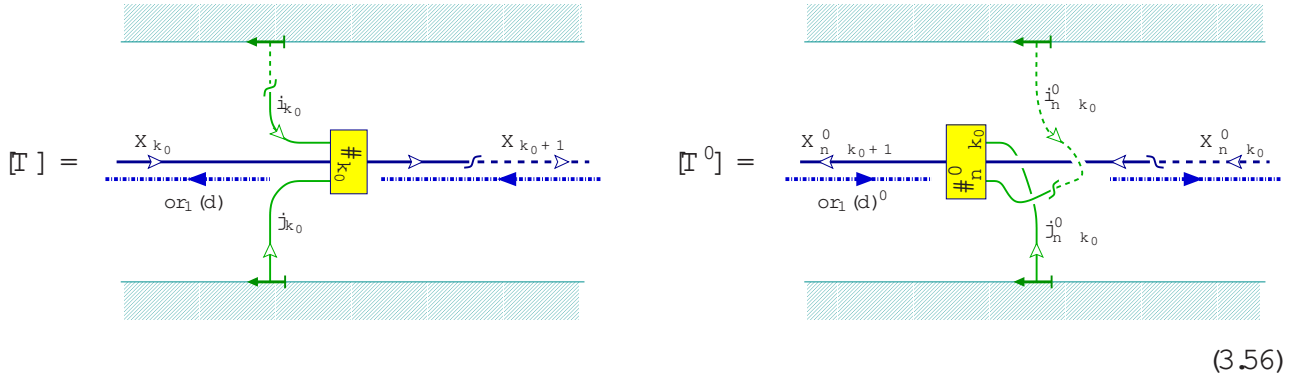
■ Choices # 2:

As for bulk fields the fact that the morphism $\#$ in a defect field is an intertwiner of A -bimodules allows one to move vertices of the dual triangulation past insertion points of defect fields.

■ Choice # 1:

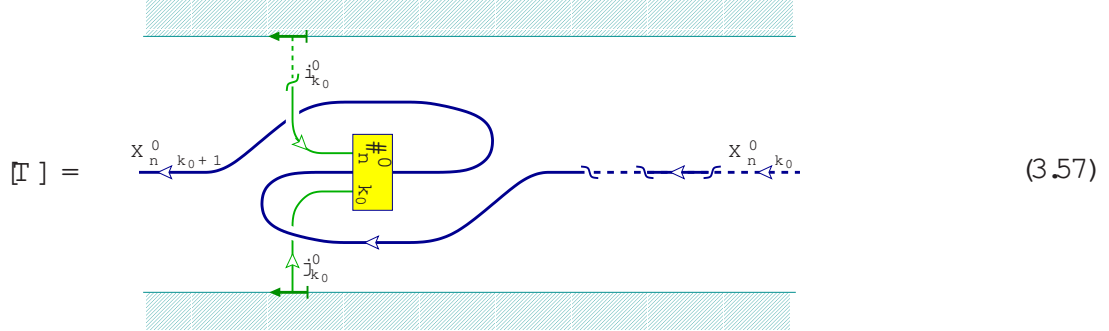
Suppose T and T^0 are two representatives of the equivalence class D labelling the defect circle. We have to establish that if T and T^0 are linked by one of the five basic relations above, then the construction leads to equivalent ribbon graphs. This can be done by straightforward, though tedious, computations. We refrain from presenting them in any detail, except for the example that T and T^0 are linked by relation 2.

If T and T^0 are linked by relation 2, then in particular $p_k = p_{n-k}$. Select a point $p = p_{k_0} = p_{n-k_0}$ and consider only the fragment of the ribbon graph for T and T^0 close to p . Suppose further that $\text{or}_1(p_{k_0}) = \text{or}_1(d)$, $\text{or}_2(p_{k_0}) = \text{or}_2(X_{k_0})$ and $\text{or}_2(p_{k_0}) = -\text{or}_2(X_{k_0+1})$. The other instances of relation 2 follow by similar considerations. Denote the fragments close to p by $[\Gamma]$ and $[\Gamma^0]$. Applying the construction above gives



Here we displayed the graphs (3.55) using blackboard framing. The upper and lower boundary in these figures represent the upper and lower boundary of the connecting manifold M_X . According to (3.43) in the graph $[\Gamma]$ we should substitute $X_{k_0} = (X_{n-k_0+1}^0)^v$, $X_{k_0+1} = (X_{n-k_0}^0)^v$,

$i_{k_0} = i_{n-k_0}^0$, $j_{k_0} = j_{n-k_0}^0$ and $\#_{k_0} = \alpha_{n-k_0}^0 - \alpha_{k_0}^0$. This results in



One can now verify that this ribbon graph fragment can be deformed into $[T^0]$ in (3.56).

4 Ribbon graphs for structure constants

The correlation function for an arbitrary world sheet X , which may have boundaries and field insertions, and which may or may not be orientable, can be computed by cutting X into smaller pieces and summing over intermediate states. This procedure is known as 'sewing'. In principle, every correlator can be obtained in this way from a small number of basic building blocks, namely the correlators of

- | three boundary fields on the disk;
- | one bulk field and one boundary field on the disk;
- | three bulk fields on the sphere;
- | one bulk field on the cross cap.

(The last of these is only needed if non-orientable world sheets are admitted.) Some correlators involving defect fields will be presented as well, namely

- | three defect fields on the sphere;
- | one defect field on the cross cap.

However, recall from the discussion in section 3.4 that this does not correspond to the most general way to treat defects. When cutting a world sheet involving defect lines into smaller pieces, one is forced to also consider fields of the type (3.31), which we will not do in this paper.

The aim of this and the next two sections is to derive expressions for the building blocks listed above in the form

$$(\text{correlator}) = (\text{const}) \quad (\text{conformal block}): \quad (4.1)$$

The constants appearing here, to be referred to as structure constants, will be obtained in sections 4.2 { 4.7 as ribbon invariants in the 3-d TFT. The conformal blocks are then introduced in section 5, and finally the connection to correlation functions is made in section 6.

Since a given world sheet X can be reduced to the fundamental building blocks in several different ways, the latter must fulfill a set of consistency conditions, the so-called sewing or

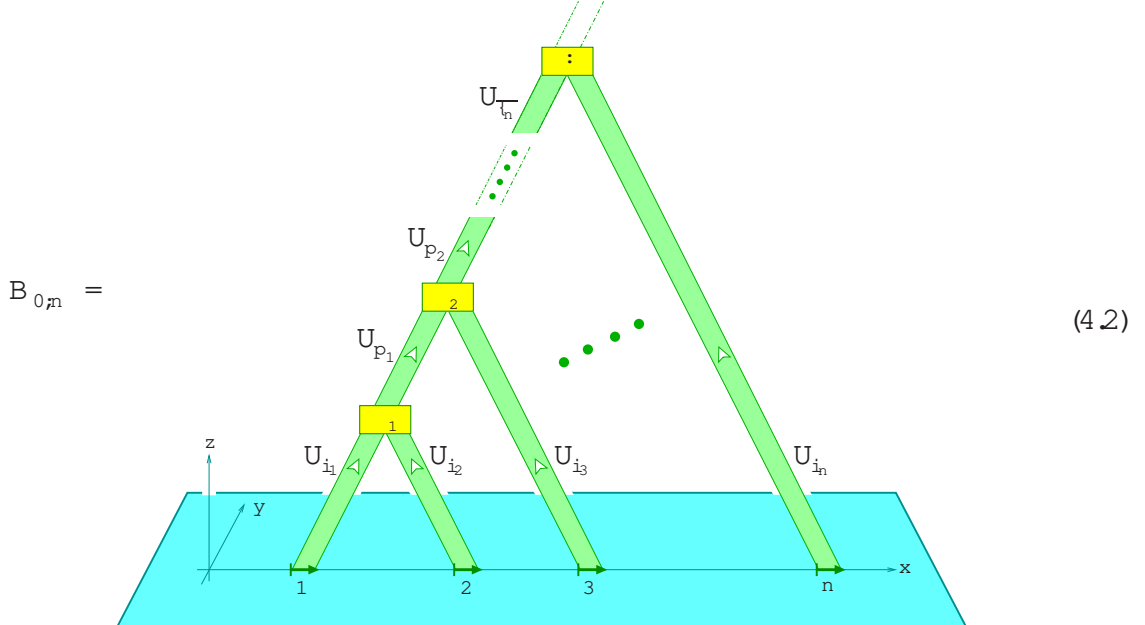
factorisation constraints [44, 5, 45, 13, 6, 7, 22]. The correlators computed in the TFT approach satisfy these constraints by construction [4, V].

When giving the correlators on the disk and on the sphere in sections 4.2 { 4.5, we will fix a (bulk and boundary) orientation for the world sheet from the start. In this way the expressions we obtain are valid for oriented CFTs as well. In the unoriented case we can change the orientation without affecting the result for the correlator, by using the equivalence relations of section 3.

4.1 Standard bases of conformal blocks on the sphere

Let the world sheet X be one of the building blocks listed above. To compute the constants in (4.1) we first construct the ribbon graph representation in M_X of the correlator on X according to the rules given in section 3. The TFT assigns to M_X an element $C(X)$ in the space $H(\hat{X})$ of blocks on the double \hat{X} . In the cases considered here, \hat{X} is either the sphere S^2 or the disjoint union $S^2 \sqcup (-S^2)$. The constants are the coefficients occurring in the expansion of $C(X)$ in a standard basis of blocks in $H(\hat{X})$. In the present section we describe our convention for the standard basis in $H(S^2)$. In section 5 this basis will be related to products of chiral vertex operators.

Take the sphere S^2 to be parametrised as R^2 [f1 g. Define the standard extended surface $E_{0,n} [i_1; \dots; i_n]$ to be R^2 [f1 g with the standard orientation, together with the marked points $f((k,0); [k]; U_{i_k}; +)$ $jk = 1, \dots, n$ and $i_k(t) = (k+t,0)$. If it is clear from the context what representations occur at the marked points, we use the shorthand notation $E_{0,n}$ for $E_{0,n} [i_1; \dots; i_n]$. Let the cobordism $B_{0,n} = B_{0,n} [i_1; \dots; i_n; p_1; \dots; p_{n-3}; 1; \dots; n-2]$ be given by the three-manifold $f(x; y; z) \in R^3$ [f1 g together with the ribbon graph

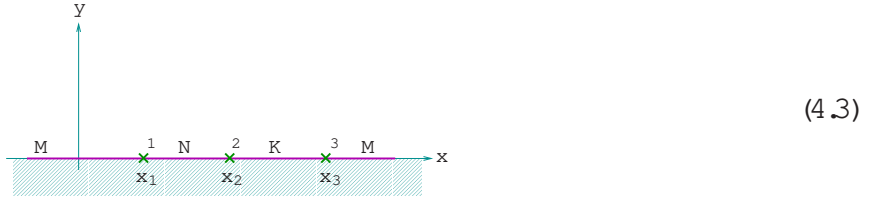


where the i_m label the basis elements (I.2.29) in the spaces of three-point couplings. For example $i_1 = 1, \dots, N_{i_2 i_1 p_1}$ labels the basis of $H_{0,n} (U_{i_2} \sqcup U_{i_1}; U_{p_1})$. Note that in (4.2) all ribbons are oriented in such a way that their black side is facing the reader. The linear map

$Z(B_{0,n};;E_{0,n}) : \mathbb{C}! H(E_{0,n})$, applied to $12 \mathbb{C}$, and with all possible choices of the labels p_1, \dots, p_n and $1, \dots, n$, gives the standard basis in the space $H(E_{0,n})$. For a proof that this is indeed a basis, see e.g. lemma 2.1.3 in chapter IV of [19] or section 4.4 of [20]. Situations in which the insertion points are at different positions or in which the arcs are oriented in a different way can be obtained from (4.2) by continuous deformation.

4.2 Boundary three-point function on the disk

Consider the correlator of three boundary fields on a disk. For future convenience we regard the disk as the upper halfplane plus a point. What is shown in the picture below is a piece of the upper halfplane:

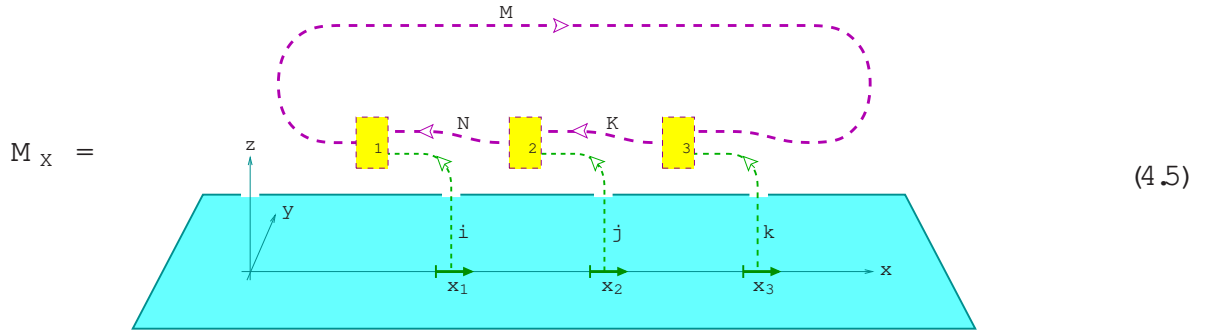


On the world sheet we choose the standard orientation for bulk and boundary, as indicated. The three boundary fields are given by

$$\begin{aligned} \mathbf{1} &= (N; M; U_i; \mathbf{1}; x_1; [\mathbf{1}]); & \mathbf{2} &= (K; N; U_j; \mathbf{2}; x_2; [\mathbf{2}]); \\ \mathbf{3} &= (M; K; U_k; \mathbf{3}; x_3; [\mathbf{3}]); \end{aligned} \quad (4.4)$$

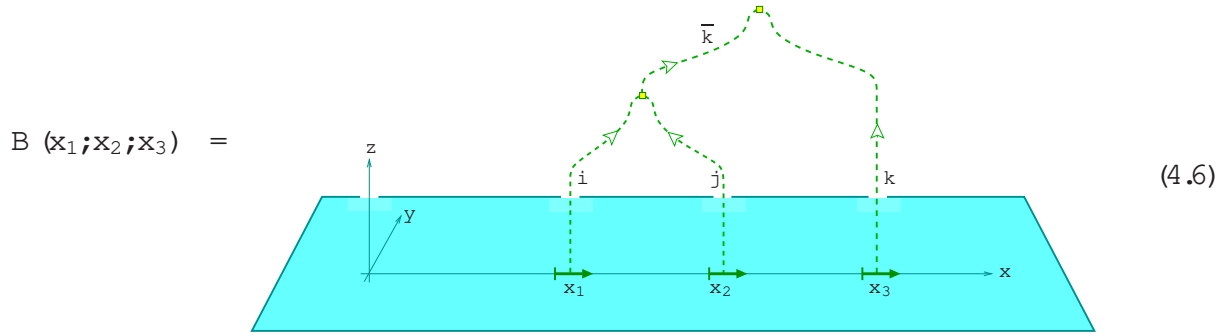
Here the coordinates of the insertion points satisfy $0 < x_1 < x_2 < x_3$, and the arc germs $[\cdot]$ at these points are given by $\gamma(t) = (x_i + t; 0)$ for $i = 1, 2, 3$. Further, U_i, U_j, U_k are simple objects, while M, N, K are left A -modules.

Following the procedure for boundary fields described in section 3.2, one finds that the correlator is determined by the cobordism



In more detail, this cobordism is obtained as follows. First note that in the situation at hand any A -ribbons resulting from a dual triangulation of the world sheet X can be eliminated by repeatedly using the moves (I.5.11) and (I.5.12). Thus only the module ribbons with the field insertions as in figure (3.14) remain. As explained in section 3.1, all ribbons are inserted with orientation opposite to that of the world sheet. Also note that the three-manifold displayed in (4.5) is topologically equivalent to the one indicated in (3.12).

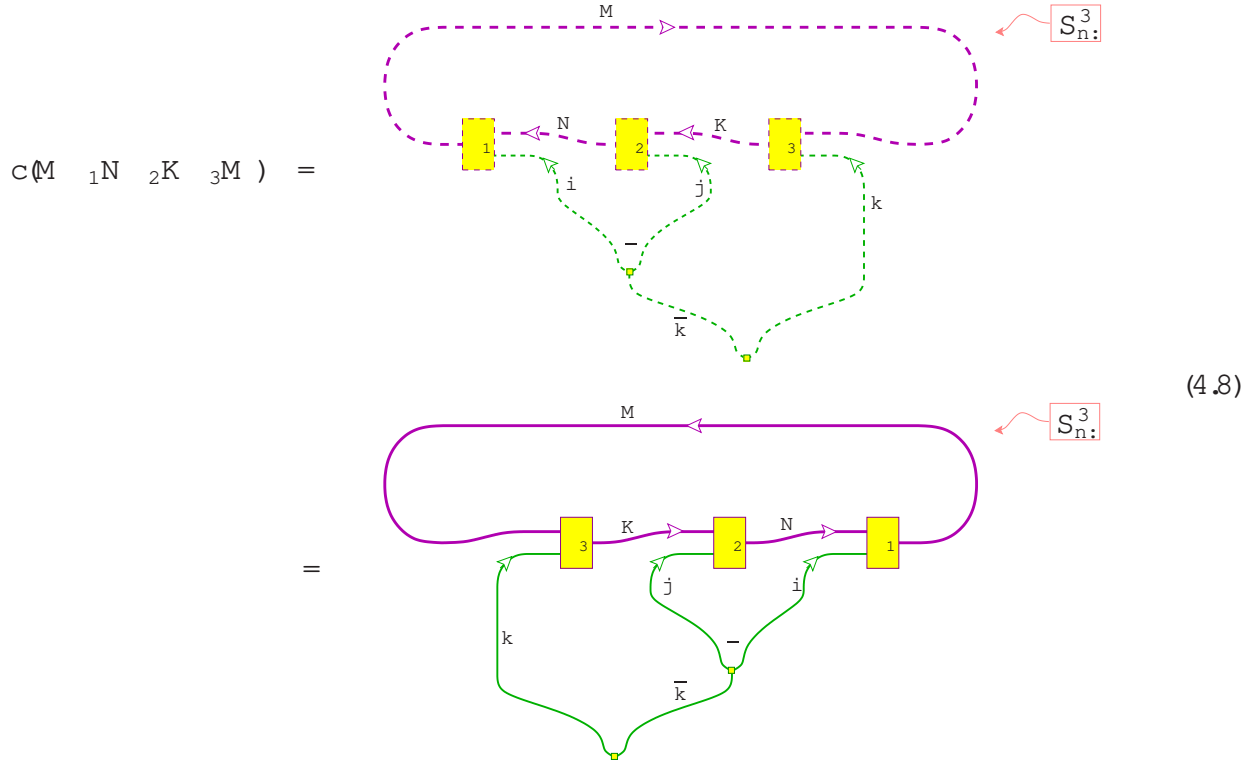
According to section 4.1, the structure constants $c(M_1 N_2 K_3 M)$ are defined to be the coefficients occurring when expanding (4.5) in terms of a standard basis for the space of blocks $H(\hat{X})$. In the case under consideration, \hat{X} is the sphere with field insertions at x_1, x_2, x_3 . The standard basis is given by the cobordism s



which are obtained from (4.2) by shifting the insertion points appropriately. The defining equation for the structure constants thus reads

$$Z(M_x;;;\hat{X}) = \sum_{i,j,k} c(M_1 N_2 K_3 M) Z(B(x_1, x_2, x_3);;;\hat{X}) : = 1 \quad (4.7)$$

To determine the coefficients c we compare both sides of the equality with $Z(\bar{B}(x_1, x_2, x_3);;\hat{X};;)$ from the left, where \bar{B} is the cobordism dual to B . This removes the summation and results in the desired ribbon invariant expressing c :



Here the second equality amounts to rotating the ribbon graph in S^3 by 180 degrees, so that one is looking at the white sides of the ribbons, rather than their black sides. Also, we introduced

the notation S_n^3 to indicate the graphical representation of the normalised invariant of a ribbon graph in S^3 . Recall from the end of section I.5.1 that when the picture of a ribbon graph in a three-manifold M is drawn, it represents the invariant $Z(M)$ except when $M = S^3$, in which case it rather represents $Z(M) = S_{0,0}$. Since $S_{0,0} = Z(S^3)$, this amounts to assigning the value 1 to the empty graph in S^3 . To stress this difference, we label figures representing normalised invariants in S^3 by S_n^3 , rather than by S^3 . (This notational distinction was not made in [I, II, III], where the normalisation convention for S^3 is used implicitly.) Recall also that, by definition, we have

$$S_{0,0}^2 = \sum_{i \in I} \dim(U_i)^2 : \quad (4.9)$$

Let us express the constant $c(M_1 N_2 K_3 M)$ in terms of the basis introduced in (2.5). To this end we take the modules $M; N; K$ to be simple. A correlator labelled by reducible modules can be expressed as a sum of correlators labelled by simple modules. We set

$$M = M_1 ; N = M_2 ; K = M_3 \quad (4.10)$$

and

$$1 = (i) ; \quad 2 = (j) ; \quad 3 = (k) ; \quad (4.11)$$

It is then straightforward to compute the invariant (4.8) from relation (2.8) for the fusing matrix of the module category \mathcal{G}_A . The result is

$$c(M_1 N_2 K_3 M) = \dim(M) \cdot \sum_{i=1}^M G[A]_{2-i}^{(ji)} \cdot G[A]_{3-i}^{(kk)} : = 1 \quad (4.12)$$

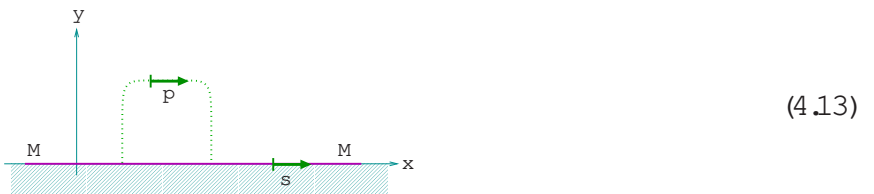
The dot ' ' stands again for a multiplicity label that can only take a single value, the corresponding morphism space being one-dimensional.

Formula (4.12) is in agreement with equation (4.16) of [22]. Note that in [22], the quantities ${}^{(1)}F$ are taken as an input, whereas the corresponding quantities $G[A]$ can be computed (with some effort) in terms of the multiplication of A and the fusing matrices F of C , see section 2.3.

Expressions for the structure constants of three boundary fields in rational conformal field theory have been obtained previously in various cases for models with charge conjugation invariant [14, 22, 46, 4] and non-diagonal models [47, 48].

4.3 One bulk and one boundary field on the disk

The next correlator we consider is that of a bulk field and a boundary field on the disk, which we again describe as the upper half plane:

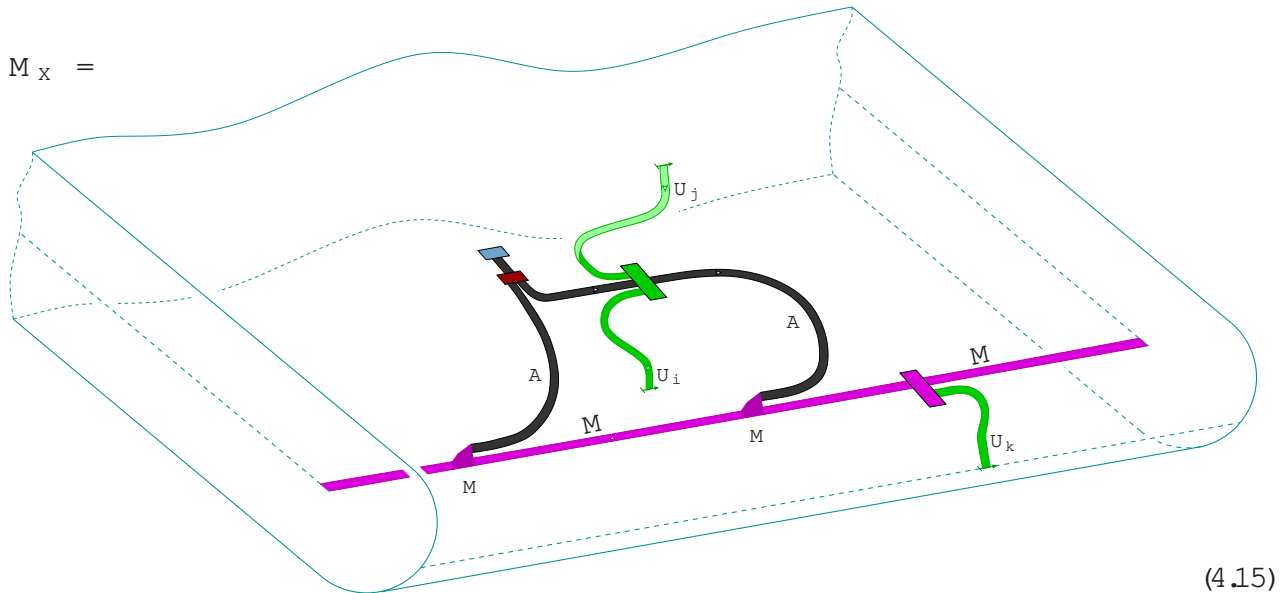


The dotted line indicates the dual triangulation that we will use later on in the construction of the ribbon graph. The bulk and boundary fields are the tuples

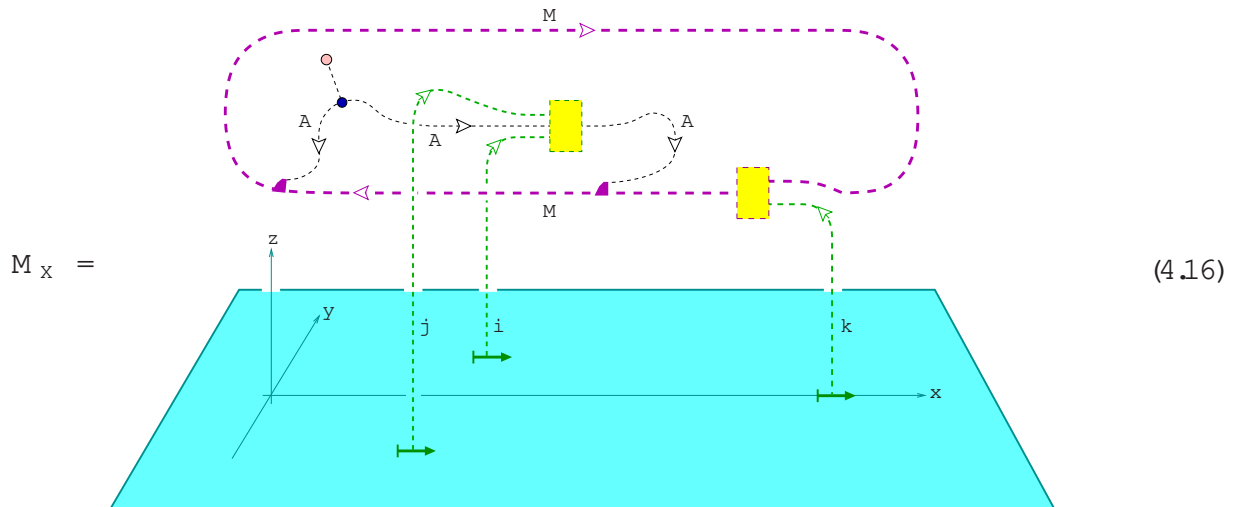
$$= (i; j; \{p; \} ; \text{or}_2) \quad \text{and} \quad = (M; M; U_k; \{s; \} ;) \quad (4.14)$$

where $i, j \in I$ label simple objects, $2 \text{Hom}_{A, A}(U_i \rightarrow A \rightarrow U_j; A)$ and $2 \text{Hom}_A(M \rightarrow U_k; M)$. Further, the insertion points are $p(x; y)$ and $s(s; 0)$ with $y > 0$ and $s > x > 0$, and the two arc germs are given by $(t) = (x + t; y)$ and $(t) = (s + t; 0)$, respectively. The orientation or_2 is the standard orientation of the upper halfplane at the insertion point of the bulk field.

The construction of section 3 yields the following ribbon graph inscribed in the connecting manifold:

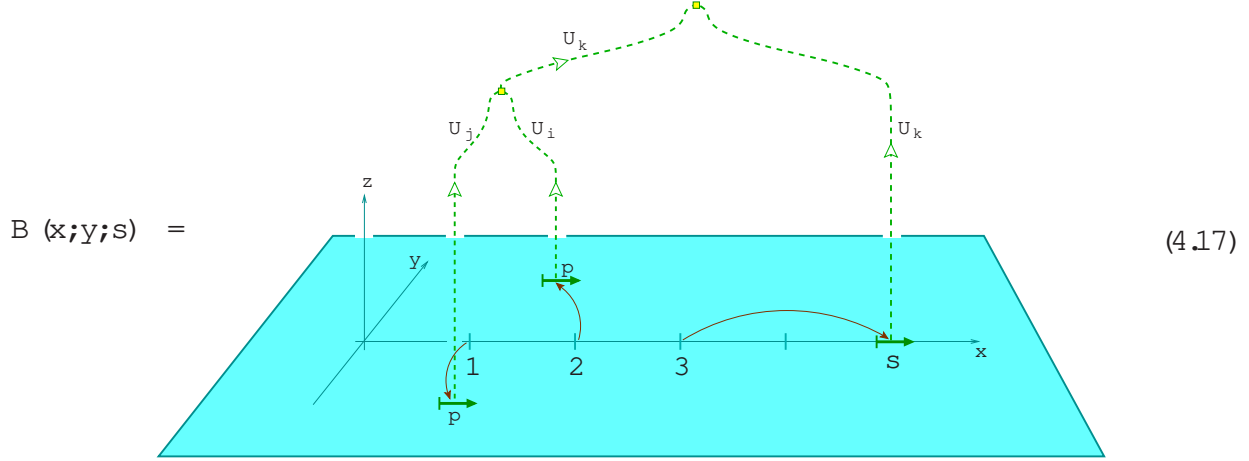


Here the three-manifold has been drawn as in (3.12). Also, in (4.15) it is understood that the M -ribbon that leaves the picture to the left and to the right is closed to a large loop. One may now 'unfold' the boundary ∂M_x so as to arrive at the equivalent representation of the three-manifold used also in (4.5). This yields



To verify that this cobordism is indeed the same as (4.15), one best works in the full ribbon representation and translates the picture to blackboard framing only at the very end.

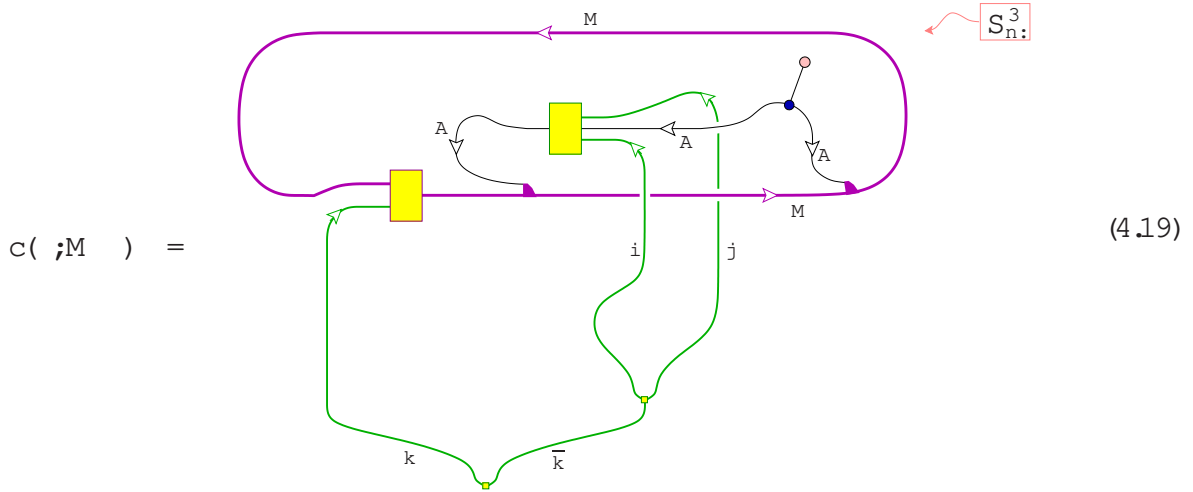
The basis of blocks in $H(\hat{X})$ in which we expand $Z(M_x;;;\hat{X})$ is given by



Also indicated in the figure is the continuation path that one has to choose starting from the standard situation (4.2). The structure constants $c(\cdot; M \cdot)$ are the expansion coefficients of (4.16) in terms of (4.17),

$$Z(M_x;;;\hat{X}) = \sum_{\text{terms}} c(\cdot; M \cdot) Z(B(x; y; s);;;\hat{X}): \quad (4.18)$$

Using the cobordism dual to $B(x; y; s)$ selects one term in the sum on the right hand side and thus yields, after a rotation by 180°, the ribbon graph



Remark 4.1 :

An interesting special case is the correlator of one bulk field on the upper half plane, without any boundary field insertion. The corresponding structure constant $c(\cdot; M \cdot)$ can be obtained from (4.19) by taking the boundary field to be the identity, $= (M; M; 1; id_M; [])$. Doing so,

one gets

$$\begin{aligned}
 c(\ ; M) = & \quad \text{Diagram (4.20)} \\
 & \text{A ribbon graph with a yellow square node labeled } A. \\
 & \text{A green loop labeled } i \text{ enters from the left.} \\
 & \text{A purple loop labeled } M \text{ enters from the top.} \\
 & \text{A green loop labeled } i \text{ exits to the right.} \\
 & \text{A purple loop labeled } M \text{ exits to the bottom.} \\
 & \text{A dashed box labeled } \tilde{\ } \text{ contains a red arrow pointing to } S_n^3.
 \end{aligned} \tag{4.20}$$

To obtain (4.20) from (4.19), one needs to get rid of one of the A -ribbons that are attached to the M -ribbon, by first moving the two representation morphisms close to each other, and then using the representation property (I.4.2), taking the resulting multiplication morphism past (which is allowed because commutes in particular with the left action of A on itself). The resulting A -loop can be omitted owing to specialness, so that one is left with the unit. To arrive at (4.20) it then only remains to deform the resulting ribbon graph a bit.

A ribbon graph of the form (4.20) was already encountered in the definition of the quantity S^A in (II.3.89). It follows that

$$c(\ ; M) = \frac{S^A(M; U_i; \tilde{\ })}{S_{0,0}}; \tag{4.21}$$

where $\tilde{\ }$ is the morphism enclosed in a dashed box in (4.20).

Next we express the invariant (4.19) in a basis, making the simplifying assumption that $N_{ij}^k \in \mathbb{F}_0; 1g$ and that $hU_i; A \in \mathbb{F}_0; 1g$. This implies in particular that A is haploid and thus simple. By convention, the bimodules are then labelled in such a way that $X_0 = A$. Let us choose the boundary condition and the morphisms for the bulk and boundary field in $c(\ ; M)$ as

$$M = M; \quad =_{(k)}; \quad =_{(i0j)0}; \tag{4.22}$$

Note that (4.19) can be slightly simplified by removing the A -ribbon that arrives at in the same way as explained in remark 4.1. Substituting (4.22) into (4.19) leads to the ribbon graph

$$\begin{aligned}
 C(\quad; M \quad) &= \text{Diagram} \\
 &= \sum_{m \in \mathbb{N}; a} X^m X^a \left[\begin{smallmatrix} (i_0 j_0) & 0 \\ 0 & 1 \end{smallmatrix} \right]^{0 ja} \left[\begin{smallmatrix} M & (m) \\ a & (n) \end{smallmatrix} \right]^{m n} I(i; j; k; a; m; n); \tag{4.23}
 \end{aligned}$$

where in the second step we have substituted the expansions of $_{(k)}$ and $_{(i_0 j_0)}$ given in (2.39) and (2.40). The coefficients M , introduced in (4.56), express a representation morphism in a basis. The function $I(i; j; k; a; m; n)$ is the ribbon invariant

$$I(i; j; k; a; m; n) = \text{Diagram} \tag{4.24}$$

To evaluate this invariant one first applies the appropriate relation from appendix II A.1 to the dashed box marked [1]. Next one inserts a complete basis (2.31) at [2] and removes all braidings with the help of (2.41). Finally one applies an F-move (II.2.36) to [3], so as to obtain

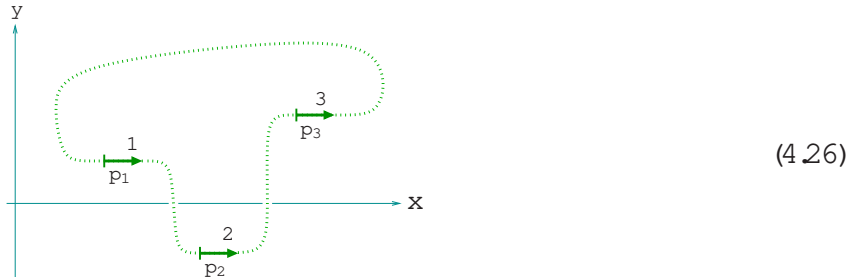
$$I(i; j; k; a; m; n) = G_{n0}^{(m; k; k)m} R^{(n; a)m} \dim(U_m) \sum_p^X \frac{n-i}{p} F_{ap}^{(n; i; j)m} G_{pk}^{(n; i; j)m} : \quad (4.25)$$

The correlators for one bulk field and one boundary field on the upper half plane, i.e. the structure constants describing the coupling of bulk to boundary fields, have first been considered in [13]. There, a constraint is derived which these coefficients have to solve and an explicit expression for their square is found for the case of the charge conjugation invariant. Since then, solutions for the coefficients themselves have been found, both for models with charge conjugation invariant and for more general cases [14, 22, 47, 49, 4]. Also, in equation (5.6) of [23] the bulk-boundary coefficients of spinless bulk fields are expressed through 1F .

The coupling of a bulk field to the identity on the boundary, i.e. the one-point function of a bulk field on the disk as in remark 4.1, is easier to obtain than the general bulk-boundary structure constants, as it can already be recovered from the NIM-rep data (multiplicities in the tensor products of C and C_A) and does not require knowledge of the 6j-symbols [50, 13]. These coefficients, which determine the boundary state, have been calculated for many models.

4.4 Three bulk fields on the sphere

We now turn to the correlator of three bulk fields on the sphere. Analogously as in the discussion of the disk, we describe the sphere as R^2 plus a point. The correlator then takes the form



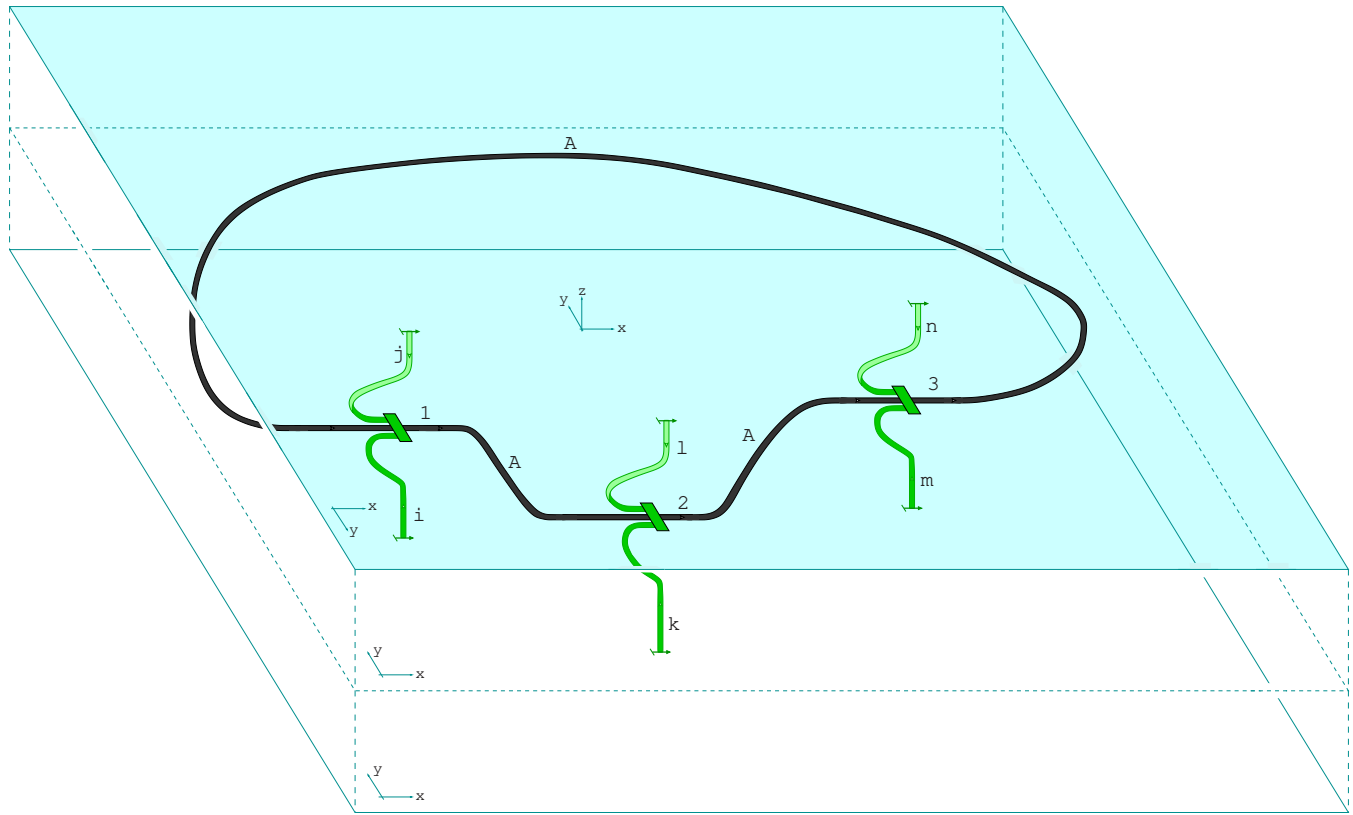
The dotted line again indicates the dual triangulation that will be used in the construction of the ribbon graph. The three bulk fields are tuples

$${}_1 = (i; j; {}_1; p_1; [{}_1]; or_2); \quad {}_2 = (k; l; {}_2; p_2; [{}_2]; or_2); \quad {}_3 = (m; n; {}_3; p_3; [{}_3]; or_2); \quad (4.27)$$

Here $i; j; k; l; m; n$ label simple objects. ${}_1$ is a morphism in $\text{Hom}_{A_A}(U_i \rightarrow A \rightarrow U_j; A)$, and similarly one has ${}_2 \in \text{Hom}_{A_A}(U_k \rightarrow A \rightarrow U_l; A)$ and ${}_3 \in \text{Hom}_{A_A}(U_m \rightarrow A \rightarrow U_n; A)$. The three fields are inserted at p_1, p_2 and p_3 , respectively, with arc germs $[{}_1], [{}_2], [{}_3]$ given by ${}_{1,2,3}(t) = p_{1,2,3} + (t; 0)$. The orientations or_2 around the insertion points of the three bulk fields are given by the standard orientation of R^2 .

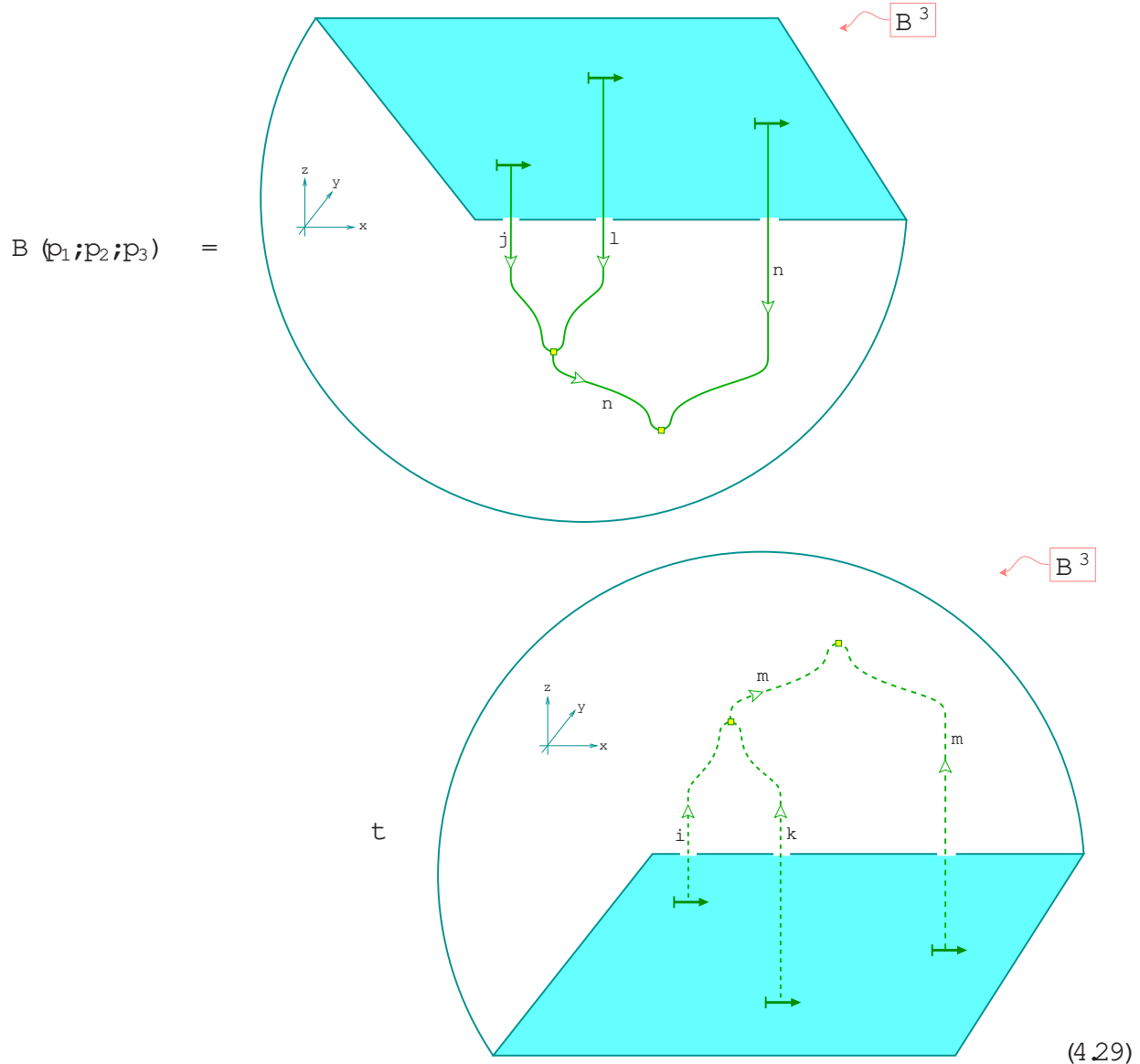
The construction of section 3 gives the following ribbon graph inscribed in the connecting manifold:

$$M_X =$$



(4.28)

As a basis for the space $H(\hat{X})$ we take the cobordisms



where the symbol B^3 indicates that the manifolds are solid three-balls, with orientations as indicated, while \sqcup denotes the disjoint union of the two three-manifolds. Expanding (4.28) in terms of (4.29) defines the bulk structure constants $c_{(1,2,3)}$ via

$$Z(M_X, \hat{X}) = \sum_{\hat{X}} c_{(1,2,3)} Z(B(p_1, p_2, p_3), \hat{X}); \quad (4.30)$$

By gluing the cobordism dual to $B(p_1, p_2, p_3)$ we get rid of the summation on the right hand

side, thus obtaining the ribbon graph

$$c_{(1,2,3)} = \frac{1}{S_{0,0}} \quad \text{Diagram:} \quad \begin{array}{c} \text{A} \\ \text{S}_n^3 \end{array} \quad (4.31)$$

The diagram shows a ribbon graph with three yellow rectangular vertices labeled 1, 2, and 3. Each vertex has a dashed green line labeled 'A' entering it. The graph is composed of green and dashed green lines. Labels include 'n' at the top, 'i' and 'k' on the left, 'j' and 'l' on the right, and 'm' at the bottom. A red arrow points to a red box labeled S_n^3 .

The additional factor $1 = S_{0,0}$ comes from the normalisation of the cobordism dual to $B(p_1; p_2; p_3)$, which consists of two copies of B^3 .

Let us assume that the algebra A is simple, and thus by convention $X_0 = A$. Also, we choose the morphisms entering the three bulk fields in $c_{(1,2,3)}$ as

$$1 = \frac{1}{(i0j)0}; \quad 2 = \frac{2}{(k0l)0}; \quad 3 = \frac{3}{(m0n)0}; \quad (4.32)$$

Inserting these expressions in (4.31) and rotating the resulting graph in such a way that the white side of the A -ribbons faces the reader results in

$$c_{(1,2,3)} = \frac{1}{S_{0,0}} \quad \text{Diagram:} \quad \begin{array}{c} \text{S}_n^3 \\ \text{X}_0 \end{array} \quad (4.33)$$

The diagram shows a ribbon graph with three yellow rectangular vertices labeled 1, 2, and 3. Each vertex has a dashed green line labeled 'X_0' entering it. The graph is composed of green and dashed green lines. Labels include 'n' at the top, 'i' and 'k' on the left, 'j' and 'l' on the right, and 'm' at the bottom. A red arrow points to a red box labeled S_n^3 .

Applying now the definition (2.27) of the $F[A]$ bimatrices twice, first to the pair $1, 2$ of morphisms, and then to the remaining two bimodule morphisms, the invariant (4.33) becomes

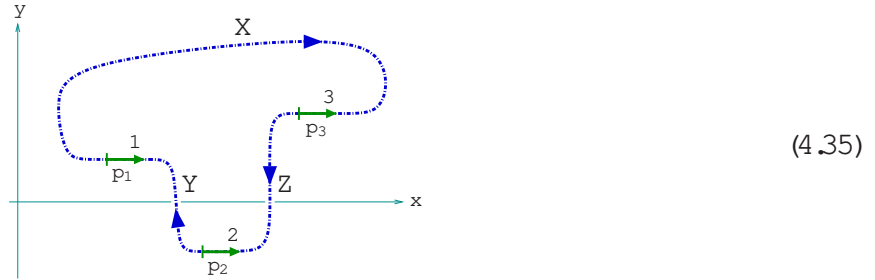
$$c_{(1,2,3)} = \frac{\dim(A)^X}{S_{0,0}} \quad F[A]_{1,0,2; m,n}^{(k,i0j)0}, F[A]_{0,3; 0,0}^{(m,0n)0}; \quad (4.34)$$

Multiplying this with the inverse of the two-point correlator, one finds that the bulk OPE coefficients are given precisely by entries of the matrix $F[A]$, as announced in remark 2.3.

Of the various types of structure constants considered in this paper, the coefficient for the correlator of three bulk fields has the longest history. Explicit expressions have first been obtained for the A-series Virasoro minimal models [12, 51], and subsequently for many models with charge conjugation invariant [52, 53, 54, 55, 56] and more general theories [57, 58, 59, 60, 61, 62, 63, 64, 65, 22].

4.5 Three defect fields on the sphere

The calculation for three defect fields is almost the same as for three bulk fields. This is not surprising, as a bulk field is just a special kind of defect field, namely the one connecting the invisible defect to the invisible defect. We consider three defect fields on a defect circle,



The three defect fields are tuples

$$\begin{aligned} \mathbf{1} &= (X; \text{or}_2; Y; \text{or}_2; i; j; \#_1; p_1; [1]; \text{or}_2); \\ \mathbf{2} &= (Y; \text{or}_2; Z; \text{or}_2; k; l; \#_2; p_2; [2]; \text{or}_2); \\ \mathbf{3} &= (Z; \text{or}_2; X; \text{or}_2; m; n; \#_3; p_3; [3]; \text{or}_2); \end{aligned} \quad (4.36)$$

Here or_2 is the standard orientation of \mathbb{R}^2 , i, j, k, l, m, n label simple objects, and $\#_{1,2,3}$ are morphisms

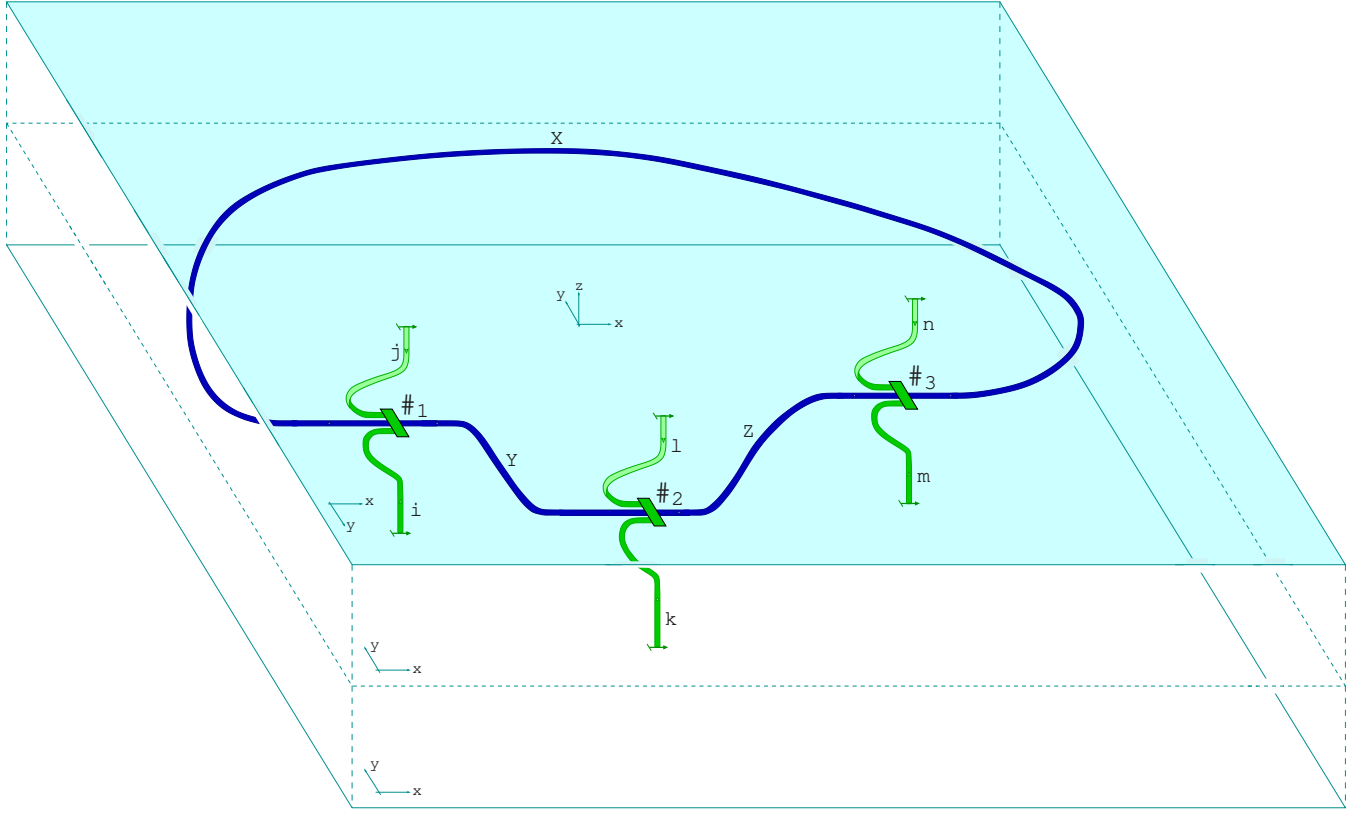
$$\begin{aligned} \#_1 &\in \text{Hom}_{\mathcal{A}}(U_i \rightarrow X; U_j; Y); \\ \#_2 &\in \text{Hom}_{\mathcal{A}}(U_k \rightarrow Y; U_l; Z); \\ \#_3 &\in \text{Hom}_{\mathcal{A}}(U_m \rightarrow Z; U_n; X); \end{aligned} \quad (4.37)$$

The three fields are inserted at p_1, p_2, p_3 , with arc germs $[1,2,3]$ given by $\mathbf{1,2,3}(t) = p_{1,2,3} + (t; 0)$.

The ribbon graph differs from the one for three bulk fields only in that the annular A-ribbon

is replaced by the appropriate bimodule ribbons. Thus we obtain

$$M_X =$$



(4.38)

Expanding this in the basis (4.29) defines the structure constants of three defect fields via

$$Z(M_X, \dots, \hat{X}) = \sum_X c(X; \#_1; Y; \#_2; Z; \#_3; X) Z(B(p_1; p_2; p_3); \dots; \hat{X}); \quad (4.39)$$

Using the cobordism dual to $B(p_1; p_2; p_3)$ yields a ribbon invariant very similar to (4.31):

$$c(X; \#_1; Y; \#_2; Z; \#_3; X) = \frac{1}{S_{0,0}} \quad \text{Diagram (4.40) showing a green ribbon with cusps #1, #2, and #3, connected to a blue dashed box labeled S_n^3. The diagram is enclosed in a dashed box. Labels i, j, l, m, n are present. Arrows indicate orientation along the ribbon. A red arrow points to the label S_n^3. The diagram is labeled (4.40).}$$

The calculation of the invariant (4.40) runs along the same line as in the case of three bulk fields. Let us choose

$$X = X ; Y = X ; Z = X ; \#_1 = \begin{smallmatrix} 1 \\ (i \ j) \end{smallmatrix} ; \#_2 = \begin{smallmatrix} 2 \\ (k \ l) \end{smallmatrix} ; \#_3 = \begin{smallmatrix} 3 \\ (m \ n) \end{smallmatrix} : \quad (4.41)$$

Inserting this in (4.40) leads to a ribbon invariant similar to (4.33), which can again be evaluated with the help of the definition (2.27). We find

$$c(X ; \#_1; X ; \#_2; X ; \#_3; X) = \frac{\dim(X)}{S_{0,0}} F[A]_{1 \ 2; m \ n}^{(ki \ jl)} F[A]_{3 \ 00}^{(mm \ nn)} : \quad (4.42)$$

Just like for three bulk fields, multiplying this expression with the inverse of the two-point correlator one finds that the OPE coefficients for defect fields are entries of the matrix $F[A]$.

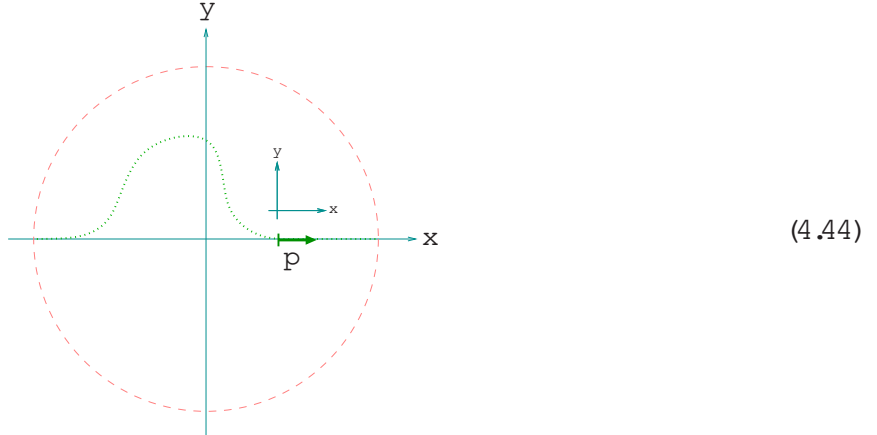
4.6 One bulk field on the cross cap

After dealing with the fundamental correlators allowing to obtain all orientable world sheets by sewing, we finally consider the additional world sheet that is needed to construct all non-orientable surfaces as well, i.e. the cross cap. Correspondingly, the algebra A is now a Jandl algebra.

We present the cross cap as $R^2 =$, with the equivalence relation identifying points according to the rule $u \sim_{RP^2} (u)$, where in standard coordinates $x; y$ on R^2 , $_{RP^2}$ acts as

$$_{RP^2}(x; y) = \frac{1}{x^2 + y^2} (x; y) : \quad (4.43)$$

Consider now the correlator of one bulk field on the cross cap, with the bulk field given by $= (i; j; ; p; []; or_2)$:

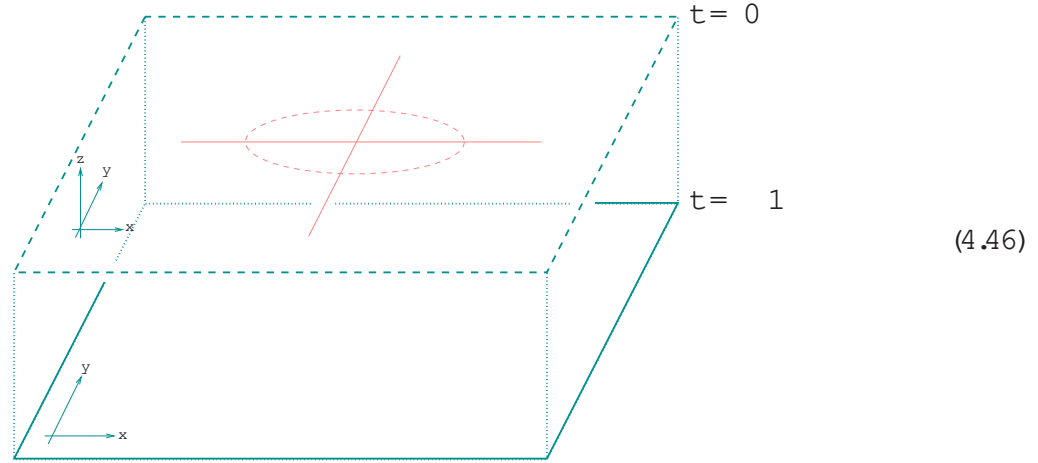


As before, $i; j \in I$, $2 \text{Hom}_{A \bar{A}}(U_i \rightarrow A \rightarrow U_j; A)$ and $(t) = p + (t; 0)$, where p is the insertion point of the bulk field. The local orientation or_2 around p is chosen as indicated in figure (4.44). The interior of the dashed circle is a fundamental domain of the equivalence relation $u \sim_{RP^2} (u)$. On its boundary, i.e. for $j \neq 1$, points are identified according to $u \sim u$.

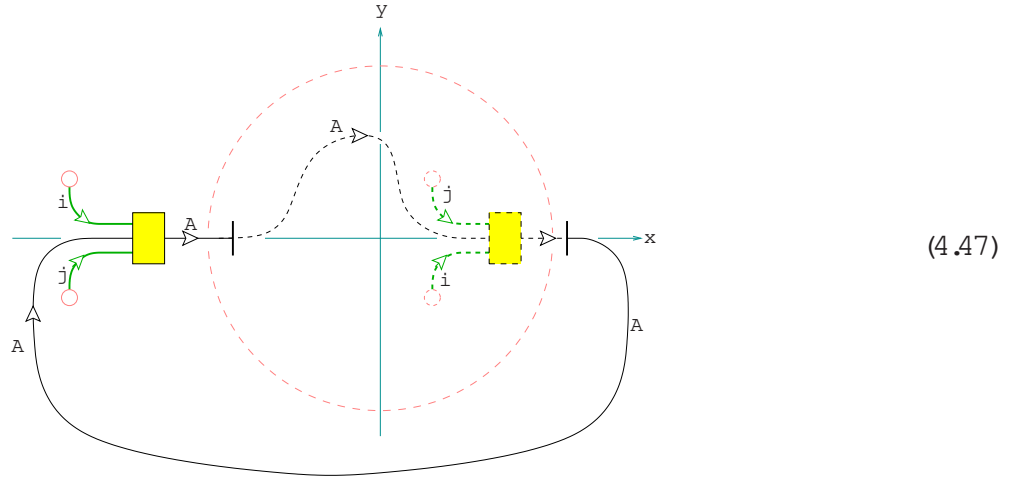
Similarly as in (II.3.10), one can write the connecting manifold as

$$M_X = \hat{X} [1; 0] = \quad \text{with} \quad (u; 0) \sim_{RP^2} (u; 0) \quad \text{for all } u \in \hat{X} : \quad (4.45)$$

For the cross cap we obtain in this way the three-manifold



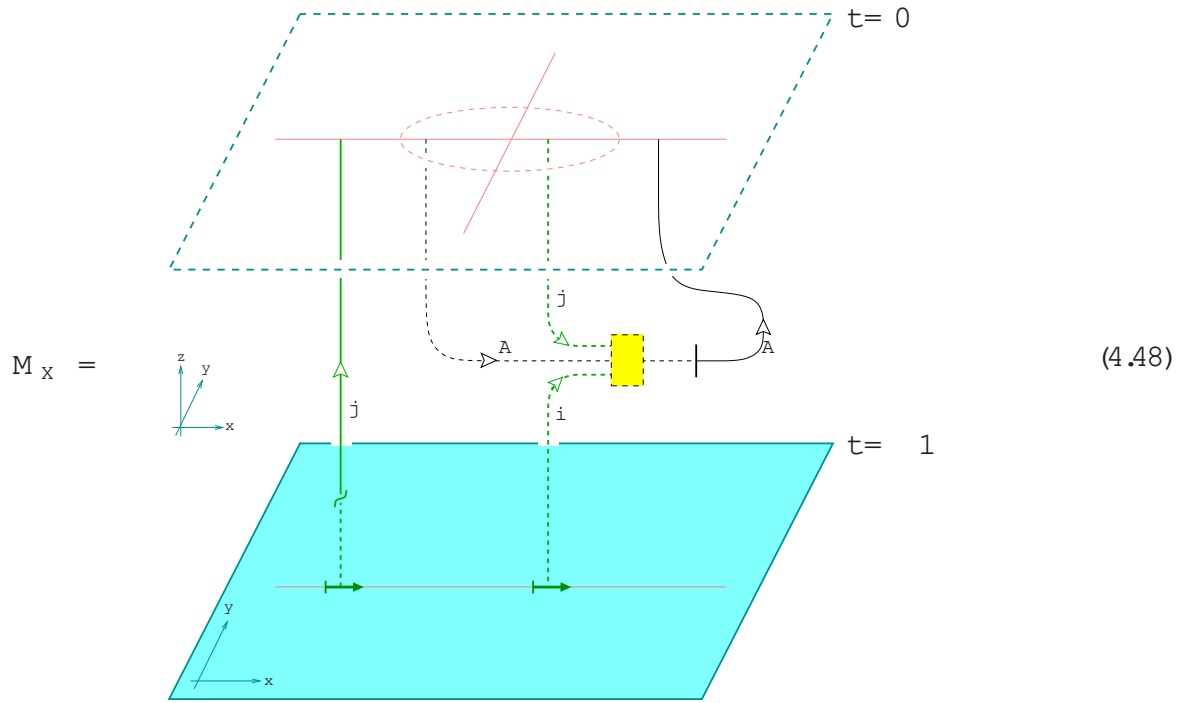
with orientations as indicated, and with points in the $t=0$ -plane to be identified according to $u \in \mathbb{RP}^2(u)$. Next we draw the ribbon graph embedded in the $t=0$ -plane:



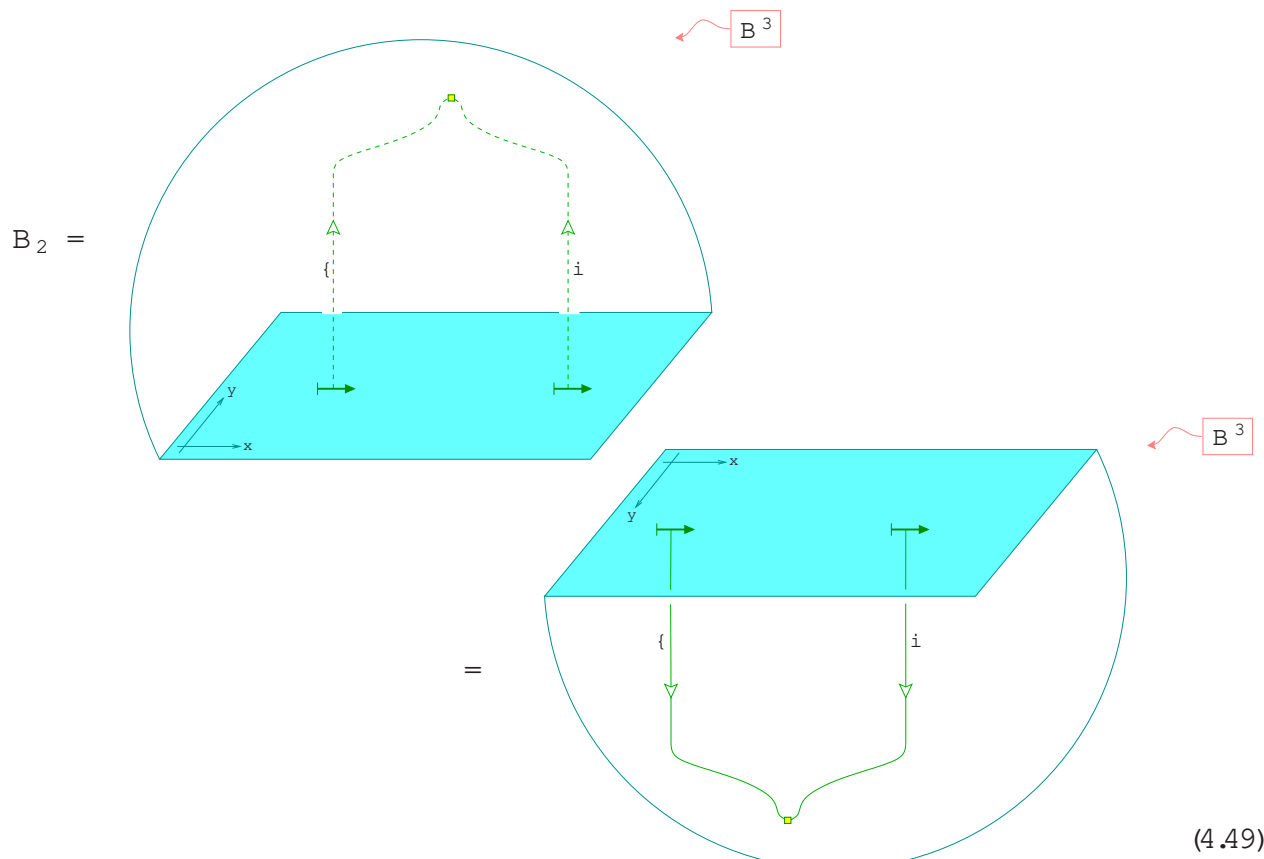
Note that there is only a single field insertion, but as a consequence of the identification $u \in \mathbb{RP}^2(u)$ the ribbon graph is duplicated in the picture. In (4.47) the U_i - and U_j -ribbons end in dashed circles; this way we indicate the points at which they leave the $t=0$ -plane so as to connect to the marked points on the boundary of M_x . Recall also the notation (II:3.4) for the element connecting two A-ribbons with opposite orientation.

The complete ribbon graph, lifted out of the $t=0$ -plane to $t < 0$ and rotated into blackboard

framing, looks as follows (again one better uses full ribbon notation to verify this move):



The space $H(\hat{X})$ in this case is one-dimensional if $j = \{$ and zero-dimensional otherwise. For $j = \{$ we select



as the cobordism describing the basis element in the space of blocks. The structure constant appearing in

$$Z(M_X; \cdot; \hat{X}) = c(\cdot) Z(B_2; \cdot; \hat{X}) \quad (4.50)$$

is again found by composing $Z(M_x;;;\hat{X})$ with the cobordism dual to (4.49). After a suitable rotation of the three-manifold, this results in

(4.51)

In the second equality, after deforming the ribbon graph, we use that ϕ is a morphism of bimodules, $\text{Hom}_{A\text{-}A}(U_i \otimes A \otimes U_j; A)$. Comparing to (II.3.91), we conclude that the resulting ribbon graph is just

$$C(\cdot) = \{U_i; \cdot^0\} = S_{0,i^0}; \quad (4.52)$$

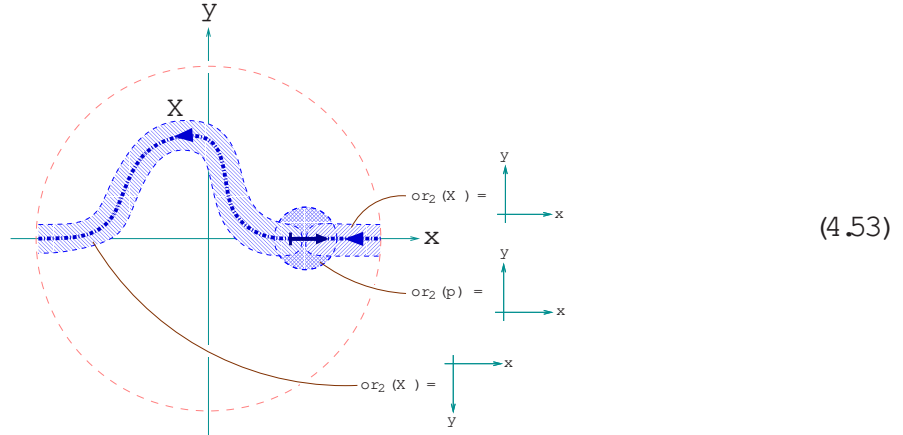
where \circ is the morphism inside the dashed box on the right hand side of (4.51). \mathcal{R} is the ribbon invariant that was introduced in (II.3.90), which was computed in a basis in (II.3.110).

One-point functions on a cross cap have been first obtained for free bosons, fermions and ghosts in [66, 67] and for the Ising model in [7]. The cross cap Ishibashi states were discussed in [68]. A set of cross cap one-point functions for the Cardy case in rational CFTs was given in [69, 4], and for the D-series of $su(2)$ in [70]. Simple current techniques allow one to find more solutions in the Cardy case, as well as more general simple current invariants [71, 72, 73, 74, 75]. In particular, Gepner (and related) models have recently received a lot of attention, see e.g. [76, 77, 78].

4.7 One defect held on the cross cap

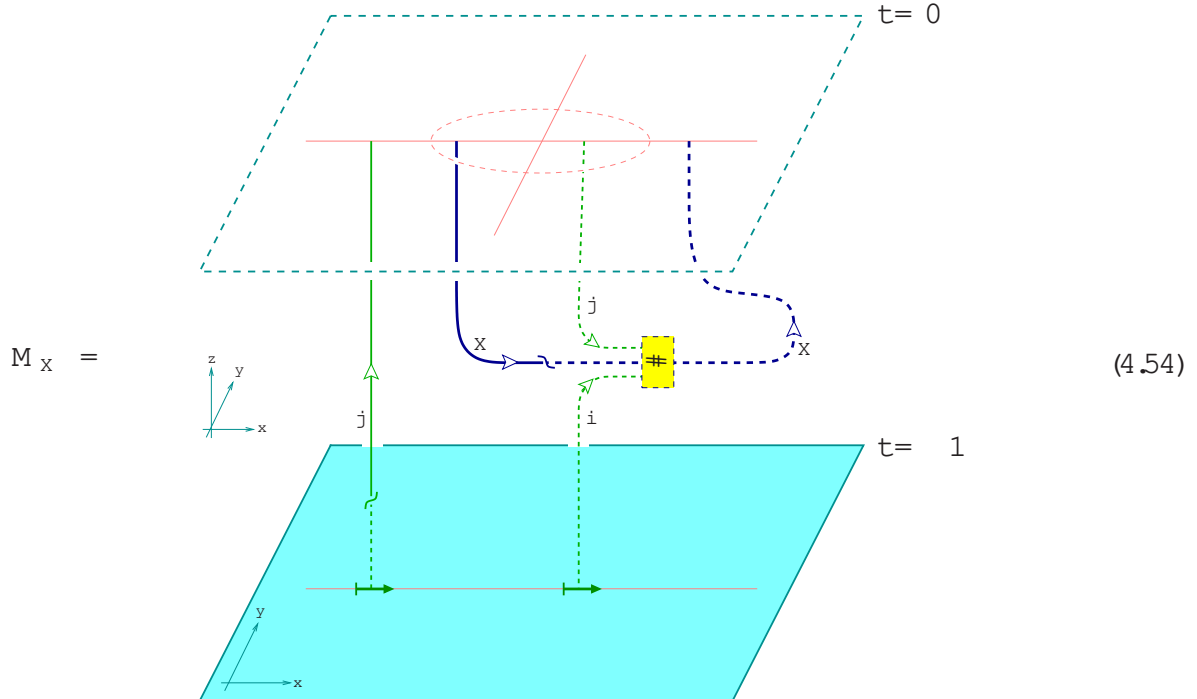
As already noted in section 4.5, replacing bulk fields by defect fields changes very little in the calculation of a correlator. Thus we discuss the correlator of one defect field on the cross cap

only very briefly. The geometric setup for the correlator is



where the defect field is given by $\phi = (X; \text{or}_2; X; \text{or}_2; i; j; \#; p; [;] \text{or}_2)$ with $\phi(t) = p + (t; 0)$ and $\# \in \text{Hom}_{\mathbb{A} \otimes \mathbb{A}}(U_i + X^s, U_j; X)$. The choice of $\#$ implies that at the insertion point of the defect field the defect runs parallel to the real axis. The orientations $\text{or}_2(p)$ around the insertion point and $\text{or}_2(X)$ around the defect line are chosen as indicated. When giving $\text{or}_2(X)$ one must take the orientation-reversing identification of points on \mathbb{R}^2 into account.

The connecting manifold M_X can be found by the same method that led to (4.48). The only difference is that the A -ribbon gets replaced by an X -ribbon, and that there is a half-twist in accordance with (3.55). The resulting ribbon graph is, in blackboard framing,



Composing with the dual of the cobordism (4.49) one determines the constant $c(X; \#)$ appearing

in the relation $Z(M_X;;;\hat{X}) = c(X;;)Z(B_2;;;\hat{X})$ to be

$$c(X;;) = \frac{1}{S_{0,0}} \quad (4.55)$$

To work out the invariant (4.55) we need to introduce a bit more notation. Note that the morphism $\#$ entering the data for the defect field is an element of $\text{Hom}_{A\mathbb{A}}(U_i^+ X^s U_i; X)$. If we choose X to be the simple bimodule X , then also $X^s = (X)^s$ is a simple bimodule. Define a map

$$s : K \rightarrow K \quad (4.56)$$

via $(X)^s = X_{s(\)}$. We explicitly choose, once and for all, a set of isomorphisms s

$$s \in \text{Hom}_{A\mathbb{A}}(X;;(X_{s(\)})^s) : \quad (4.57)$$

This is similar to the choice of $\iota \in \text{Hom}(U_i; (U_i)^-)$ made in (I.2.23). For our purposes we need to expand the inverse of s in a basis,

$$s^{-1} = \sum_i x^{h_{U_i} x^{-i}} (s^{-1})^{-1} x \quad (4.58)$$

In writing this relation we used that as objects in C , X and $(X_{s(\)})^s$ are both equal to X . They only differ in the left and right actions of A .

After these preliminaries, let us evaluate the invariant (4.55). We make again the simplifying assumption that $N_{ij}^k \neq 0$. Let us choose

$$X = X \quad \text{and} \quad \# = \text{id}_{U_i} - (s_{s(\)})^{-1} \text{id}_{U_i} : \quad (4.59)$$

Substituting this into (4.55) results in

$$c(X;) = \frac{1}{S_{0;0}}$$

$$= \frac{1}{S_{0;0}} x x [(is())^x y x [(s())^1 x_2 I(i; x; y) : \quad (4.60)$$

In the second equality we have replaced $(is())^x$ and $(s())^1$ by their expansions (2.40) and (4.58), respectively. If one in addition drags the points where the U-ribbon touches the identification plane along the paths indicated¹³ one obtains the following representation of the invariant $I(i; x; y)$:

$$I(i; x; y) = \quad (4.61)$$

To compute $I(i; x; y)$, we apply the relation (II:3.73) to the morphism that is indicated by the dashed box. Thereby $I(i; x; y)$, which according to (4.61) is the invariant of a graph in RP^3 , is

¹³ When moving the U-ribbon one must carefully take into account the identification. As discussed at the end of section II:3.5 this introduces additional twists.

expressed as the invariant of a graph in S^3 . In the latter form, $I(i;x;y)$ is straightforward to evaluate; we find

$$I(i;x;y) = S_{0,0} \sum_{j \in I}^X S_{0;j} \sum_{j \in I}^2 \frac{x}{y} \frac{1}{R^{(iy)x}} G_{x0}^{(y i)0} S_{jy} = P_{0,y} \frac{x G_{x0}^{(y i)0} y}{t_y R^{(iy)x}} : \quad (4.62)$$

In the second step we made use of the definition of the P -matrix [79, 80], see (II.3.122), and used the notations

$$P_{ij} = \hat{P}_{ij}^1; \quad \hat{P}_{ij} = (\hat{T}^{1=2} S \hat{T}^2 S \hat{T}^{1=2})_{ij}; \quad \hat{T}_{ij} = t_i^{-1} \delta_{ij}; \quad \hat{T}_{ij}^{1=2} = t_i^{-1} \delta_{ij}; \quad (4.63)$$

Finally, $P = S_{0,0} \sum_{k \in C}^1 (\dim U_k)^2$ is the charge of the modular category C . If C is the representation category of a RVOA, it is given by $P = e^{\frac{ic=4}{16}}$, with c the central charge of the chiral CFT.

4.8 Example: The Cardy case

In this section we apply the TFT formalism to the simplest situation, i.e. to the algebra $A = 1$. This case has already been treated¹⁴ in [46, 4]. Furthermore we make again the simplifying assumption that $N_{ij} \leq 2$ for all i, j .

With the exception of the structure constants for three defect fields on the sphere (4.68) and one defect field on the cross cap (4.75), the results of this section are not new and merely serve to illustrate the general formalism developed above. References to previous results in the literature are listed at the end of sections 4.2 & 4.6 above.

Field content

As is immediate from (I.5.30) and (I.5.19), for $A = 1$ the torus partition function is given by the charge conjugation modular invariant, $Z(1)_{ij} = \delta_{ij}$. Thus there is a bulk field ϕ_i for each simple object. In the notation of section 3.3, we choose

$$\phi_i = \phi_i; \quad \phi_i; p; []; \text{ or } (p); \quad (4.64)$$

where the morphism $\phi_i = \phi_{(i0)0}$ is given by the basis element introduced in (2.44).

The boundary conditions are in one-to-one correspondence with the simple objects U_i , too, and the annulus coefficients are given by the fusion rules [50]. Thus we have $J = I$ and $A_i = N_i$, compare remark I.5.21(i). Nonetheless we continue use greek letters to label boundary conditions. Let us denote the field that changes a boundary condition ϕ_i to ϕ_k and is labelled by the simple object U_k by ϕ_k . Thus in terms of the notation of section 3.2, we choose

$$\phi_k = M; M; U_k; \phi_k; []; \quad (4.65)$$

where the morphism $\phi_k = \phi_{(k0)0}$ is the basis element defined in (2.44).

The defects are in one-to-one correspondence with the simple objects U_i as well, so that $K = I$. Moreover, the twisted partition functions are again expressed in terms of the fusion

¹⁴ In [46, 4] the structure constants were derived for a specific normalisation of the bulk and boundary fields. We find it helpful to reproduce the results with normalisations kept arbitrary. Also, structure constants of defect fields were not considered in [46, 4].

rules [40]; as follows from the ribbon representation (I.5.151), we have $Z_{kl}^j = \sum_{k_2 \in I} N_{kl}^m N_m$. The number Z_{kl}^j gives the multiplicity of defect fields carrying chiral and antichiral labels U_k and U_l , respectively, that change a $-$ -defect into a $-$ -defect. Let us denote such fields by $_{kl}^j$. To be specific, in the notation of 3.4 we choose

$$_{kl}^j = (X; \text{or}_2(p); X; \text{or}_2(p); k; l; p; []; \text{or}_2(p)); \quad (4.66)$$

where $_{(k-1)}$. The multiplicity label j takes all values in I for which $N_{-1} N_k \neq 0$.

Three boundary fields

Let us first consider the case of three boundary fields i , j and k on the disk, changing boundary conditions from \dots to \dots to \dots as we move along the real axis. Substituting the expression (2.47) for the fusion matrices of G_A into the general expression (4.12) immediately results in

$$c(M_i M_j M_k) = \sum_{i,j,k} G_{k}^{(j,i)} G_{0}^{(k,k)} \dim(U) : \quad (4.67)$$

Recall that the constants i etc. give the normalisation of the boundary fields.

Remark 4.2:

In view of the results in [14, 22, 46, 4, 23] one might have expected that the F -matrices appear in (4.67), rather than their inverses G . This is, however, merely an issue of normalisation and of labelling of the boundary conditions, and illustrates the fact that the labelling of boundary conditions by simple objects is not canonical. Indeed, at the end of this section we will see that by suitably changing the normalisation of the boundary fields, in addition to relabelling the boundary conditions as γ , the structure constants (4.67) can equivalently be expressed in terms of F -matrices.

Three defect fields

Next we consider three defect fields. The structure constant of three bulk fields can then be obtained as a special case thereof. We consider a circular defect consisting of three segments of defect types \dots , \dots and \dots , respectively, see (4.35). The change of defect type is effected by three defect fields $_{ij;1}^j$, $_{kl;2}^j$ and $_{mn;3}^j$. The corresponding structure constant is obtained by substituting (2.49) into (4.42), resulting in

$$\begin{aligned} & c(X; _{ij;1}^j; X; _{kl;2}^j; X; _{mn;3}^j; X) \\ &= \sum_{ij;1}^j \sum_{kl;2}^j \sum_{mn;3}^j \frac{R^{(ij)n} R^{(mn)0}}{t_i t_j t_n} \frac{\dim(U)}{S_{0,0}} \\ & \quad X G_{1n}^{(i_1 i_2)} G_{2m}^{(j_1 j_2)} F_{2m}^{(k_1)} G_{00}^{(m-n)} G_{00}^{(n-n)} F_{30}^{(m-m)} : \end{aligned} \quad (4.68)$$

The constants $_{ij;1}^j$ etc. determine the normalisation of the defect fields.

Three bulk elds

The structure constants of three bulk elds i, j and k on the sphere are obtained by restricting formula (4.68) to the case $= = = 0$. The expression then simplifies a lot, leading to

$$c(i; j; k) = \frac{1}{t_i t_j t_k} \frac{G_{0k}^{(i|j)} | F_{|k}^{(jik)0}}{S_{0,0} \dim(U_k)} : \quad (4.69)$$

Here t_i^{0j} etc. give the normalisation of the bulk elds. In deriving this formula we made use of the relation

$$G_{00}^{(ppp)p} = R^{(pp)0} \frac{1}{p} \dim(U_p) : \quad (4.70)$$

which can be verified analogously as the corresponding equation for F in (I.2.45).

The normalisation of the bulk elds can be read off from the two-point structure constant, divided by the squared norm of the vacuum (expressed as the two-point function of the identity eld). Setting $m = 0$ and $j = \{$ in (4.69) and using once more (4.70) gives

$$\frac{c(i; \{)}{c(1; 1)} = \frac{t_i^{\{}}}{\dim(U_i)} : \quad (4.71)$$

One bulk and one boundary eld

Consider now the correlator for one bulk eld i and one boundary eld k on the disk, with boundary condition labelled by M . To evaluate the general expression (4.23), first note that the expansion coefficients of the representation morphism are now trivial, $\frac{M^{(m)}}{0; (m)} = 1$. Also recall relation (2.45) for the expansion coefficients of F and G . We then find

$$c(i; M; k) = t_i^{-1} \frac{1}{t_i t_k} G_{0k}^{(kk)} \frac{1}{\dim(U_i)} \sum_p^X \frac{t_i^{|p}}{t_p} F_{0p}^{(i0)} G_{pk}^{(i0)} : \quad (4.72)$$

Of particular interest is the correlator of one just bulk eld on disk, which is obtained from (4.72) by setting $k = 1$. Using the identities

$$F_{0p}^{(i0)} G_{p0}^{(i0)} = \frac{\dim(U_p)}{\dim(U_i) \dim(U_i)} \quad \text{and} \quad s_{i;|} = \sum_{k \neq i}^X \frac{t_i^{|k}}{t_k} N_{ik}^{(k)} \dim(U_k) ; \quad (4.73)$$

one finds

$$c(i; M) = \frac{1}{t_i} \frac{t_i^{\{}}}{\dim(U_i)} s_{i;} : \quad (4.74)$$

The phase t_i^{-1} will cancel a corresponding phase in the correlator, see equation (6.27) below. Also note that here one might have expected $s_{i;}$ instead of $s_{i;|}$. This difference amounts to the freedom to choose the labelling of the boundary conditions at will. Indeed, our labelling is related to the one leading to $s_{i;}$ by $\$$; we will return to this point at the end of the section.

One defect field on the cross cap

Consider a defect of type σ on a cross cap, together with a defect insertion σ_{ij} . To evaluate (4.60) we need to make a definite choice for the isomorphism s . First note that for $A = 1$ one has $s(\sigma) = \sigma$ for all $\sigma \in K$. It is convenient to choose $s = t \text{id}_U$. One then finds

$$c(X; \sigma_{ij}) = \frac{1}{\dim(U_i)} R^{(i)} \frac{t}{t_i t} G^{(i)} \frac{P_{0j}}{S_{0,0}} : \quad (4.75)$$

One bulk field on the cross cap

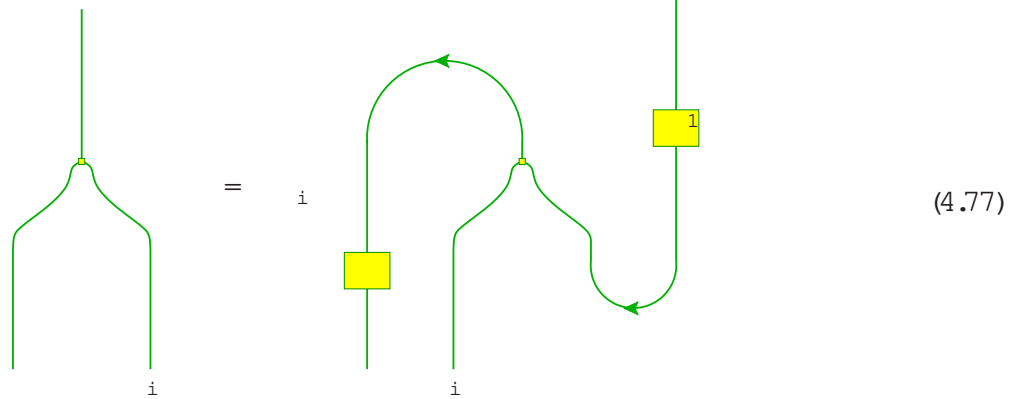
The structure constants of one bulk field σ_i on the cross cap are obtained by setting $\sigma = 0$ in (4.75):

$$c(\sigma_i) = \frac{1}{\dim(U_i)} \frac{P_{0i}}{S_{0,0}} : \quad (4.76)$$

Change of normalisation for boundary fields

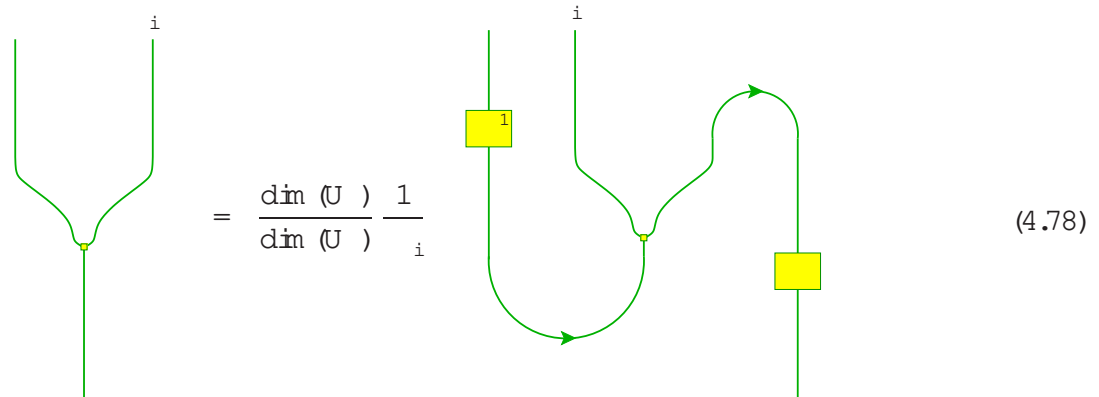
Let us now return to the question of expressing the structure constant (4.67) of three boundary fields in terms of F -matrices instead of their inverses G . We would like to demonstrate that there is a normalisation of the boundary fields in which (4.67) is expressed in terms of F , but with all boundary labels i, j, k replaced by their conjugates.

Introduce numbers σ_i by relating two different basis vectors of $\text{Hom}(U_i, U_i)$, according to



$$(4.77)$$

A short computation shows that this implies the relation



$$= \frac{\dim(U_i)}{\dim(U_j)} \frac{1}{\sigma_j} \quad (4.78)$$

between the dualbasis vectors. Consider now the ribbon representation of $G_{\mathbf{k}}^{(j|i)}$ as in (I2.40). Take the trace of that relation and replace the three basis vectors $_{(i)}$, $_{(j)}$ and $_{(k)}$ by the corresponding right hand sides of (4.77) and (4.78). It is then not difficult to see that the resulting ribbon graph can be deformed to equal the trace of the left hand side of (I2.37). Altogether we obtain

$$G_{\mathbf{k}}^{(j|i)} = \frac{i}{k} F_{\mathbf{k}}^{(j|i)} : \quad (4.79)$$

Substituting this relation into (4.67) results in the equality

$$c(M_{i|M_j|M_k}) = (i|i)(j|j)(k|k) F_{\mathbf{k}}^{(j|i)} F_{\mathbf{0}}^{(k|k)} \dim(U) : \quad (4.80)$$

We conclude that by changing the normalisation of the boundary fields and renaming the boundary conditions as $!$, one arrives at the usual expression of the boundary structure constants in terms of F -matrix elements.

5 Conformal blocks on the complex plane

In the study of CFT correlators there are two different aspects, a complex-analytic and a purely topological one. The construction of the correlators, as presented in detail in sections 2–4 for the fundamental correlators $h_{i|h_i}$ and $h_{i|h_i}$, as well as for the defect correlators $h_{i|h_i}$ and $h_{i|h_i}$, proceeds entirely at the topological level. Given this construction, one would next like to address the complex-analytic aspect of the correlators, thereby obtaining them as actual functions of the insertion points. This aspect is treated in the present section and in section 6. We start in sections 5.1 and 5.2 by recalling the concepts of vertex algebras and bundles of conformal blocks.

The relation between the 3-d TFT formulation of the correlators and the complex-analytic description relies on a number of assumptions, thus restricting the class of vertex algebras V to which our construction can be applied. First, we require the category $\text{Rep}(V)$ of representations of V to be a modular tensor category. Sufficient conditions on V which ensure this property of $\text{Rep}(V)$ have been given in [18].

Given V we can define bundles of conformal blocks for Riemann surfaces with marked points. Our second condition is to demand that these spaces are finite-dimensional, and that for surfaces of arbitrary genus the conformal blocks give rise to the same monodromy and factorisation data as the 3-d TFT constructed from $\text{Rep}(V)$. So far there is no complete treatment of this issue in the literature. However, many results have been obtained, see e.g. [9, 81, 82, 20, 83, 84]. For the purposes of this paper we do not need a complex-analytic construction of correlators in its full generality, though, as we only consider particularly simple cases, namely the fundamental correlators listed above. For these, at most conformal three-point blocks on the Riemann sphere are needed.

For the purposes of this paper, we will call the class of vertex algebras satisfying these conditions rational. From now on we take V to be rational in this sense.

Another important issue is the metric dependence of the correlation functions through the Weyl anomaly, which arises whenever the Virasoro central charge of V is nonzero. Here again we do not need a general treatment, because we will be interested in the ratio of a correlator and of the corresponding correlator with all field insertions removed (see section 6.1 below).

The presence of field insertions does not affect the metric-dependence of a correlator, and hence the Weyl anomaly cancels in such ratios.

5.1 Chiral vertex operators

In this section we describe the space of conformal blocks on the Riemann sphere P^1 , realised as $P^1 = \mathbb{C} \setminus \{1\}$. To this end we collect a few notions from the theory of vertex algebras, in particular that of an intertwiner between representations of vertex algebras. However, this section neither is intended as a review of vertex algebras, nor is it as general as it could be in a vertex algebra setting. Rather, the main purpose is to specify some notations and conventions needed in the description of the CFT correlation functions. For a much more detailed exposition of vertex algebras the reader may consult e.g. [82, 83, 85].

Vertex algebras and intertwiners

One formalisation of the physical concept of a chiral algebra for a conformal field theory is the structure of a conformal vertex algebra V . This is a vector space R , the space of states, which is $\mathbb{Z}_{\geq 0}$ -graded with finite-dimensional homogeneous subspaces, equipped with some additional structure. In particular, there is a state-field correspondence, assigning to every $W \in R$ a field $W(z) = Y(W; z) \in \text{End}(R)[[z; z^{-1}]]$. Here $\text{End}(V)[[z]]$, for V a vector space, denotes the space of formal power series in the indeterminate z with coefficients in $\text{End}(V)$. The state space R , also called the vacuum module, contains a distinguished vector v , the vacuum state, for which the associated field is the identity, $Y(v; z) = \text{id}_R$, and for which $Y(u; z)v = u + O(z)$ for all $u \in R$. The grading of the state space R is given by the conformal weight. The vacuum v is a non-zero vector in the component of weight zero, which we assume to be one-dimensional. The component of weight two contains the Virasoro vector v_{vir} , whose associated field $Y(v_{\text{vir}}; z) = T(z)$ is the (holomorphic component of the) stress tensor.

We will be interested in representations of the vertex algebra V and intertwiners between them. A representation of V of lowest conformal weight consists of a $(+\mathbb{Z}_{\geq 0})$ -graded vector space R and a map $\phi : R \rightarrow \text{End}(R)[[z^{-1}]]$, subject to some additional consistency conditions. An intertwining operator between three modules R_i, R_j, R_k with conformal highest weights $i; j; k$ is a map

$$V_{jk}^i(\phi; z) : R_j \rightarrow z^{i-j-k} \text{Hom}(R_k; R_i)[[z^{-1}]], \quad (5.1)$$

satisfying a condition to be described in a moment.

In the sequel we make the simplifying assumption that certain power series of our interest possess a non-empty domain of convergence when the indeterminate z is replaced by a complex variable, again denoted by z ; they can then be regarded as complex-valued functions analytic in that domain. For instance, suppose we are given some fields $\phi_i(z) \in z^i \text{Hom}(R_i; R_{i+1})[[z^{-1}]]$, which may be either fields $W(z)$ in the chiral algebra (in which case $R_{i+1} = R_i$) or intertwining operators $V_{p;i+1}^i(v; z)$ for some V -representation R_p and some $v \in R_p$. For any two homogeneous vectors $a \in R_1$ and ¹⁵ $b \in R_{n+1}$ we have

$$\langle b | \phi_n(z_n) \phi_{n+1}(z_{n+1}) a \rangle \in z_1^{-1} \cdots z_n^{-1} \mathbb{C}[[z_1^{-1}; \dots; z_n^{-1}]] \quad (5.2)$$

¹⁵ Here R_i is the restricted dual of the vector space R_i , which by definition is the direct sum of the duals of the (finite-dimensional) homogeneous subspaces of R_i , i.e. $R_i = \bigoplus_{n=0}^{\infty} R_{(n)}$ for $R_i = \bigoplus_{n=0}^{\infty} R_{(n)}$.

with suitable numbers i . It is then assumed that, when taking the z_j in the power series (5.2) to be complex variables (and thereby interpreting them as field insertion points in the complex plane), this series converges for all $(z_1; z_2; \dots; z_n) \in \mathbb{C}^n$ satisfying $j_1 > \dots > j_n > 0$.

As another example where we assume convergence, let us formulate the condition for $V_{jk}^i(\cdot; z)$ to be an intertwining operator. For $a \in R_i$, $b \in R_j$ and $c \in R_k$, consider the three formal power series

$$\begin{aligned} f_1(z) &= (a;_i W(z)) V_{jk}^i(b;_w c); \\ f_2(z) &= (a;_i V_{jk}^i(j W(z-w)) b;_w c); \\ f_3(z) &= (a;_i V_{jk}^i(b;_w) k W(z)) c; \end{aligned} \quad (5.3)$$

which are elements of $w^{i-j-k} \mathbb{C}[[z^{-1}; w^{-1}; (z-w)^{-1}]]$. What we assume is that, with z and w interpreted as complex variables, each of these three series has a non-zero domain of convergence. Usually $f_1(z)$ converges for $j > j_1$, $f_2(z)$ for $j < j_2$ and $f_3(z)$ for $j > j_3$. Then the condition for $V_{jk}^i(\cdot; w)$ to be an intertwining operator is that the three functions $f_{1,2,3}(z)$ coincide upon analytic continuation and can have poles only at $z = 0, w$ and 1 .

As already mentioned, we demand that $\text{Rep}(V)$ is a modular tensor category. In particular, V has only finitely many inequivalent irreducible representations, and every V -representation is fully reducible. We choose, once and for all, a set

$$\{S_i\}_{i \in I} \subset \text{Rep}(V) \quad (5.4)$$

of representatives of isomorphism classes of irreducible V -modules. By S_k we denote the element in this list that is isomorphic to the dual module $(S_k)^\perp$. We also take $S_0 = R$.

The morphisms of the tensor category V are intertwiners of V -modules. In particular, $\text{Hom}_V(S_j, S_k; S_i)$ is the vector space of intertwiners $V_{jk}^i(\cdot; z)$ between S_j, S_k and S_i . As V is rational, the dimension N_{jk}^i of this space is finite.

Choice of basis for intertwining operators

We choose bases

$$\{V_{jk}^{ij}(\cdot; z)\}_{j=1, \dots, N_{jk}^i} \subset \text{Hom}_V(S_j, S_k; S_i) \quad (5.5)$$

in the spaces of intertwiners $V_{jk}^i(\cdot; z)$. We do not restrict this choice, except when S_j or S_k is the vacuum module. Take first $j=0$; then $N_{0k}^i = k_i$. Thus $V_{0i}^i(\cdot; z) : S_i \otimes \text{End}(S_i)[[z^{-1}]]$ is unique up to multiplication by a scalar. As a basis, we take the representation morphism itself, $V_{0i}^i = \text{id}_{S_i}$. Then in particular the field corresponding to the vacuum v is the identity,

$$V_{0i}^i(v; z) = \text{id}_{S_i} : \quad (5.6)$$

Similarly, for $k=0$ we normalize $V_{i0}^i(\cdot; z) : S_i \otimes \text{Hom}(S_0; S_i)[[z^{-1}]]$ via the condition that

$$V_{i0}^i(u; z)v = u + O(z) : \quad (5.7)$$

for all $u \in S_i$.

Two- and three-point conformal blocks

Let v be the unique vector of weight zero in R satisfying $v(v) = 1$. For X a product of intertwiners, we write $h_0 j X \mathcal{J}i$ for the number $v(Xv)$.

For products of at most three intertwiners, the functional dependence of $h_0 j X \mathcal{J}i$ on the insertion points is fixed by conformal invariance. For the case of two intertwiners one finds explicitly

$$h_0 j V_{kk}^0(v; z_2) V_{k0}^k(u; z_1) \mathcal{J}i = (z_2 - z_1)^{2-k(u)} B_{kk}(v; u); \quad (5.8)$$

with $B_{kk}(v; u) = h_0 j V_{kk}^0(v; 2) V_{k0}^k(u; 1) \mathcal{J}i$:

Here we take $u \in S_k$ and $v \in S_k$ to be homogeneous of conformal weight $_{k(u)}$ and $_{k(v)}$, respectively. The two-point conformal block vanishes unless $_{k(u)} = _{k(v)}$.

For three intertwiners one gets

$$h_0 j V_{kk}^0(w; z_3) V_{ji}^k(v; z_2) V_{i0}^i(u; z_1) \mathcal{J}i$$

$$= (z_3 - z_2)^{i(u)} (z_3 - z_1)^{j(v)} (z_2 - z_1)^{k(w)} B_{kji}(w; v; u);$$

with $B_{kji}(w; v; u) = 2^{j(v) + i(u) + k(w)} h_0 j V_{kk}^0(w; 3) V_{ji}^k(v; 2) V_{i0}^i(u; 1) \mathcal{J}i$; (5.9)

where $u \in S_i$, $v \in S_j$ and $w \in S_k$ and, as before, $_{i(u)}$, $_{j(v)}$ and $_{k(w)}$ are the conformal weights of the respective vectors.

Local coordinate changes

For discussing the relationship to three-dimensional topological field theory in the next section, one needs to introduce the group $\text{Aut}0$ of local coordinate changes or, equivalently, locally invertible function germs. We describe $\text{Aut}0$ briefly; for details see e.g. section 6.3.1 of [82].

The group $\text{Aut}0$ can be identified with a subset of the formal power series $\mathbb{C}[[z]]$ consisting of those $f \in \mathbb{C}[[z]]$ that are of the form $f(z) = a_1 z + a_2 z^2 + \dots$ with $a_1 \neq 0$. Since a V -module R is in particular a V -module, there is an action R of $(\text{Aut}0)_{\text{opp}}$ on the module R ,

$$R : \text{Aut}0 \rightarrow \text{End}(R) \quad \text{such that} \quad R(\text{id}) = \text{id} \quad \text{and} \quad R(f \circ g) = R(g)R(f); \quad (5.10)$$

This action R is constructed as follows. For the coordinate change $f \in \text{Aut}0$ that is given by $f(z) = \sum_{k=1}^1 a_k z^k$, set $D = \sum_{j=1}^1 v_j t^{j+1} \frac{d}{dt}$, with the coefficients v_j determined by solving $v_0 \exp(D)t = f(t)$ order by order in t . The first few coefficients are

$$v_0 = a_1; \quad v_1 = \frac{a_2}{a_1}; \quad v_2 = \frac{a_3}{a_1} - \frac{a_2}{a_1}^2; \quad (5.11)$$

The operator R is then given by $R(f) = \exp \left(\sum_{j=1}^1 v_j L_j \right) v_0^{-L_0}$. Actually we will later rather need the inverse of $R(f)$, which takes the form

$$R(f)^{-1} = v_0^{L_0} \exp \left(\sum_{j=1}^1 v_j L_j \right); \quad (5.12)$$

For example, if j_i is a Vir-highest weight vector of L_0 -eigenvalue λ , then for the first two levels one finds

$$\begin{aligned} R(f)^1 j_i &= (f^0) j_i \quad \text{and} \\ R(f)^1 L_1 j_i &= (f^0) f^0 L_1 j_i + f^{(0)} = f^0 j_i; \end{aligned} \quad (5.13)$$

with f^0 and $f^{(0)}$ denoting derivatives of f at $z=0$, i.e. $f^0 = a_1$ and $f^{(0)} = 2a_2$. Define a functional t via

$$t(f)(z) := f(z+t) - f(t); \quad (5.14)$$

Then for vertex operators we have the identity [81, section 5.4]

$$Y(v; f(z)) = R(f)^1 Y(R(z(f))v; z)R(f); \quad (5.15)$$

where again f satisfies $f(0) = 0$ and $f^0(0) \neq 0$.

5.2 Spaces of conformal blocks

Extended Riemann surfaces

Recall from section 3.1 that the 3-d TFT assigns to every extended surface E a vector space $H(E)$. On the other hand, for the (chiral) 2-d CFT we need surfaces with a complex structure. The appropriate objects here are extended Riemann surfaces. An extended Riemann surface E^c is given by the following data:

- A compact Riemann surface without boundary, also denoted by E^c .
- A finite ordered set of marked points, i.e. triples $(p_i; [\gamma_i]; R_i)$, where the $p_i \in E^c$ are mutually distinct points, $[\gamma_i]$ is a germ of injective holomorphic functions from a small disk $D \subset \mathbb{C}$ around 0 to E^c such that $[\gamma_i](0) = p_i$, and R_i is a module of the vertex algebra V .
- A Lagrangian subbundle ${}^c H_1(E^c; \mathbb{Z})$ (that is, a \mathbb{Z} -subbundle c of $H_1(E^c; \mathbb{Z})$) such that the intersection form h ; i vanishes on c and that any $x \in H_1(E^c; \mathbb{Z})$ obeying $hx; yi = 0$ for all $y \in {}^c$ lies in c .

Given extended Riemann surfaces E^c and E'^c with marked points $(p_i; [\gamma_i]; R_i)$ and $(p'_i; [\gamma'_i]; R'_i)$, respectively, an isomorphism $f: E^c \rightarrow E'^c$ of extended Riemann surfaces is a holomorphic bijection of the underlying Riemann surfaces that is compatible with the (ordered) marked points in the sense that

$$(p_i; [\gamma_i]; R_i) = (f(p_i); [f \circ \gamma'_i]; R'_i); \quad (5.16)$$

Bundles of conformal blocks

Let E^c be an extended Riemann surface with marked points $(p_i; [\gamma_i]; R_i)$, $i = 1, 2, \dots, n$. Denote by $(R_1 \otimes \dots \otimes R_n)R$ the space of linear functions¹⁶ $R_1 \otimes \dots \otimes R_n \rightarrow \mathbb{C}$. To an extended Riemann surface E^c the chiral CFT assigns the space of conformal blocks on E^c , denoted by $H^c(E^c)$. It is defined as a subspace¹⁷ of $(R_1 \otimes \dots \otimes R_n)R$. As mentioned at the beginning

¹⁶ Here \otimes denotes the tensor product of complex vector spaces, not the tensor product in $\text{Rep}(V)$.

¹⁷ The subspace $H^c(E^c) \subset (R_1 \otimes \dots \otimes R_n)R$ is described via a compatibility condition with the action of V . For details we refer e.g. to [86, section 4] and [82, chapter 9].

of section 5 we assume all $H^c(E^c)$ to be finite-dimensional. One can show that if E^c and \tilde{E}^c are isomorphic as extended Riemann surfaces, then $H^c(E^c) = H^c(\tilde{E}^c)$. Note that this is an equality of subspaces of $(R_1 \cup \dots \cup R_n)R$, not just an isomorphism. In other words, there exists a well-defined assignment $[E^c] \mapsto H^c(E^c)$ on isomorphism classes $[E^c]$ of extended Riemann surfaces.

Denote by $\hat{M}_{g,n}(R_1; \dots; R_n)$ the moduli space of extended Riemann surfaces of genus g with n marked points, such that the k th point is labelled by the module R_k . If the choice of representations is obvious from the context, or not important to the argument, we will write $\hat{M}_{g,n}$ in place of $\hat{M}_{g,n}(R_1; \dots; R_n)$. The same convention will be applied to related objects defined below. Consider the trivial vector bundle

$$\hat{M}_{g,n}(R_1; \dots; R_n) \rightarrow (R_1 \cup \dots \cup R_n)R \rightarrow \hat{M}_{g,n}(R_1; \dots; R_n); \quad (5.17)$$

Each point in $\hat{M}_{g,n}$ is an isomorphism class $[E^c]$ of extended Riemann surfaces, to which we can assign the subspace $H^c(E^c) \subset (R_1 \cup \dots \cup R_n)R$. This defines a subbundle of (5.17), the bundle of conformal blocks on $\hat{M}_{g,n}(R_1; \dots; R_n)$; we denote it by

$$\hat{B}_{g,n}(R_1; \dots; R_n) \rightarrow \hat{M}_{g,n}(R_1; \dots; R_n); \quad (5.18)$$

The bundle $\hat{B}_{g,n}$ comes equipped with a projectively flat connection, the Knizhnik-Zamolodchikov connection, see [87] and e.g. [82, chapter 17]. Via parallel transport, this connection allows us to assign an isomorphism $U : H^c(E^c) \rightarrow H^c(\tilde{E}^c)$ to every curve $\gamma : [0; 1] \rightarrow \hat{M}_{g,n}$ with $\gamma(0) = [E^c]$ and $\gamma(1) = [\tilde{E}^c]$.

Two examples of the map U

We will later use two instances of the map U , the case that corresponds to a change of local coordinates and the case that amounts to moving the insertion points. Restricting to these two directions in $\hat{M}_{g,n}$ (moving insertion points and changing local coordinates while the complex structure of the underlying Riemann surface remains unaltered) results in a flat (not only projectively flat) connection. U then depends only on the homotopy class of γ .

In both examples considered below, E^c denotes an extended Riemann surface with marked points $(p_i; \ell_i; R_i)$, $i = 1; 2; \dots; n$. We will consider curves with $\gamma(0) = [E^c]$.

For the first example, define a family $E^c(t)$ of extended Riemann surfaces by taking $E^c(t)$ to be given by E^c , with the local coordinate at the k th marked point replaced by $\ell_k(t)$ with $t : D^n \rightarrow D^n$ such that $t(0) = 0$ and $t_0 = \text{id}$. This defines a curve in $\hat{M}_{g,n}$ by setting $\gamma(t) = [E^c(t)]$. For this curve the map U takes the form, for $v \in H^c(E^c)$,

$$(U \circ \gamma)(v_1; \dots; v_n) = (v_1; \dots; \hat{R}(\gamma^{-1}(v_k); \dots; v_n) \circ H^c(\tilde{E}^c)); \quad (5.19)$$

where $\tilde{E}^c = E^c(1)$. Note that we cannot directly take the map $R(\gamma^{-1}(v_k))$ as defined in (5.12) because if R_k has non-integral conformal weight, then the expression $(\gamma^{-1}(v_k))_k$ in (5.13) is only defined up to a phase. Instead, we set

$$\hat{R}(\gamma^{-1}(v_k)) = \hat{r}(1); \quad (5.20)$$

where

$$\hat{\iota} : [0;1] \rightarrow \text{End}(R_k) \quad (5.21)$$

$$t \mapsto R(\iota_t)^{-1};$$

and where now $R(\iota_t)^{-1}$ is the map defined in (5.12), with the phase ambiguity resolved by demanding $\hat{\iota}$ to be continuous and to obey $\hat{\iota}(0) = \text{id}$.

For the second example consider the curves $(t) = E^c(t)$ with $t \in \mathbb{C}$. Here $E^c(t)$ is again equal to E^c , but with the k th marked point replaced this time by $(p_k^t; \iota_k(t); R_k)$, where $\iota_k(t) = \iota + t$ and $p_k^t = \iota_k(t(0))$. If ι_k is defined on D , then $\iota_k(t)$ is a well-defined local coordinate around p_k^t as long as $t \in D$. With these definitions, in $E^c = E^c(1)$ the point $p_k = \iota_k(0)$ has been moved to $p_k^t = \iota_k(t)$. The map U must obey, for each $t \in \mathbb{C}$,

$$\frac{d}{dt} (U(t))(v_1; \dots; v_n) \Big|_0 = (v_1; \dots; L_{-1} v_k; \dots; v_n); \quad (5.22)$$

Renumbering marked points

Given an extended Riemann surface E^c with marked points $(p_i; \iota_i; R_i)$, $i = 1, 2, \dots, n$, and a permutation of $f_1, 2, \dots, n$, one can define a new extended Riemann surface $E^c = P(E^c)$ by taking the same underlying Riemann surface, but now ordering the marked points as $(p_i; \iota_i; R_i) = (p_{\iota^{-1}(i)}; \iota_{\iota^{-1}(i)}; R_{\iota^{-1}(i)})$.

In the same spirit, one can define an isomorphism $P : H^c(E^c) \rightarrow H^c(P(E^c))$ of conformal block spaces via $(P(v))(v_1; \dots; v_n) = (v_{\iota(1)}; \dots; v_{\iota(n)})$, where $v_k \in R_k = R_{\iota^{-1}(k)}$. This extends to a bundle isomorphism, which we will also denote by P ,

$$P : \hat{B}_{0,n}(R_1; \dots; R_n) \rightarrow \hat{B}_{0,n}(R_{\iota^{-1}(1)}; \dots; R_{\iota^{-1}(n)}); \quad (5.23)$$

Conformal blocks on the Riemann sphere

Let us describe the bundle $\hat{B}_{0,n}$ more explicitly. Define the standard extended Riemann surface $E_{0,n}^c[i_1; i_2; \dots; i_n]$ to be the Riemann sphere, realised as $\mathbb{C} \setminus \{f_1, \dots, f_n\}$, with marked points $f_k; \iota_k; S_{i_k}$ for $k = 1, 2, \dots, n$, with ι_k given by $\iota_k(z) = z + k$. When it is clear from the context what representations occur at the marked points, we use again the shorthand notation $E_{0,n}^c$ for $E_{0,n}^c[i_1; i_2; \dots; i_n]$. A basis for $H^c(E_{0,n}^c)$ is provided by the conformal blocks

$$_{0,n}^c[i_1; \dots; i_n; p_1; \dots; p_{n-3}; \iota_1; \dots; \iota_{n-2}] \quad (5.24)$$

given by a product of intertwiners,

$$_{0,n}^c : v_1 \in \mathbb{V}_{i_1} \otimes \dots \otimes \mathbb{V}_{i_n} \quad v_n \in \mathbb{V}_{\iota_1} \otimes \dots \otimes \mathbb{V}_{\iota_{n-2}} \quad (5.25)$$

where the $i_1; \dots; i_n$ and $\iota_1; \dots; \iota_{n-2}$ are multiplicity labels.

The moduli space $\hat{M}_{0,n}$ is connected, and the Knizhnik-Zamolodchikov connection on $\hat{M}_{0,n}$ is flat. To define the bundle $\hat{B}_{0,n}$, pick a curve from $E_{0,n}^c$ to some $E^c \in \hat{M}_{0,n}$. Then we have $H^c(E^c) = U(H^c(E_{0,n}^c))$, as a subspace of $(S_{i_1} \otimes \dots \otimes S_{i_n})S$. Note that while this defines the subspace, it does not provide a canonical basis, since U itself depends on the homotopy

class of \mathbb{C} , whereas the image of U does not.) In fact, if E^c is given by $\mathbb{C} [f_1, g]$ with marked points $(z_k; l_k; S_{i_k})$, then a basis of $H^c(E^c)$ can be given in terms of products of intertwiners,

The choice of branch cuts that are required when evaluating (5.26) is related to the path in $M_{0,n}^{+}(i_1; \dots; i_n)$ chosen to obtain (5.26) from (5.25).

5.3 Relation to TFT state spaces

In the three-dimensional topological field theory given by the Chern–Simons path integral, the space of states on a component of the boundary of a three-manifold can be thought of as the space of conformal blocks of the corresponding WZW model on that same surface [2]. One can in fact extract the Knizhnik–Zamolodchikov equation for field insertions on the complex plane from the Chern–Simons path integral [3].

In our approach to topological and conformal field theory the path integral does not play any role. Instead, the space of states for the 3-d TFT and the space of conformal blocks for the 2-d CFT are constructed independently, and it is a separate task to find an isomorphism between the two spaces. In this section we make such an isomorphism explicit in the case that the surface is the Riemann sphere. The TFT that is used in the present and the following section is the one obtained from the modular tensor category $C = \text{Rep}(V)$ of representations of the chiral algebra V .

Extended surfaces from extended Riemann surfaces

To an extended Riemann surface E^c one can assign an extended surface

$$E = F(E^c) \quad (5.27)$$

as follows. As a two-manifold, E coincides with E^c . Further, a marked point $(p; []; R)$ on E^c becomes the marked point $(p; []; R; +)$ on E , where the arc-germ $[]$ is defined by $[t] = [t]$, that is, by the real axis of the local coordinate system around p . The Lagrangian subspace of $H_1(E; R)$ is obtained as $=^c z R$ from $^c H_1(E^c; Z)$. The assignment F thus acts on extended Riemann surfaces by forgetting the complex structure and by replacing germs of local coordinates by germs of arcs.¹⁸ For instance, recalling the definition of the standard extended surfaces $E_{0,n} [i_1; \dots; i_n]$ in section 4.1 and of the standard extended Riemann surfaces $E_{0,n}^c [i_1; \dots; i_n]$ above, we see that

$$F(E_{0,n}^c) = E_{0,n} : \quad (5.28)$$

¹⁸ This also constitutes the main reason for using a slightly different definition of extended surface as compared to section 12.4. While there is no canonical way to associate an arc to a germ of local coordinates, there is no problem in assigning a germ of arcs in the way described.

The topological counterparts of P and U

Recall that for an extended Riemann surface E^c , $P(E^c)$ describes a permutation of the order of the marked points on E^c . Since the set of marked points on an extended surface E is not ordered, we simply have

$$F \circ P = F : \quad (5.29)$$

To be able to formulate the analogue of U in the two examples discussed in section 5.2 above, we need the following concepts. By a family $E^c(t)$ of extended Riemann surfaces over a Riemann surface E we mean that each extended surface $E^c(t)$ is given by E together with a set of marked points $(p_k^t; \ell_k^t; R_k)$ such that p_k^t and ℓ_k^t depend smoothly on t . A family $E^c(t)$ of extended surfaces over a two-manifold E is defined in the same way. If $E^c(t)$ is a family of extended Riemann surfaces over E , then $F(E^c(t))$ is a family of extended surfaces over $F(E)$.

To a family $E^c(t)$ with $t \in [0;1]$ we can assign a curve in the moduli space $M_{g,n}^\wedge$ by setting $E^c(t) := [E^c(t)]$. We then also get the isomorphism $U_{E^c} : H^c(E^c(0)) \rightarrow H^c(E^c(1))$.

On the topological side, from a family $E(t)$ over E , with $t \in [0;1]$, we can construct a cobordism $M_E : E(0) \rightarrow E(1)$. As a three-manifold, M_E is given by the cylinder $[0;1]$. The ribbon graph in M_E is fixed by demanding that the ribbons intersect the slice of M_E at time t as prescribed by the marked points on $E(t)$. The topological counterpart of U_{E^c} is then the linear map $Z(M_E) : H(E(0)) \rightarrow H(E(1))$ that is supplied by the TFT.

In this context the Riemann sphere with marked points is special: any curve in $M_{0,n}^\wedge$ can be obtained as $[E^c]$ for a family of extended Riemann surfaces over a single fixed base Riemann surface, which we take to be $\mathbb{C} \setminus \{f_1\}$. For surfaces of higher genus one needs to vary the complex structure moduli of the underlying Riemann surfaces as well. From here on we restrict our attention to the Riemann sphere with marked points.

The isomorphism in the case of the Riemann sphere

Let $[E^c] \in M_{0,n}^\wedge$. We would like to describe an isomorphism

$$\Theta : H^c(E^c) \rightarrow H(F(E^c)) \quad (5.30)$$

between the space of conformal blocks associated to the extended Riemann surface E^c and the space of states of the TFT on the extended surface $F(E^c)$.

The TFT encodes the monodromy data of the conformal blocks. This must be reflected in the isomorphism Θ . More precisely, we require Θ to fulfil

$$\Theta \circ P = \Theta \quad \text{and} \quad \Theta \circ U_{E^c} = Z(M_{F(E^c)}) \circ \Theta \quad (5.31)$$

for any permutation P and any family $E^c(t)$ over $\mathbb{C} \setminus \{f_1\}$. In addition to (5.31), the isomorphism Θ must be consistent with cutting and gluing of extended Riemann surfaces. For extended surfaces of higher genus, there are further conditions arising from varying the complex structure moduli of the underlying Riemann surface. We will not analyse the latter two types of conditions in this paper. Instead we assume that Θ does satisfy these conditions, and content ourselves with describing Θ for points in $M_{0,n}^\wedge$ and illustrating its consistency with (5.31) in some examples.

For the Riemann sphere we fix the isomorphism Θ by demanding that the standard conformal block $_{0,n} 2 H(E_{0,n}^c)$ from (5.25) gets mapped to the state described by the cobordism $B_{0,n}$ from (4.2),

$$\begin{aligned} \Theta([_{0,n} i_1; \dots; i_n; p_1; \dots; p_{n-3}; i_1; \dots; i_{n-2}]) \\ = Z(B_{0,n}[i_1; \dots; i_n; p_1; \dots; p_{n-3}; i_1; \dots; i_{n-2}];; E_{0,n}[i_1; \dots; i_n]) 1 : \end{aligned} \quad (5.32)$$

Since $\hat{M}_{0,n}$ is connected, relation (5.31) can be used to determine Θ for all points in $\hat{M}_{0,n}$, starting from its value at the point $E_{0,n}^c$ as given by (5.32). This way defining Θ is consistent if (5.31) holds for every closed loop in $\hat{M}_{0,n}$. The first property in (5.31) just means that Θ is independent of the ordering of the marked points of the extended Riemann surface. The second property in (5.31) can be reformulated as follows. Two representations $_{0,n}^c$ and $_{0,n}$ of $_{1}(\hat{M}_{0,n})$ on $H^c(E_{0,n}^c)$ and on $H(E_{0,n})$, respectively, are given by

$$_{0,n}^c([c]) = U_c \quad \text{and} \quad _{0,n}([c]) = Z(M_{F(c)}) ; \quad (5.33)$$

where the c are paths starting and ending on $E_{0,n}^c$ and E^c is a family over $\mathbb{C}[f_1]$ such that $E^c = c$. The isomorphism Θ must intertwine these two representations,

$$\Theta \circ _{0,n}^c = _{0,n} \circ \Theta : \quad (5.34)$$

Below we will verify the intertwining property in two examples, and sketch an argument for it to hold in general at the end of section 5.4.

Example: Closed path resulting in a twist

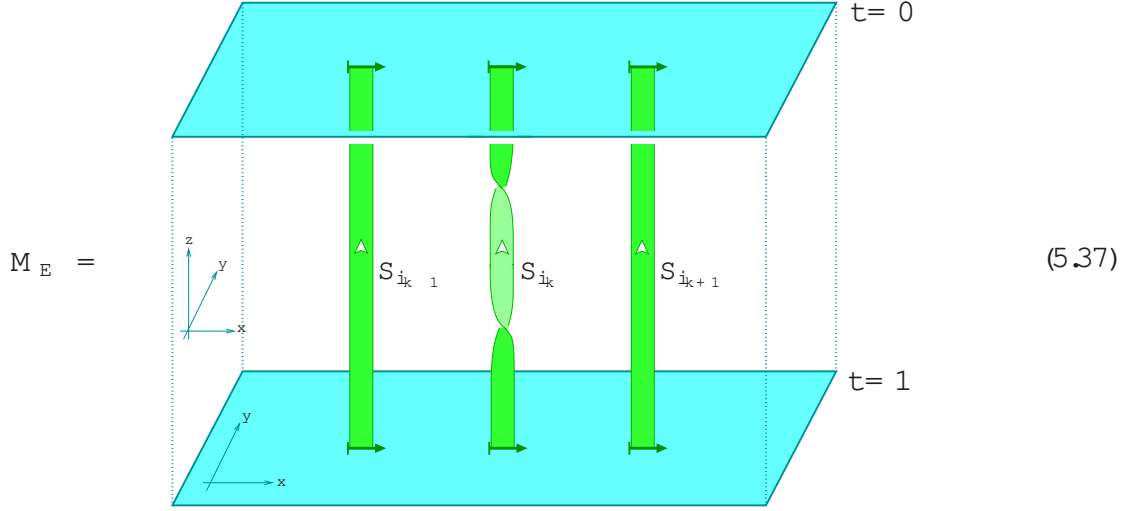
Define a family of extended Riemann surfaces $E^c(t)$ over $\mathbb{C}[f_1]$ by taking $E^c(t)$ to be equal to $E_{0,n}^c[i_1; \dots; i_n]$, except that the k th marked point gets replaced by $(k; i_k; t; S_{i_k})$ with $t(z) = e^{2\pi i z}$. Using U to compute the transport of a block $_{0,n}$ along the closed path E^c gives

$$(U_{E^c} \circ _{0,n})(v_1; \dots; v_n) = e^{2\pi i i_k} _{0,n}(v_1; \dots; v_n) : \quad (5.35)$$

To see this, start from formula (5.19) and use (5.13) and (5.21) so as to deduce first that $R(t)^{-1}v_k = e^{2\pi i v_k} v_k$ and then, also using that $i_k = (v_k) \bmod Z$, that $\hat{R}(t)v_k = e^{2\pi i i_k} v_k$. We thus find

$$_{0,n}([E^c]) = \bigcup_{i_k=0}^1 \text{id}_{H^c(E_{0,n}^c)} : \quad (5.36)$$

Further, let $E(t) = F(E^c(t))$; then the cobordism $M_E : E(0) \rightarrow E(1)$ is given by



with the orientations of the manifold and ribbons as indicated. Once oriented by the inward pointing normal, the boundary at $t=0$ is given by $E(0) = E_{0,n}$ and the boundary at $t=1$ by $E(1) = E_{0,n}$, as it should be. By definition of the twist (see (I2.9)), the middle ribbon in (5.37) can be replaced by $\frac{1}{i_k}$ times a straight ribbon, so that

$$Z(M_E) = \frac{1}{i_k} Z(E_{0,n} [0;1]) : \quad (5.38)$$

Since Z applied to the cylinder over $E_{0,n}$ gives the identity on $H(E_{0,n})$ we obtain

$$Z([E^c]) = \frac{1}{i_k} \text{id}_{H(E_{0,n})} : \quad (5.39)$$

For the closed path considered in this example, the desired identity (5.34) thus even holds independent of θ (and hence provides a consistency check of the conventions described in section 3.1).

Example: Closed path resulting in a double braiding

In this example we deal again with a family $E^c(t)$ over $\mathbb{C}[f1,g]$. We consider the situation that each of the extended Riemann surfaces $E^c(t)$ has three marked points, $(1; \gamma_1(z); S_i)$, $(p_2^t; \gamma_2^t(z); S_j)$ and $(3; \gamma_3(z); S_k)$, with the functions γ_i given by $\gamma_1(z) = z+1$, $\gamma_2^t(z) = z+1+e^{2\pi i t}$, $\gamma_3(z) = z+3$ and $p_2^t = \gamma_2^t(0)$. Note that $E^c(0) = E^c(1) = E_{0,3}^c[i; j; k]$. A basis for the conformal blocks in $H^c(E_{0,3}^c)$ is given by (5.9) with $z_1 = 1$, $z_2 = 2$, $z_3 = 3$. Transporting along E^c from 0 to t results in the conformal block ${}_{t,2} H(E^c(t))$ given by

$$\begin{aligned} {}_{t,2} H(u; v; w) &= h_0 \mathcal{J} V_{kk}^0(w; 3) V_{ji}^k(v; 1+e^{2\pi i t}) V_{i0}^j(u; 1) \mathcal{J} \\ &= B_{kji}(w; v; u) (2 e^{2\pi i t})^{(u)(v)(w)} 2^{(v)(u)(w)} e^{2\pi i t((w)(u)(v))} : \end{aligned} \quad (5.40)$$

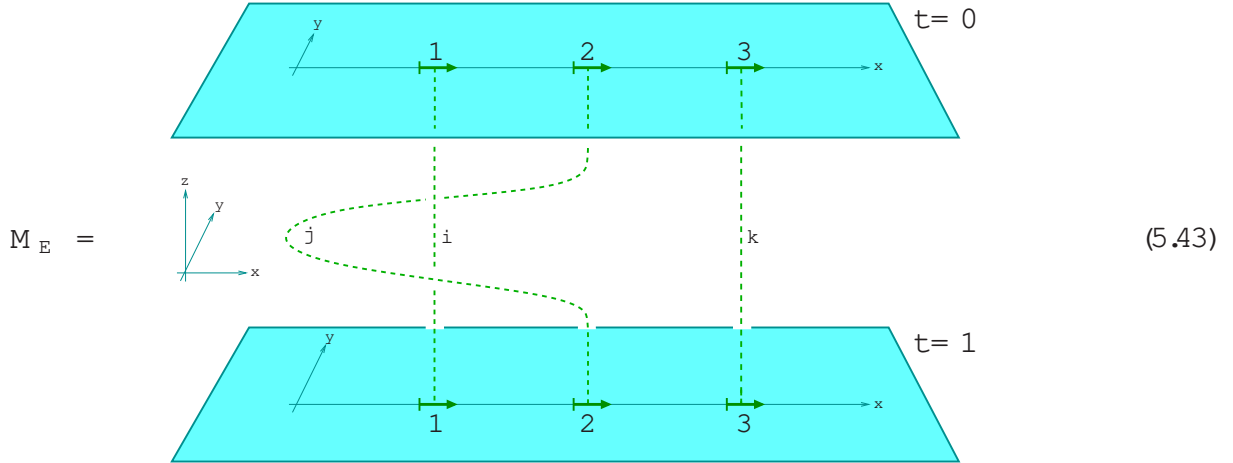
This block is obtained by setting $z_1 = 1$, $z_2 = 1+e^{2\pi i t}$ and $z_3 = 3$ in (5.9), as follows from (5.22) together with the property $V_{jk}^i(L_1 v; z) = \frac{d}{dz} V_{jk}^i(v; z)$ of the intertwiners. Setting $t=1$ we obtain

$${}_{1,2} H(u; v; w) = e^{2\pi i (k-i-j)} H(u; v; w) ; \quad (5.41)$$

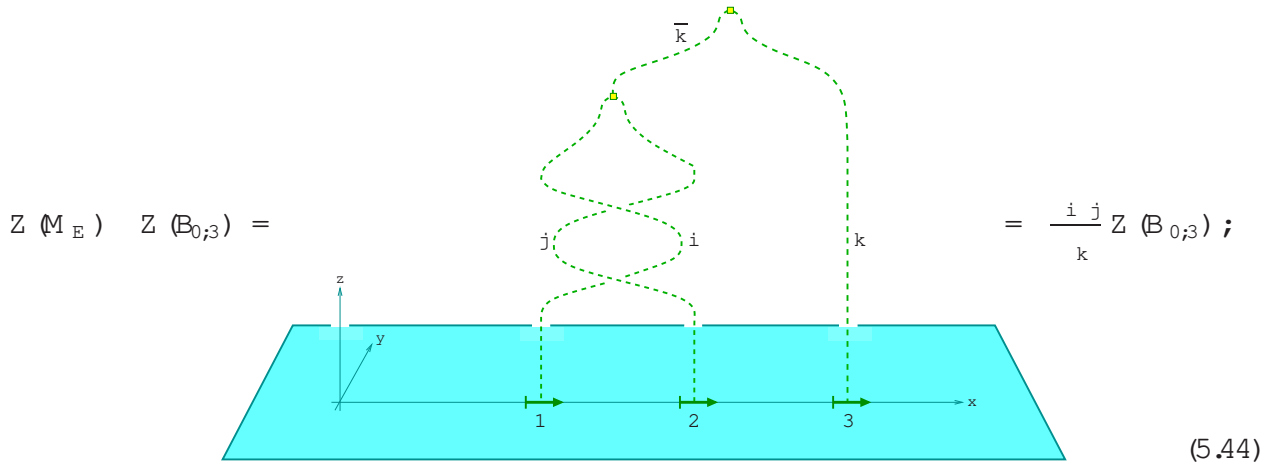
where we also used $(u) = \dots \bmod Z$ etc. Thus

$${}_{0;3}^c ([\mathbb{E}^c]) = \frac{i \ j}{k} \text{id}_{H^c(\mathbb{E}^c_{0;3})} : \quad (5.42)$$

Regarding the topological side, the cobordism M_E is easily found to be



Composing this cobordism with $B_{0;3}$ results in



where we applied (I2.41) twice and then substituted (I2.43) (or rather the corresponding relations for R instead of R). Thus for ${}_{0;3}$ we get

$${}_{0;3}^c ([\mathbb{E}^c]) = \frac{i \ j}{k} \text{id}_{H^c(\mathbb{E}^c_{0;3})} : \quad (5.45)$$

This shows that also in this example the identity (5.34) holds independently of θ , giving another consistency check of the conventions in section 3.1.

5.4 The braid matrices

It is common to express various quantities of interest in terms of matrices $B^{(ijk)1}$ ($B^{(ijk)1}_{pq}$) which are certain specific combinations of fusing matrices F and braiding matrices R [10, 9].

Conversely, one can recover F and R from B . In terms of conformal blocks, the braid matrices B can be deduced from the exchange of two insertion points in a four-point block on the sphere. Using the map @ one then verifies that this definition of B is equivalent to the one used in the 3-d TFT context.

Braid matrices in modular tensor categories

Similarly to the definition of the fusing matrices in (I2.36), for a modular tensor category C one defines the braid matrices $B^{(ijk)1}$ to be the matrices whose entries appear as coefficients in the relation

$$\begin{array}{c}
 \text{Diagram: A green loop with vertices labeled } i, j, k \text{ at the bottom and } p, q \text{ at the top. The loop is oriented such that it crosses itself.} \\
 = \sum_{q} \sum_{p} B_{p; q}^{(ijk)1} \\
 \text{Diagram: A green loop with vertices labeled } i, j, k \text{ at the bottom and } q \text{ at the top. The loop is oriented such that it does not cross itself.}
 \end{array} \quad (5.46)$$

If instead the inverse braiding is used one obtains the inverse braid matrices $B^{(ijk)1}$.

The braid matrices can be expressed in terms of the fusing matrices F from (I2.36) and the braid matrices R from (I2.41) as

$$B_{p; q}^{(ijk)1} = \sum_{p} R^{(k i) p} F_{p; q}^{(j k i) 1} R^{(i q) 1} : \quad (5.47)$$

This can be verified by first applying an inverse R -move to the morphism $\text{Hom}(U_i \otimes U_k; U_p)$ on the left hand side of (5.46), then performing an F -move, and finally an R -move applied to the resulting morphism in $\text{Hom}(U_q \otimes U_i; U_1)$.

Setting $k = 0$ in (5.46) and comparing to (I2.41), and recalling also convention (I2.33), one arrives at the relation

$$R^{(i j) k} = B_{i; j}^{(i j 0) k} : \quad (5.48)$$

Note that by convention the couplings in the one-dimensional morphism spaces involving the tensor unit $U_0 = 1$ are not spelt out explicitly.

Furthermore, using (I2.42) the relation (5.47) is easily inverted:

$$F_{p; q}^{(ijk)1} = \sum_{p} R^{(k j) p} B_{p; q}^{(k i j) 1} R^{(q k) 1} : \quad (5.49)$$

Thus one can obtain both R and F from the braid matrices B . One may wonder whether it is possible to recover the twists κ and the quantum dimensions $\dim(U_k)$ as well. For this to be the case, we need to assume that the quantum dimensions are all positive. Then we can take the absolute value of (I2.45) so as to find

$$\dim(U_k) = F_{00}^{(k k k) k} R^{(k k) 0}^{-1} : \quad (5.50)$$

The twist is then directly given by (I.2.45),

$$k = \dim(U_k) F_{00}^{(k k k)k} R^{(k k)0} : \quad (5.51)$$

Up to equivalence, a modular tensor category is determined by the list of isomorphism classes of simple objects f_{U_k} , the dimensions N_{ij}^k of the morphism spaces $\text{Hom}(U_i, U_j; U_k)$, and the numbers

$$\dim(U_k); \quad k; \quad R^{(i j)k}; \quad F_p^{(i j k)1} : \quad (5.52)$$

The considerations above show that, upon the assumption that the quantum dimensions are positive, instead of (5.52) it is sufficient to give the numbers

$$B_p^{(i j k)1} : \quad (5.53)$$

Braid matrices from four-point conformal blocks

The braid matrices also appear upon analytic continuation of the standard four-point conformal blocks. In short, one takes the standard four-point block and exchanges the field insertions at the points 2 and 3 via analytic continuation. The result can be expanded in terms of standard blocks, and the coefficients occurring in that expansion are the braid matrices. A more precise description is as follows.

Define a family $E^c(t)$ of extended Riemann surfaces over \mathbb{C} [fig] by taking $E^c(t)$ to have field insertions

$$(1; [r_1]; S_i); \quad (w_t; [r_2^t]; S_j); \quad (z_t; [r_3^t]; S_k); \quad (4; [r_4]; S_l); \quad (5.54)$$

where $r_1(\) = +1$, $r_4(\) = +4$,

$$r_2^t(\) = \frac{1}{2}e^{-\frac{\pi}{2}t} + \frac{5}{2}; \quad r_3^t(\) = -\frac{1}{2}e^{-\frac{\pi}{2}t} + \frac{5}{2}; \quad (5.55)$$

and $w_t = r_2^t(0)$, $z_t = r_3^t(0)$. It follows in particular that $E^c(0) = E_{0,4}^c[i; j; k; l]$. For $E^c(1)$ we must also take into account the ordering of the marked points, resulting in $P_{(23)}(E^c(1)) = E_{0,4}^c[i; k; j; l]$, where (23) denotes the transposition that exchanges 2 and 3. Transporting the conformal block $[i; j; k; l; p; ;]2 H^c(E_{0,4}^c)$ along E^c from 0 to 1 results in the block ${}_{t=2} H^c(E^c(t))$ given by

$${}_{t=2} (v_1; v_2; v_3; v_4) = h_0 j V_{11}^0(v_4; 4) V_{kp}^{\frac{1}{2}}(v_3; z_t) V_{ji}^p(v_2; w_t) V_{i0}^{\frac{1}{2}}(v_1; 1) j \quad (5.56)$$

with $z_t = \frac{1}{2}e^{-\frac{\pi}{2}t} + \frac{5}{2}$ and $w_t = -\frac{1}{2}e^{-\frac{\pi}{2}t} + \frac{5}{2}$. Since v_1 is in the space $H^c(E^c(1))$ we can apply to it the map $P_{(23)}: H^c(E^c(1)) \rightarrow H^c(E_{0,4}^c[i; k; j; l])$ and expand the result in the standard basis for the latter space,

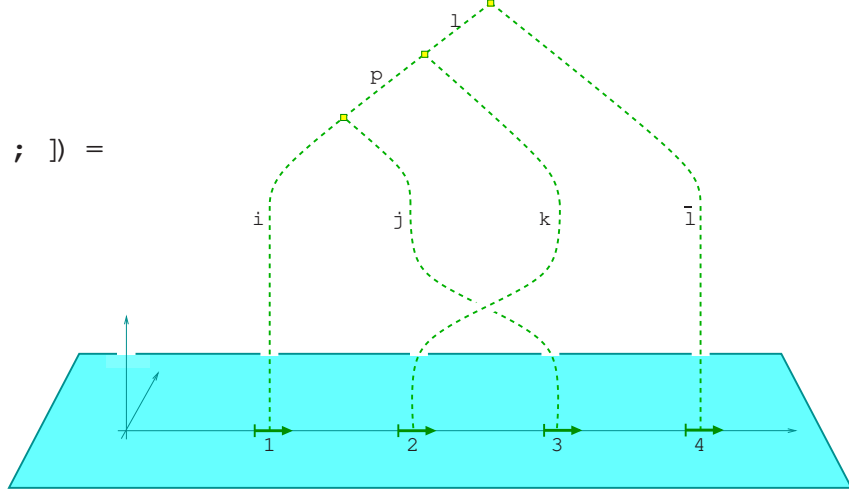
$$\begin{aligned} P_{(23)}(v_1)(u_1; u_2; u_3; u_4) &= \sum_{X_1} (u_1; u_3; u_2; u_4) \\ &= \sum_{q} B_p^{(j k i)1} {}_{0,4} [i; k; j; l; q; ;](u_1; u_2; u_3; u_4); \end{aligned} \quad (5.57)$$

By definition of the braiding in the representation category $C = \text{Rep}(V)$ of the chiral algebra, the matrices $B_p^{(i j k)1}$ which appear in (5.57) are the same as those defined in (5.46) through a relation between morphisms in C , see e.g. [88] for details.

Compatibility of @ and braiding

A gain one obtains a family $E(t)$ of extended surfaces by applying F to the family $E^c(t)$. For the associated cobordism M_E , composed with a cobordism $B_{0,4}$ describing the standard basis of $H(E_{0,4})$, one finds

$$Z(M_E) - Z(B_{0;4}[i;j;k;l;p; ;]) =$$



$$= \sum_{q=1}^{\infty} \sum_{p=1}^{\infty} B_{p,q}^{(j,k,i)} Z(B_{0,4}[i;k;j;l;q; \dots]) : \quad (5.58)$$

We can now verify the relation (5.34) for the braiding on a basis $_{0,4}^{\text{c}}[i;j;k;l;p; ;]$ of the space $H^c(E_{0,4}^c[i;j;k;l])$ as follows:

Here the first and third step just use the definition of \mathcal{C} in (5.32), the second and fourth step are the equalities in (5.58) and (5.57), respectively, and the final step amounts to the definition $\mathcal{C}_1 = \bigcup_{E \in \mathcal{C}} \{i; j; k; l; p; \dots\}$ together with the first of the properties (5.31).

Consistency of @

Let us now sketch how compatibility with the braiding implies (5.34). Let γ be a closed path in $M_{0,n}^+$ starting and ending at $E_{0,n}^c$. γ can always be written as the composition of two paths γ_1 and γ_2 , of which γ_1 only changes the local coordinates but leaves the insertion points fixed, while γ_2 only moves the insertion points, with all local coordinates remaining of the form $\gamma_k(z) = z + p_k$.

The paths γ_1 and γ_2 are closed already by themselves, and hence can be treated separately. For paths of type γ_1 relation (5.34) holds by an argument similar to the one used in the first example above. A path of type γ_2 furnishes an element of the braid group with n strands,

which has the special property that the strand starting at position k also ends at position k . The braid group is generated by moves $g_{k,k+1}$ that exchange two neighbouring strands. It is thus sufficient to verify the relation $U_{E^c} = Z(M_E)$ for such elements. This in turn follows by a similar argument as used for the four-point conformal block above, taking also into account that the braid matrices $B^{(ijk)1}$ control the behaviour of the intertwiners themselves under analytic continuation, not only that of the four-point block,

$$V_{kp}^{1;}(v_3; z) V_{ji}^{p;}(v_2; w) = \sum_q B_{p; q}^{(jk)i} V_{jq}^{1;}(v_2; w) V_{ki}^{q;}(v_3; z); \quad (5.60)$$

where the left hand side is understood as analytic continuation from $jw \rightarrow j < j$ to $jw \rightarrow j > j$, taking w clockwise around z .

6 The fundamental correlation functions

Ultimately, we would like to obtain the correlators of a CFT as functions of the world sheet moduli and of the field insertions. To this end we must combine the results from the previous sections with additional information about the world sheet. In particular, for non-zero central charge the correlators C do depend explicitly on the world sheet metric g and not only on the conformal equivalence class of metrics, see e.g. [89]. Thus, to find the value of a correlator it is not enough to know the conformal structure of the world sheet, but rather the metric itself is relevant. In sections 6.2 { 6.7 we will treat certain ratios of correlators in which the Weyl anomaly cancels.¹⁹

6.1 Riemannian world sheets

In sections 3 and 4 we were concerned with the 3-d TFT, and accordingly only needed the world sheet as a topological manifold. To obtain the correlator as a function, rather than as a vector in the TFT state space, we need the world sheet metric. To distinguish the two settings, we will use the terms topological world sheet and Riemannian world sheet.

Definition

By a Riemannian world sheet X^g we mean a compact, not necessarily orientable, two-manifold with metric g which may have non-empty boundary, defects and field insertions.

In section 3 we found that on the topological world sheet the fields, boundaries and defects are labelled by equivalence classes of certain tuples. The same holds true for insertions on the Riemannian world sheet, but the quantities entering the tuples are slightly different. We will only describe the tuples and refrain from giving the equivalence relations explicitly. They take a similar form as in the topological case, and will not be needed for the applications below.

Define a local bulk coordinate germ $[f]$ to be a germ of injective functions $f: D \rightarrow X^g$ of an arbitrarily small disk $D = fz \subset \mathbb{C}$ $j < g$ to X^g such that $f(0)$ lies in the interior of X^g . On the disk D we take the standard metric induced by $\mathbb{C} = \mathbb{R}^2$. The maps f are

¹⁹ These ratios, in turn, are obtained from unnormalised correlators $C(\dots)$, as opposed to the (normalised) expectation values h_i which obey $h_i = 1$. It is the correlators C which appear in factorisation constraints, and which give, e.g., the torus and annulus partition functions.

required to be conformal, i.e. satisfy $f \circ g = (x; y)(dx^2 + dy^2)$. Define further a local boundary coordinate germ $[d]$ to be a germ of injective functions $d: H \rightarrow X^g$ of an arbitrarily small semi-disk $H = \{z \in \mathbb{C} \mid |z| < \epsilon \text{ and } \operatorname{Im}(z) \geq 0\}$ to X^g such that $d(x) \in X^g$ for $x \in H$. Again on H we take the standard metric and require the map d to be conformal.

Since the definition of local coordinate germs depends only on the conformal structure on X^g , we denote fields on X^g with a superscript c to distinguish them from their topological counterparts in section 3. The possible field insertions on X^g are as follows.

- A bulk field c is a tuple

$${}^c = (i; j; \#; [f]); \quad (6.1)$$

where $i, j \in I$ label simple objects, $\#$ is a morphism in $\operatorname{Hom}_{A, A}(U_i \rightarrow A, U_j; A)$, and $[f]$ is a local bulk coordinate germ.

- A boundary field c is a tuple

$${}^c = (M; N; R; \#; [d]); \quad (6.2)$$

where M and N are left A -modules, R is an object of C , $\# \in \operatorname{Hom}_A(M \rightarrow R; N)$, and $[d]$ is a local boundary coordinate germ.

- A defect field c is a tuple

$${}^c = (X; \operatorname{or}_2(X); Y; \operatorname{or}_2(Y); i; j; \#; [f]); \quad (6.3)$$

where X, Y are A -bimodules, $\operatorname{or}_2(X)$ is a local orientation of X^g around the defect segment labelled by X , and similarly for $\operatorname{or}_2(Y)$. Further, $i, j \in I$ and $\# \in \operatorname{Hom}_{A, A}(U_i \rightarrow Z, U_j; Z^0)$, where Z, Z^0 are defined as in (3.38). $[f]$ is a local bulk coordinate germ which must fulfill the condition that $f(x)$ lies on the defect circle if x lies on the real axis.

As an additional datum, the boundary and bulk insertions are ordered, i.e. if there are m boundary fields and altogether n bulk and defect fields, we have to pick maps from f_1, f_2, \dots, f_m to the set of boundary fields and from f_1, f_2, \dots, f_n to the set of bulk/defect fields. Thinking of bulk fields as a special type of defect fields, we write

$${}^c_k = (M_k; N_k; R_k; \#_k; [d_k]) \quad \text{and} \quad {}^c_k = (X_k; \operatorname{or}_2(X)_k; Y_k; \operatorname{or}_2(Y)_k; i_k; j_k; \#_k; [f_k]) \quad (6.4)$$

for the k th boundary and defect field, respectively, and their defining data. The ordering is needed because below we construct an extended Riemann surface from X^g , and in that situation the marked points from an ordered set.

The complex double of X^g

From a Riemannian world sheet X^g we can obtain an extended Riemann surface \hat{X}^g , the complex double of X^g . It is constructed as follows.

If there are no field insertions on X^g , then \hat{X}^g is simply the orientation bundle over X^g , divided by the usual equivalence relation, i.e.

$$\hat{X}^g = \operatorname{Or}(X^g) = \{ (x; \operatorname{or}_2) \sim (x; \operatorname{or}_2) \mid (x; \operatorname{or}_2) \text{ for } x \in X^g \} \quad (6.5)$$

Since a metric (or just a conformal structure) together with an orientation defines a complex structure, we obtain a complex structure on $Or(X^g)$. The equivalence relation leading from $Or(X^g)$ to \hat{X}^g respects this complex structure. In terms of charts it amounts to identifying a subset of the upper half plane with the conjugate subset of the lower half plane along the real axis. Thus \hat{X}^g is a compact Riemann surface without boundary.

If in addition there are eld insertions on X^g , one obtains an ordered set of marked points on \hat{X}^g as follows.

- Each boundary $\text{eld } c = (M; N; R; \cdot; d)$ gives rise to a single marked point $(p; [\cdot]; R)$ on \hat{X}^g , where

$$\iota(z) = \begin{cases} [d(z); \text{or}_2(d)] & \text{for } \text{Im}(z) > 0; \\ [d(z); -\text{or}_2(d)] & \text{for } \text{Im}(z) < 0; \end{cases} \quad (6.6)$$

Here $\text{or}_2(d)$ denotes the local orientation of X^g obtained from the push-forward of the standard orientation on \mathbb{C} via d . One can verify that ι is an injective analytic function from a small disk in \mathbb{C} to \hat{X}^g . The insertion point p is equal to $\iota(0)$. Finally, if c has label k from the ordering of elds , we also assign the number k to the marked point (6.6).

- Each bulk / defect $\text{eld } c = (i; j; \cdot; f)$ or defect $\text{eld } c = (X; \text{or}_2(X); Y; \text{or}_2(Y); i; j; \#; f)$ gives rise to two marked points $(p_i; [\cdot]; S_i)$ and $(p_j; [\cdot]; S_j)$ on \hat{X}^g . Here

$$\iota_i(z) = [f(z); \text{or}_2(f)] \quad \text{and} \quad \iota_j(z) = [f(z); -\text{or}_2(f)] \quad (6.7)$$

are analytic functions, and $p_{i;j} = \iota_{i;j}(0)$. If the bulk / defect eld has label k from the ordering on X^g , the two marked points (6.7) are assigned the numbers $m + 2k - 1$ and $m + 2k$, respectively, with m the number of boundary elds .

We also need to fix a Lagrangian subbundle $c \in H_1(\hat{X}^g; \mathbb{Z})$. This is again done via the inclusion $:X^g \rightarrow M_X$ (here M_X is the connecting manifold for X^g , considered as a topological manifold), which gives rise to a map $:H_1(\hat{X}^g; \mathbb{Z}) \rightarrow H_1(M_X; \mathbb{Z})$. We take c to be the unique Lagrangian subbundle that contains $\ker(\cdot)$.

Holomorphic factorisation

Given a Riemannian world sheet X^g , the correlation function $C(X^g)$ of the CFT for that world sheet is a linear function

$$C(X^g) : \begin{matrix} \mathcal{O}^n \\ R_k \\ k=1 \end{matrix} \longrightarrow \begin{matrix} \mathcal{O}^n \\ (S_{i_1} \quad S_{j_1}) \\ l=1 \end{matrix} \longrightarrow \mathbb{C} : \quad (6.8)$$

Any correlation function must solve the chiral Ward identities coming from the holomorphic (and anti-holomorphic) elds in the theory, in particular those coming from elds in the chiral algebra. This leads to the principle of holomorphic factorisation [8], which can be simply formulated as the statement that

$$C(X^g) \in H^c(\hat{X}^g); \quad (6.9)$$

i.e. that the correlator for X^g is an element of the space of conformal blocks on the complex double of X^g .

Metric dependence

Consider a Riemannian world sheet X^g . Under a Weyl transformation $g \mapsto g^0 = e^c g$ for some $c : X^g \rightarrow \mathbb{R}$, the correlator changes by a factor:

$$C(X^{g^0}) = e^{cS[\cdot]} C(X^g); \quad (6.10)$$

where c is the central charge and $S[\cdot]$ is the (suitably normalized) Liouville action, see e.g. [89] for details.

If one works with ratios of correlators, the prefactor can be cancelled in the following manner. Let X^g be the Riemannian world sheet obtained from X^g by removing all field insertions and labelling all boundaries and defects by the algebra A . Then $C(X^g)$ is just a complex number, rather than a function as in (6.8), but it shows the same behaviour (6.10) under Weyl transformations of the metric as $C(X^g)$. It follows that the ratio

$$C(X^g) = C(X^g) \quad (6.11)$$

only depends on the conformal equivalence class of the metric g . It is these ratios, rather than the correlators themselves, that we will present below for the fundamental correlators.

The topological world sheet and its double

Let us define an operation F which assigns to a Riemannian world sheet X^g a topological world sheet $X = F(X^g)$ as follows.

If there are no field insertions on X^g , then X is obtained from X^g by just forgetting the metric. If in addition there are field insertions on X^g , then the corresponding insertions on the topological world sheet X are obtained as follows.

- A boundary field $\circ = (M; N; V; \dots; d)$ on X^g gives an insertion $= (M; N; V; \dots; p; [\cdot])$ on X , where $p = d(0)$ and $(t) = d(t)$.
- A bulk field $\circ = (i; j; \dots; f)$ on X^g gives an insertion $= (i; j; \dots; p; [\cdot]; \text{or}_2(p))$ on X , where $p = f(0)$ and $(t) = f(t)$. The local orientation $\text{or}_2(p)$ of X^g is given by $\text{or}_2(f)$, i.e. the push-forward of the standard orientation of \mathbb{C} via f .
- Similarly, for a defect field $\circ = (X; \text{or}_2(X); Y; \text{or}_2(Y); i; j; \#; f)$ on X^g one gets an insertion $\circ = (X; \text{or}_2(X); Y; \text{or}_2(Y); i; j; \#; p; [\cdot]; \text{or}_2(p))$ on X .

With these definitions one can verify that the diagram

$$\begin{array}{ccc} X^g & \xrightarrow{F} & X \\ \nearrow \# & & \nearrow \# \\ \hat{X}^g & \xrightarrow{F} & \hat{X} \end{array} \quad (6.12)$$

with F the map from extended Riemann surfaces to extended surfaces defined in section 5.3, commutes.

The TFT construction describes the correlator as a state of the TFT, $C(X) \in \mathcal{H}(\hat{X})$. In order to obtain the correlator $C(X^g) \in \mathcal{H}(\hat{X}^g)$ we thus need an isomorphism

$$\circ : \mathcal{H}(\hat{X}^g) \xrightarrow{\cong} \mathcal{H}(\hat{X}) \quad (6.13)$$

Since the metric g does not appear in the topological construction, θ should have some dependence on g . Here we are interested in correlators (or rather, the ratios (6.11)) on the upper half plane and on the complex plane (together with the point at infinity). In both cases we consider the standard metric²⁰ $dx^2 + dy^2$. For this metric we take the isomorphism θ to be the one defined in section 5.3.

6.2 Boundary three-point function on the upper half plane

Let A be a symmetric special Frobenius algebra in C . Take the Riemannian world sheet X^g to be the upper half plane together with three field insertions

$$_1 = (N; M; S_i; _1; [d_1]); \quad _2 = (K; N; S_j; _2; [d_2]); \quad _3 = (M; K; S_k; _3; [d_3]) \quad (6.14)$$

on its boundary. Here $M; N; K$ are left A -modules, the three fields are inserted at positions x_i satisfying $0 < x_1 < x_2 < x_3$, and the local boundary coordinate germs $[d_n]$ around these points are given by $\text{arcs } d_n(z) = x_n + z$. Note that $F(X^g)$ gives precisely the topological world sheet displayed in figure (4.3).

The complex double of X^g is the extended Riemann surface consisting of the Riemann sphere $\hat{X}^g = \mathbb{P}^1$, parametrised as $\mathbb{C} \setminus \{f_1, g\}$, and the three marked points $(x_1; f_1; S_i)$, $(x_2; f_2; S_j)$ and $(x_3; f_3; S_k)$, with the local coordinates given by $f_n(z) = x_n + z$, $n = 1, 2, 3$. The correlator $C(X^g)$ is an element of the space of conformal blocks $H^c(\hat{X}^g)$. A basis of this space is provided by the three-point blocks (5.9). One can thus write the correlator as a linear combination

$$C(X^g)(u; v; w) = \sum_{i=1}^{N_{ij}^k} c(M_{-1}N_{-2}K_{-3}M) h_{0j} V_{kk}^0(w; x_3) V_{ji}^k(v; x_2) V_{i0}^i(u; x_1) \delta_{ij}; \quad (6.15)$$

where $u \in S_i$, $v \in S_j$ and $w \in S_k$. The constants $c(M_{-1}N_{-2}K_{-3}M)$ are precisely those determined by the TFT-analysis in (4.8). This follows from applying the map θ to both sides of (6.15), which results in (4.7). Altogether, for the ratio (6.11) we find, using the explicit form (5.9) of the three-point block,

$$\frac{C(X^g)(u; v; w)}{C(X^g)} = \frac{\sum_{i=1}^{N_{ij}^k} c(M_{-1}N_{-2}K_{-3}M)}{\dim(A)} B_{kji}(w; v; u) \frac{(x_3 - x_2)^{-i(u)} (x_3 - x_1)^{-j(v)} (x_2 - x_1)^{-k(w)}}{(x_3 - x_1)^{-j(v)} (x_2 - x_1)^{-k(w)} (x_2 - x_1)^{-i(u)}}; \quad (6.16)$$

The vectors $u \in S_i$, $v \in S_j$ and $w \in S_k$ tell us which fields of the infinite-dimensional representation spaces of the chiral algebra are inserted at the points $x_3 > x_2 > x_1$, and $-i(u)$, $-j(v)$, $-k(w)$ are their conformal weights. Note also that $C(X^g) = \dim(A)$. The constants c have been expressed in a basis in (4.12); for the Cardy case they are given by (4.67).

²⁰ This makes both world sheets non-compact, but they are still conformally equivalent to compact world sheets. We could have chosen a compact metric instead, but since the ratios (6.11) are invariant under Weyl-transformations this makes no difference.

Remark 6.1:

Even though the correlator of three boundary fields is built directly from a single conformal block, rather than from a bilinear combination of blocks like the correlator of three bulk fields, it is not, in general, an analytic function of the insertion points. As an example, take the correlator of two equal boundary fields²¹ ϕ , which for $x_2 > x_1$ is given by

$$C = C(M \quad M \quad M) B_{ii}(u;u) (x_2 - x_1)^{2-i(u)} \quad (6.17)$$

For $x_1 > x_2$ one finds the same answer up to an exchange $x_1 \leftrightarrow x_2$, so that for all values of x_1, x_2 we can write

$$C = C(M, M, M) B_{ii}(u; u) x_2 - x_1^2; \quad (6.18)$$

which is not analytic in x_1 and x_2 (unless $\beta \in \mathbb{Z}$, which is a very special case). It is thus not quite appropriate to say that the theory on the boundary is chiral.

Remark 6.2:

Consider the case $M = N = K = A$, i.e. on each boundary segment the boundary condition is given by A , regarded as a left module over itself. Using the Frobenius reciprocity relation $\text{Hom}_A(A \otimes U; A) = \text{Hom}(U; A)$ (see e.g. proposition I.4.12), the elements of $\text{Hom}_A(A \otimes S_k; A)$ can be expressed as

$$= m \quad (\mathbf{i}\mathbf{d}_A^T \quad \mathbf{b}_{k_i}^A) ; \quad (6.19)$$

where m is the multiplication morphism of A and b_k^A denotes the basis (2.38) of $\text{Hom}(S_k; A)$. The ribbon graph (4.8) then takes the form

$$c(A_1 A_2 A_3 A) = \text{Diagram} = \text{Diagram} \quad (6.20)$$

In the second equality one uses associativity of the multiplication, the transformations (I:3.49), as well as the specialness relation $m = \text{id}_A$. One can now substitute the expression of the multiplication in a basis as in (I:3.7) to evaluate the ribbon invariant (6.20). This yields

$$C(A_{-1}A_{-2}A_{-3}A) = \begin{smallmatrix} X \\ & m_j^k & ; & m_k^0 \\ & i & ; & k \end{smallmatrix} " \quad \begin{smallmatrix} A \\ 0 \end{smallmatrix}; \quad : \quad (6.21)$$

²¹ This is zero in general, in particular if $i \in \{ \}$. But there are many examples, like the Virasoro minimal models, where it can be non-zero.

Using the OPE of boundary fields as defined in (I.3.11) to evaluate the correlator $h_0 j_{3-2-1} \partial_i$ and comparing the result to (6.21) gives

$$m_{j;i}^{k;} = C_{j;i}^{k;} : \quad (6.22)$$

This is nothing but the relation (I.3.14) that was already established in section I.3.2. In words it says that the boundary OPE on the boundary condition labelled by A is equal to the multiplication on the algebra A .

6.3 One bulk and one boundary field on the upper half plane

The next correlator we consider is that of one bulk field and one boundary field on the upper half plane. Let X^g be the upper half plane with field insertions

$$c = (i; j; ; [f]) \quad \text{and} \quad c = (M; M; S_k; ; [d]); \quad (6.23)$$

where $i, j, k \in I$ label simple objects, $2 \text{Hom}_{A, A}(S_i \otimes A \otimes S_j; A)$ and $2 \text{Hom}_A(M \otimes S_k; M)$. Further, $[f]$ is a local bulk coordinate germ and $[d]$ a local boundary coordinate germ, with $f(z) = z + iy$ and $d(s) = s + iy$ for z in the upper half plane and s on the real axis. In fact we take $z = x + iy$ and $s > x > 0$.

The complex double of X^g is the extended Riemann surface \hat{X}^g consisting of the Riemann sphere \mathbb{C} [f1] and the three marked points $(s; [l_1]; S_k)$, $(x + iy; [l_2]; S_i)$ and $(x - iy; [l_3]; S_j)$, with the local coordinates given by $'_1(s) = s + iy$, $'_2(z) = x + iy + iy$ and $'_3(z) = x - iy + iy$. We select a basis f^g in the space of conformal blocks $H^c(\hat{X}^g)$ as

$$\begin{aligned} &= h_0 j V_{kk}^0(w; z_3) V_{ij}^k(u; z_2) V_{j0}^j(v; z_1) \partial_i \\ &\quad z_1 = x - iy; z_2 = x + iy; z_3 = s \\ &= B_{kij}(w; u; v) e^{\frac{i}{2}(-k(w) - i(u) - j(v))} s^{-x + iy} (s - x)^2 + y^2^{-2(-i(u) - j(v))} \\ &\quad (s - x)^2 + y^2^{-i(u) + j(v) - k(u) - 2y^{-k(w) - i(u) - j(v)}}; \end{aligned} \quad (6.24)$$

where in the first line it is understood that the points $z_{1,2,3}$ are taken to their present position from the standard block (5.25) with $z_n = n$ via continuation along the contours indicated in figure (4.17). In particular, the connection to B in (4.17) is $\theta(z) = Z(B(x, y; s); ; ; \hat{X})$. Applying θ^{-1} to both sides of (4.18) thus yields

$$C(X^g) = \frac{X}{c(M)}; \quad (6.25)$$

where the constants $c(M)$ are given by the ribbon invariant (4.19).

We conclude that the correlator ratio for one bulk field and one boundary field on the upper half plane is of the form

$$\begin{aligned} \frac{C(X^g)(w; u; v)}{C(X^g)} &= \frac{\hat{X}^{ijk}}{\dim(A)} \frac{c(M)}{c(M)} B_{kij}(w; u; v) e^{\frac{i}{2}(-k(w) - i(u) - j(v))} \\ &\quad s^{-x + iy}^{-2(-i(u) - j(v))} (s - x)^2 + y^2^{-i(u) + j(v) - k(u) - 2y^{-k(w) - i(u) - j(v)}}; \end{aligned} \quad (6.26)$$

where $u \in V^2 S_i \otimes S_j$ gives the bulk field and $w \in S_k$ the boundary field.

Remark 6.3 :

The special case of one bulk field on the upper halfplane without any boundary field insertion (compare remark 4.1) is obtained by setting $\mathbf{c} = (M; M; 1; \text{id}_M; g)$ as well as $w = \text{Ji}_2 S_0$. Then (6.26) becomes

$$\frac{C(X^g)(u;v)}{C(X^g)} = \frac{c(\cdot; M)}{\dim(A)} B_{ij}(u;v) e^{-i_i(u)} 2y^{-2-i_i(u)} : \quad (6.27)$$

In (6.27) the two-point block (5.8) appears, which vanishes unless $j = i$ and $i_i(u) = i_j(v)$. Note that in the Cardy case, the phase in (6.27) combines with the factor t_i in (4.74) to a sign $(-1)^{i_i(u) - i_i}$.

6.4 Three bulk fields on the complex plane

We now turn to the correlator of three bulk fields on the complex plane, i.e. X^g is $\mathbb{C}[\mathbf{f}_1, g]$ together with three field insertions

$$c_1 = (i; j; 1; [\mathbf{f}_1]); \quad c_2 = (k; l; 2; [\mathbf{f}_2]); \quad c_3 = (m; n; 3; [\mathbf{f}_3]): \quad (6.28)$$

Here $i, j, k, l, m, n \in \mathbb{N}$ label simple objects; 1 is an element of $\text{Hom}_{A, A}(S_i \otimes A \otimes S_j; A)$, and similarly one has $2 \in \text{Hom}_{A, A}(S_k \otimes A \otimes S_l; A)$ and $3 \in \text{Hom}_{A, A}(S_m \otimes A \otimes S_n; A)$. The three fields are inserted at the positions z_1, z_2, z_3 with local bulk coordinate germs $[\mathbf{f}_{1,2,3}]$ given by $\mathbf{f}_{1,2,3}(\cdot) = z_{i,2,3} + \cdot$.

The complex double of X^g is the extended Riemann surface \hat{X}^g given by two copies of the Riemann sphere $\mathbb{C}[\mathbf{f}_1, g]$ together with six marked points, three on each connected component. Recall that we have chosen an orientation of X^g from the outset. Let \hat{X}_+^g be the connected component of \hat{X}^g that has the same orientation as X^g , and \hat{X}_-^g be the component with opposite orientation. We have $\hat{X}^g = \mathbb{P}^1$. The three marked points on the component \hat{X}_+^g are $(z_1; [\mathbf{f}_1]; R_i)$, $(z_2; [\mathbf{f}_2]; R_k)$ and $(z_3; [\mathbf{f}_3]; R_m)$, while on \hat{X}_-^g the marked points are $(z_1; [\mathbf{f}_1]; R_j)$, $(z_2; [\mathbf{f}_2]; R_l)$, $(z_3; [\mathbf{f}_3]; R_n)$. Here $z = x + iy$ is the point complex conjugate to $z = x - iy$. The local coordinates are given by $\mathbf{f}_i(\cdot) = z_i + \cdot$ and $\mathbf{f}_{\tilde{i}}(\cdot) = z_i - \cdot$, for $i = 1, 2, 3$. We select a basis \mathbf{f}_g in $H^0(\hat{X}^g)$ via the cobordism (4.29),

$$@(\cdot) = Z(B(z_1; z_2; z_3); \cdot; \hat{X}^g); \quad (6.29)$$

i.e. \cdot is a product of two three-point blocks (5.9). Applying \mathbf{c}^{-1} to both sides of (4.30) results in

$$C(X^g) = \frac{X}{c(1, 2, 3)} ; \quad (6.30)$$

with $c(1, 2, 3)$ given by the ribbon invariant (4.31).

To find the explicit functional dependence of the correlator on the insertion points, we use that the conformal block (6.29) is a product of two three-point blocks. Rearranging the individual factors in a suitable way we arrive at the expression

$$\begin{aligned} \frac{C(X^g)(v_i; \dots; v_n)}{C(X^g)} &= \frac{\mathbb{X}_{ik}^m \mathbb{X}_{jl}^n}{\dim(A)} \frac{S_{0,0} c(1, 2, 3)}{c(1, 2, 3)} B_{mki}(v_m; v_k; v_i) B_{nlj}(v_n; v_l; v_j) \\ &\quad \frac{z_1}{z_3} \frac{z_2}{z_2} \frac{z_3}{z_1} \frac{z_1}{z_1} \frac{z_2}{z_2} \frac{z_3}{z_1} \exp[i'_{32}(s_1 - s_2 - s_3) + i'_{31}(s_2 - s_1 - s_3) + i'_{21}(s_3 - s_1 - s_2)] \end{aligned} \quad (6.31)$$

for the correlator ratio for three bulk elds. Here $\arg(z_i - z_j)$, and we abbreviated

$$\begin{aligned} w_1 &= \arg(z_i) + \arg(z_j); & w_2 &= \arg(z_k) + \arg(z_l); & w_3 &= \arg(z_m) + \arg(z_n); \\ s_1 &= \arg(z_i) - \arg(z_j); & s_2 &= \arg(z_k) - \arg(z_l); & s_3 &= \arg(z_m) - \arg(z_n); \end{aligned} \quad (6.32)$$

The function (6.31) is a continuous (but not analytic) function of the insertion points z_1, z_2, z_3 . It does not have branch cuts, because $s_{1,2,3} \neq 0$ which, in turn, follows from the fact that a bulk eld transforming in the chiral/antichiral representation i, j exists only if $Z(A)_{ij} \neq 0$. The matrix $Z(A)_{ij}$ commutes with the matrix $\hat{T}_{kl} = \delta_{kl} \delta_{ik}$ (this is part of modular invariance, see theorem I.5.1), implying that $Z(A)_{ij} = (\delta_{i=j}) Z(A)_{ij}$, i.e. $i = j$ for $Z(A)_{ij} \neq 0$.

6.5 Three defect elds on the complex plane

As already seen in section 4.5, the calculation for three defect elds differs only slightly from the one for three bulk elds. X^g is now the complex plane with eld insertions

$$\begin{aligned} \overset{c}{1} &= (X; \text{or}_2; Y; \text{or}_2; i; j; \#_1; [f_1]); & \overset{c}{2} &= (Y; \text{or}_2; Z; \text{or}_2; k; l; \#_2; [f_2]); \\ \overset{c}{3} &= (Z; \text{or}_2; X; \text{or}_2; m; n; \#_3; [f_3]); \end{aligned} \quad (6.33)$$

Here or_2 is the standard orientation of the complex plane, $i, j, k, l, m, n \in \mathbb{Z}$ labels simple objects, and the morphisms $\#_{1,2,3}$ are elements of the relevant spaces of bimodule morphisms:

$$\begin{aligned} \#_1 &\in \text{Hom}_{A, A}(S_i \otimes X \otimes S_j; Y); & \#_2 &\in \text{Hom}_{A, A}(S_k \otimes Y \otimes S_l; Z); \\ \#_3 &\in \text{Hom}_{A, A}(S_m \otimes Z \otimes S_n; X); \end{aligned} \quad (6.34)$$

The three elds are inserted at z_1, z_2 and z_3 , with local bulk coordinate germs $[f_{1,2,3}]$ given by $f_{1,2,3}(x) = z_{1,2,3} + \dots$.

Here it is important to note that in (4.35) we have chosen the defect circle to run parallel to the real axis in a neighbourhood of the defect eld insertions z_i . Otherwise the local bulk coordinate germs $[f_i]$ must be modified so as to assure the condition that $f_i(x)$ lies on the defect if x lies on the real axis. We further take $j_3 > j_2 > j_1$ as indicated in figure (4.35).

The complex double of X^g is the same as for the case of three bulk elds. Correspondingly the conformal blocks needed to express the correlator (4.35) are the same, too, and we can expand

$$C(X^g) = \sum_{i=1}^X C(X; \#_1; Y; \#_2; Z; \#_3; X); \quad (6.35)$$

with blocks as defined in (6.29). The ribbon invariant for the coefficient is given by (4.38), as calculated in section 4.5. In the same manner as we arrived at the explicit form of the correlator (6.31) of three bulk elds, for three defect elds we then find

$$\begin{aligned} \frac{C(X^g)(v_i, \dots, v_n)}{C(X^g)} &= \frac{\sum_{i=1}^X \sum_{j=1}^X S_{0,0} C(X; \#_1; Y; \#_2; Z; \#_3; X)}{\dim(A)} B_{mki}(v_m; v_k; v_i) B_{nij}(v_n; v_l; v_j) \\ &\quad \cdot \frac{j_3 - z_2}{z_3 - z_2} j_1^{w_1 - w_2 - w_3} \frac{j_3 - z_1}{z_3 - z_1} j_2^{w_2 - w_1 - w_3} \frac{j_2 - z_1}{z_2 - z_1} j_3^{w_3 - w_1 - w_2} \\ &\quad \exp(i'_{32}(s_1 - s_2 - s_3) + i'_{31}(s_2 - s_1 - s_3) + i'_{21}(s_3 - s_1 - s_2)); \end{aligned} \quad (6.36)$$

where $\arg(z_i z_j)$ and

$$\begin{aligned} w_1 &= \arg(z_i) + \arg(z_j); & w_2 &= \arg(z_k) + \arg(z_l); & w_3 &= \arg(z_m) + \arg(z_n); \\ s_1 &= \arg(z_i) - \arg(z_j); & s_2 &= \arg(z_k) - \arg(z_l); & s_3 &= \arg(z_m) - \arg(z_n); \end{aligned} \quad (6.37)$$

In contrast to the correlator of three bulk fields, the expression (6.36) is not necessarily single valued in the coordinates z_1, z_2, z_3 , since the numbers s_k do not have to be integers. This is to be expected. Indeed, if, for example, in the setup (4.35) we take the field at z_2 around the field at z_1 we must deform the defect circle in order to avoid taking the field \mathbb{C} across the defect. In this way we end up with an arrangement of defect lines different from the one we started with.

6.6 One bulk field on the cross cap

Next we consider the correlator of one bulk field on the cross cap. This surface is non-orientable; accordingly we take A to be a Jandl algebra. Analogously as in section 4.6 the world sheet X^g is given by $\mathbb{C} = \mathbb{RP}^2$ with \mathbb{RP}^2 the anti-holomorphic involution $\mathbb{RP}^2(\cdot) = -1\cdot$. The bulk insertion is $\mathbb{C} = (i; j; f; \bar{f})$ with $f(\cdot) = z + i, j; 2 \in \mathbb{I}$, and $2 \text{Hom}_{\mathbb{A}}(S_i \oplus A \oplus S_j; A)$. The complex double of X^g is the Riemann sphere $\mathbb{C} \setminus f_1$ together with the two marked points $(z; \bar{z}; R_i)$ and $(\mathbb{RP}^2(z); \bar{z}; R_j)$. The holomorphic coordinate germs are given by $\mathbb{C}(\cdot) = z +$ and $\bar{\mathbb{C}}(\cdot) = \mathbb{RP}^2(\mathbb{C}(\cdot)) = (z +)^{-1}$.

The space $H^{\mathbb{C}}(\hat{X}^g)$ is the space of two-point blocks on the Riemann sphere and hence one-dimensional, provided $j = \{$. It is spanned by the block

$$_2 = h_0 \mathbb{J}V_{i;\{}^0 R_{0;0}(\bar{f})^{-1} v_i; z V_{\{;0}^1 R_{0;0}(\bar{f})^{-1} v_{\{}; \frac{1}{z} \mathbb{J}v_i; \quad (6.38)$$

where we also made explicit the dependence on the local coordinates as in (5.26). In the correlators treated in the previous sections, all operators $R(\cdot)$ were just the identity, owing to the local coordinates taking the simple form $\mathbb{C} \setminus p^+$. In the present case this is only true for $R_{0;0}(\bar{f})^{-1}$. The correlator is thus given by

$$C(X^g)(v_i; v_{\{}) = c(\mathbb{C}) h_0 \mathbb{J}V_{i;\{}^0 v_i; z V_{\{;0}^1 R_{0;0}(\bar{f})^{-1} v_{\{}; \frac{1}{z} \mathbb{J}v_i; \quad (6.39)$$

The constant $c(\mathbb{C})$ is given by the ribbon invariant (4.51), as follows from applying \mathbb{C} to both sides of (6.39) and comparing with (4.50). This result also uses the equality $\mathbb{C}(\mathbb{C}) = Z(B_2; \mathbb{C}; \hat{X})_1$, with B_2 given by (4.49).

We conclude that the correlator ratio for one bulk field on the cross cap is

$$\frac{C(X^g)(v_i; v_{\{})}{C(X^g)} = \frac{S_{0;0} c(\mathbb{C})}{(1; \bar{f})} B_{i;\{}(v_i; R_{0;0}(\bar{f})^{-1} v_{\{}) z + \frac{1}{z})^{-2 \arg(z_i)}; \quad (6.40)$$

Here $v_i \in S_i \subset S_{\{}$ specifies the state representing the bulk field. Note that for the identity bulk insertion, in (4.52) we have $\bar{f} = \bar{f}$, the counit of A , so that $C(X^g) = (1; \bar{f}) = S_{0;0}$. Using (4.63) and (II.3.90) leads to the expression

$$(1; \bar{f}) = \sum_{a \in A} \frac{t_a P_{0;a}}{(a)}; \quad (6.41)$$

Suppose now further that v_i is a Virasoro-primary state. Then $R_{0,0}(\zeta) v_i = (z) \zeta^{-2 - \ell(v_i)} v_i$, so that in this case

$$\frac{C(X^g)(v_i; v_i)}{C(X^g)} = \frac{S_{0,0} c(c)}{(1; \zeta)} B_{i\bar{i}}(v_i; v_i) \frac{1 + \frac{1}{z} \zeta^2}{1 + \frac{1}{z} \zeta^2} v_i : \quad (6.42)$$

The constant $c(c)$ is evaluated in (4.52) and (II.3.110); in the Cardy case it takes the form (4.76).

6.7 One defect field on the cross cap

To obtain the correlator of a defect field on the cross cap one essentially repeats the calculation in the previous section. Again, $X^g = \mathbb{C} = \mathbb{RP}^2$, this time with the insertion of a defect field, given by $c = (X; \text{or}_2; X; \text{or}_2; i; j; \#; [f])$ with $f(z) = z + \# 2 \text{Hom}_{\mathbb{A}}(S_i \rightarrow X^s, S_j \rightarrow X)$. The choice of f implies that the defect runs parallel to the real axis at the insertion point of the defect field. The orientations or_2 of the neighbourhood of X are obtained as follows. Let or_2 be the local orientation around $f(0)$ induced by $[f]$. The orientation of X is obtained by transporting or_2 along the defect to the right. When passing through the identification circle, the orientation gets reversed, so that one arrives at the insertion point $f(0)$ with or_2 from the left, see figure (4.53).

The space $H^c(\hat{X}^g)$ is again spanned by the single block (6.38); the correlator is

$$C(X^g) = c(X; c) h_0 \oint_{i\bar{i}}^0 v_i; z V_{i\bar{i}; 0} R_{0,0}(\zeta) v_i; \frac{1}{z} \zeta^2 v_i : \quad (6.43)$$

where $c(X; c)$ is given by the ribbon invariant (4.55), as calculated in section 4.7. Taking the states $v_i \otimes S_i$ and $v_i \otimes S_{\bar{i}}$ describing the defect field to be Virasoro-primaries, altogether the ratio of correlators for one defect field on the cross cap becomes

$$\frac{C(X^g)(v_i; v_i)}{C(X^g)} = \frac{S_{0,0} c(X; c)}{(1; \zeta)} B_{i\bar{i}}(v_i; v_i) \frac{1 + \frac{1}{z} \zeta^2}{1 + \frac{1}{z} \zeta^2} v_i : \quad (6.44)$$

In the Cardy case, the constant $c(X; c)$ is given by (4.75).

References

- [I] J. Fuchs, I. Runkel, and C. Schweigert, TFT construction of RCFT correlators I: Partition functions, *Nucl.Phys.B* 646 (2002) 353 [[hep-th/0204148](#)]
- [II] J. Fuchs, I. Runkel, and C. Schweigert, TFT construction of RCFT correlators II: Unoriented surfaces, *Nucl.Phys.B* 678 (2003) 511 [[hep-th/0306164](#)]
- [III] J. Fuchs, I. Runkel, and C. Schweigert, TFT construction of RCFT correlators III: Simple currents, *Nucl.Phys.B* 694 (2004) 277 [[hep-th/0403158](#)]
- [V] J. Fjelstad, J. Fuchs, I. Runkel, and C. Schweigert, TFT construction of RCFT correlators V: Proof of modularity invariance and factorization, preprint to appear
- [1] J. Fuchs, I. Runkel, and C. Schweigert, Conformal correlation functions, Frobenius algebras and triangulations, *Nucl.Phys.B* 624 (2002) 452 [[hep-th/0110133](#)]
- [2] E. Witten, Quantum field theory and the Jones polynomial, *Commun.Math.Phys.* 121 (1989) 351
- [3] J. Fröhlich and C. King, The Chern-Simons theory and knot polynomials, *Commun.Math.Phys.* 126 (1989) 167
- [4] G. Felder, J. Fröhlich, J. Fuchs, and C. Schweigert, Correlation functions and boundary conditions in RCFT and three-dimensional topology, *Compos.Math.* 131 (2002) 189 [[hep-th/9912239](#)]
- [5] H. Sonoda, Sewing conformal field theories, *Nucl.Phys.B* 311 (1988) 401
- [6] D.C. Lewellen, Sewing constraints for conformal field theories on surfaces with boundaries, *Nucl.Phys.B* 372 (1992) 654
- [7] D. Fioravanti, G. Pradisi, and A. Sagnotti, Sewing constraints and non-orientable strings, *Phys. Lett.B* 321 (1994) 349 [[hep-th/9311183](#)]
- [8] E. Witten, On holomorphic factorization of WZW and coset models, *Commun.Math.Phys.* 144 (1992) 189
- [9] G. Moore and N. Seiberg, Lectures on RCFT, in: *Physics, Geometry, and Topology*, H.C. Lee, ed. (Plenum Press, New York 1990), p. 263
- [10] J. Fröhlich and C. King, Two-dimensional conformal field theory and three-dimensional topology, *Int.J.Mod.Phys.A* 4 (1989) 5321
- [11] B. Bakalov and A.N. Kirillov, On the Lego-Teichmüller game, *Transform. Groups* 5 (2000) 207 [[math.GT/9809057](#)]
- [12] V.L.S. Dotsenko and V.A. Fateev, Four-point correlation functions and operator algebra in 2D conformal invariant theories with central charge $c=1$, *Nucl.Phys.B* 251 (1985) 691
- [13] J.L. Cardy and D.C. Lewellen, Bulk and boundary operators in conformal field theory, *Phys. Lett.B* 259 (1991) 274
- [14] I. Runkel, Boundary structure constants for the A-series Virasoro minimal models, *Nucl.Phys.B* 549 (1999) 563 [[hep-th/9811178](#)]
- [15] B. Ponsot, Recent progress on Liouville field theory, preprint [hep-th/0301193](#)
- [16] J.A. Teschner, A lecture on the Liouville vertex operators, preprint [hep-th/0303150](#)
- [17] Y. Nakayama, Liouville field theory { A decade after the revolution, Master's thesis (Tokyo 2004, [hep-th/0402009](#))
- [18] Y.-Z. Huang, Vertex operator algebras, the Verlinde conjecture and modular tensor categories, preprint [math.QA/0412261](#)
- [19] V.G. Turaev, Quantum Invariants of Knots and 3-Manifolds (de Gruyter, New York 1994)

- [20] B. Bakalov and A.A. Kirillov, *Lectures on Tensor Categories and Modular Functors* (American Mathematical Society, Providence 2001)
- [21] A. Cappelli, C. Itzykson, and J.-B. Zuber, The A-D-E classification of minimal and $A_1^{(1)}$ conformal invariant theories, *Commun. Math. Phys.* 113 (1987) 1
- [22] R.E. Behrend, P.A. Pearce, V.B. Petkova, and J.-B. Zuber, Boundary conditions in rational conformal field theories, *Nucl. Phys. B* 579 (2000) 707 [[hep-th/9908036](#)]
- [23] V.B. Petkova and J.-B. Zuber, The many faces of Ocneanu cells, *Nucl. Phys. B* 603 (2001) 449 [[hep-th/0101151](#)]
- [24] V.B. Petkova and J.-B. Zuber, Conformal boundary conditions and what they teach us, in: *Non-perturbative QFT Methods and Their Applications*, Z. Horvath and L. Palla, eds. (World Scientific, Singapore 2001), p. 1 [[hep-th/0103007](#)]
- [25] V.B. Petkova and J.-B. Zuber, Conformal field theories, graphs and quantum algebras, in: *MathPhys Odyssey 2001: Integrable Models and Beyond*, M. Kashiwara and T. Miwa, eds. (Birkhäuser, Boston 2002), p. 415 [[hep-th/0108236](#)]
- [26] V.O. Ostrik, Modular categories, weak Hopf algebras and modular invariants, *Transform. Groups* 8 (2003) 177 [[math.QA/0111139](#)]
- [27] J. Fröhlich, J. Fuchs, I. Runkel, and C. Schweigert, Picard groups in rational conformal field theory, preprint [math.CT/0411507](#)
- [28] B. Pareigis, Non-additive ring and module theory I. General theory of monoids, *Publ. Math. Debrecen* 24 (1977) 189
- [29] B. Pareigis, Morita equivalence of module categories with tensor products, *Commun. in Algebra* 9 (1981) 1455
- [30] J. Bernstein, Tensor categories, preprint [q-alg/9501032](#) (Sackler Lectures)
- [31] J. Fröhlich, J. Fuchs, I. Runkel, and C. Schweigert, Correspondences of ribbon categories, preprint [math.CT/0309465](#)
- [32] J. Fuchs and C. Schweigert, Category theory for conformal boundary conditions, Fields Institute Commun. 39 (2003) 25 [[math.CT/0106050](#)]
- [33] A.A. Kirillov and V.O. Ostrik, On q -analog of McKay correspondence and ADE classification of $sl(2)$ conformal field theories, *Adv. Math.* 171 (2002) 183 [[math.QA/0101219](#)]
- [34] G. Pradisi, A. Sagnotti, and Ya.S. Stanev, Completeness conditions for boundary operators in 2D conformal field theory, *Phys. Lett. B* 381 (1996) 97 [[hep-th/9603097](#)]
- [35] T. Gannon, Boundary conformal field theory and fusion ring representations, *Nucl. Phys. B* 627 (2002) 506 [[hep-th/0106105](#)]
- [36] A. Ocneanu, Operator algebras, topology and subgroups of quantum symmetry { construction of subgroups of quantum groups, *Adv. Studies in Pure Math.* 31 (2001) 235
- [37] G. Böhm and K. Szlachányi, A coassociative C^* -quantum group with non-integral dimensions, *Lett. Math. Phys.* 38 (1996) 437 [[q-alg/9509008](#)]
- [38] G. Felder, J. Fröhlich, J. Fuchs, and C. Schweigert, The geometry of WZW branes, *J. Geom. and Phys.* 34 (2000) 162 [[hep-th/9909030](#)]
- [39] R.E. Behrend, P.A. Pearce, V.B. Petkova, and J.-B. Zuber, On the classification of bulk and boundary conformal field theories, *Phys. Lett. B* 444 (1998) 163 [[hep-th/9809097](#)]
- [40] V. Petkova and J.-B. Zuber, Generalized twisted partition functions, *Phys. Lett. B* 504 (2001) 157 [[hep-th/0011021](#)]

- [41] V L.S. Dotsenko and V A. Fateev, Conformal algebra and multipoint correlation functions in 2D statistical models, *Nucl. Phys. B* 240 (1984) 312
- [42] B. Durhuus, H P. Jakobsen, and R. Nest, Topological quantum field theories from generalized 6j-symbols, *Rev. Math. Phys.* 5 (1993) 1
- [43] R. Longo and K. H. Rehren, Nets of subfactors, *Rev. Math. Phys.* 7 (1995) 567 [[hep-th/9411077](#)]
- [44] A A. Belavin, A M. Polyakov, and A B. Zamolodchikov, Infinite conformal symmetry in two-dimensional quantum field theory, *Nucl. Phys. B* 241 (1984) 333
- [45] H. Sonoda, Sewing conformal field theories 2, *Nucl. Phys. B* 311 (1988) 417
- [46] G. Felder, J. Fröhlich, J. Fuchs, and C. Schweigert, Conformal boundary conditions and three-dimensional topological field theory, *Phys. Rev. Lett.* 84 (2000) 1659 [[hep-th/9909140](#)]
- [47] I. Runkel, Structure constants for the D-series Virasoro minimal models, *Nucl. Phys. B* 579 (2000) 561 [[hep-th/9908046](#)]
- [48] I. Brunner and V. Schomerus, On superpotentials for D-branes in Gepner models, *J. High Energy Phys.* 0010 (2000) 016 [[hep-th/0008194](#)]
- [49] J. Fröhlich, O. G randjean, A. Redknagel, and V. Schomerus, Fundamental strings in Dp-Dq brane systems, *Nucl. Phys. B* 583 (2000) 381 [[hep-th/9912079](#)]
- [50] J.L. Cardy, Boundary conditions, fusion rules and the Verlinde formula, *Nucl. Phys. B* 324 (1989) 581
- [51] V L.S. Dotsenko and V A. Fateev, Operator algebra of two-dimensional conformal theories with central charge $c = 1$, *Phys. Lett. B* 154 (1985) 291
- [52] V G. Knizhnik and A B. Zamolodchikov, Current algebra and Wess-Zumino model in two dimensions, *Nucl. Phys. B* 247 (1984) 83
- [53] A B. Zamolodchikov and V A. Fateev, Operator algebra and correlation functions in the two-dimensional $SU(2) \times SU(2)$ chiral Wess-Zumino model, *Sov. J. Nucl. Phys.* 43 (1986) 657
- [54] P. Christe and R. Flume, The four point correlations of all primary operators of the $d=2$ conformally invariant $SU(2) \times SU(2)$ model with Wess-Zumino term, *Nucl. Phys. B* 282 (1987) 466
- [55] G. M ussardo, G. Sotkov, and M. Stanishkov, Fine structure of the supersymmetric operator product expansion algebras, *Nucl. Phys. B* 305 (1988) 69
- [56] Y. K itazawa, N. Ishibashi, A. K ato, K. K obayashi, Y. M atsuo, and S. O kade, Operator product expansion coefficients in $N = 1$ superconformal field theory and slightly relevant perturbation, *Nucl. Phys. B* 306 (1988) 425
- [57] L.J. Dixon, E.J.M. Martinec, D.H. Friedan, and S.H. Shenker, The conformal field theory of orbifolds, *Nucl. Phys. B* 282 (1987) 13
- [58] J. Fuchs, Operator product coefficients in nondiagonal conformal field theories, *Phys. Rev. Lett.* 62 (1989) 1705
- [59] J. Fuchs and A. Klemm, The computation of the operator algebra in nondiagonal conformal field theories, *Ann. Phys.* 194 (1989) 303
- [60] V B. Petkova, Structure constants of the $(A; D)$ minimal $c < 1$ conformal models, *Phys. Lett. B* 225 (1989) 357
- [61] M. Douglas and S. Trivedi, Operator product coefficients in nonstandard $SU(2)$ Wess-Zumino-Witten models, *Nucl. Phys. B* 320 (1989) 461
- [62] A. K ato and Y. K itazawa, E_7 type modular invariant Wess-Zumino theory and Gepner's string compactification, *Nucl. Phys. B* 319 (1989) 474

- [63] J. Fuchs, A. Klemm, and C. Scheich, The operator algebra of the E_8 type $su(2)$ WZW theory, *Z. Physik C* 46 (1990) 71
- [64] K.-H. Rehren, Ya.S. Stanev, and I.T. Todorov, Characterizing invariants for local extensions of current algebras, *Commun. Math. Phys.* 174 (1995-6) 605 [[hep-th/9409165](#)]
- [65] V.B. Petkova and J.-B. Zuber, On structure constants of $sl(2)$ theories, *Nucl. Phys. B* 438 (1995) 347 [[hep-th/9410209](#)]
- [66] C.G. Callan, C. Lovelace, C.R. Nappi, and S.A. Yost, Adding holes and crosscaps to the superstring, *Nucl. Phys. B* 293 (1987) 83
- [67] J. Polchinski and Y. Cai, Consistency of open superstring theories, *Nucl. Phys. B* 296 (1988) 91
- [68] N. Ishibashi, The boundary and crosscap states in conformal field theories, *Mod. Phys. Lett. A* 4 (1989) 251
- [69] G. Pradisi, A. Sagnotti, and Ya.S. Stanev, Planar duality in $SU(2)$ WZW models, *Phys. Lett. B* 354 (1995) 279 [[hep-th/9503207](#)]
- [70] G. Pradisi, A. Sagnotti, and Ya.S. Stanev, The open descendants of non-diagonal $SU(2)$ WZW models, *Phys. Lett. B* 356 (1995) 230 [[hep-th/9506014](#)]
- [71] L.R. Huiszoon, A.N. Schellekens, and N. Sousa, Klein bottles and simple currents, *Phys. Lett. B* 470 (1999) 95 [[hep-th/9909114](#)]
- [72] L.R. Huiszoon, A.N. Schellekens, and N. Sousa, Open descendants of non-diagonal invariants, *Nucl. Phys. B* 575 (2000) 401 [[hep-th/9911229](#)]
- [73] L.R. Huiszoon and A.N. Schellekens, Crosscaps, boundaries and T-Duality, *Nucl. Phys. B* 583 (2000) 705 [[hep-th/0004100](#)]
- [74] J. Fuchs, L.R. Huiszoon, A.N. Schellekens, C. Schweigert, and J. Walcher, Boundaries, crosscaps and simple currents, *Phys. Lett. B* 495 (2000) 427 [[hep-th/0007174](#)]
- [75] I. Brunner and K. Hori, Notes on orientifolds of rational conformal field theories, *J. High Energy Phys.* 0407 (2004) 023 [[hep-th/0208141](#)]
- [76] I. Brunner, K. Hori, K. Hosomichi, and J. Walcher, Orientifolds of Gepner models, preprint [hep-th/0401137](#)
- [77] R. Blumenhagen and T. Weigand, Chiral supersymmetric Gepner model orientifolds, *J. High Energy Phys.* 0402 (2004) 041 [[hep-th/0401148](#)]
- [78] T.P.T. Dijkgraaf, L.R. Huiszoon, and A.N. Schellekens, Supersymmetric standard model spectra from RCFT orientifolds, preprint [hep-th/0411129](#)
- [79] Z. Bern and D.C. Dunbar, Conformal field theory on surfaces with boundaries and nondiagonal modular invariants, *Int. J. Mod. Phys. A* 5 (1990) 4629
- [80] M. Bianchi and A. Sagnotti, Twisted symmetry and open-string Wilson lines, *Nucl. Phys. B* 361 (1991) 519
- [81] Y.-Z. Huang, Two-dimensional conformal geometry and Vertex Operator Algebras (Birkhäuser, Boston 1997)
- [82] E. Frenkel and D. Ben-Zvi, Vertex Algebras and Algebraic Curves, second edition (American Mathematical Society, Providence, in press) [[www.math.berkeley.edu/~frenkel/BOOK](#)]
- [83] J. Lepowsky and H. Li, Introduction to Vertex Operator Algebras and their Representations (Birkhäuser, Boston 2004)
- [84] Y.-Z. Huang, Riemann surfaces with boundaries and the theory of vertex operator algebras, *Fields Institute Commun.* 39 (2003) 109 [[math.QA/0212308](#)]

- [85] Y.-Z. Huang and J. Lepowsky, Tensor products of modules for a vertex operator algebra and vertex tensor categories, in: *Lie Theory and Geometry*, R. Brylinski, J.-L. Brylinski, V. Guillemin, and V. G. Kac, eds. (Birkhauser, Boston 1994), p. 349 [[hep-th/9401119](#)]
- [86] C. Schweigert, J. Fuchs, and J. Walcher, Conformal field theory, boundary conditions and applications to string theory, in: *Non-perturbative QFT Methods and Their Applications*, Z. Horvath and L. Palla, eds. (World Scientific, Singapore 2001), p. 37 [[hep-th/0011109](#)]
- [87] D. H. Friedan and S. H. Shenker, The analytic geometry of two-dimensional conformal field theory, *Nucl. Phys. B* 281 (1987) 509
- [88] Y.-Z. Huang, Vertex operator algebras, the Verlinde conjecture and modular transformations, preprint (2004)
- [89] K. Gawedzki, Lectures on conformal field theory, in: *Quantum Fields and Strings: A Course for Mathematicians*, P. Deligne et al., eds. (American Mathematical Society, Providence 1999), p. 727 [www.math.ias.edu/QFT/fall/index.html]